

Computational Physics and Engineering Division

**OECD/NEA
BURNUP CREDIT CALCULATIONAL CRITICALITY BENCHMARK
PHASE I-B RESULTS**

M. D. DeHart
M. C. Brady*
C. V. Parks

*Sandia National Laboratories, Las Vegas, Nevada.

Date Published: June 1996

Prepared by the
OAK RIDGE NATIONAL LABORATORY
managed by
LOCKHEED MARTIN ENERGY RESEARCH CORP.
for the
U.S. DEPARTMENT OF ENERGY
under contract DE-AC05-96OR22464



CONTENTS

	Page
ABSTRACT	iii
1. INTRODUCTION	1
2. BENCHMARK SPECIFICATION	2
3. PARTICIPANTS AND ANALYSIS METHODS	5
4. RESULTS AND DISCUSSION	15
5. CONCLUDING REMARKS	85
6. REFERENCES	86
APPENDIX A. THE EFFECT ON REACTIVITY OF THE DIFFERENCES IN THE COMPUTED ISOTOPIC COMPOSITION OF SPENT FUEL	87
A.1 INTRODUCTION	88
A.2 METHOD	88
A.3 RESULTS	89
A.4 REFERENCES	95
APPENDIX B. REVISED PSI RESULTS FOR THE BURNUP CREDIT CRITICALITY BENCHMARK, PART I-B	97

LIST OF FIGURES

Figure	Page
1. Relative U-234 concentrations	30
2. Relative U-235 concentrations	31
3. Relative U-236 concentrations	32
4. Relative U-238 concentrations	33
5. Relative Pu-238 concentrations	34
6. Relative Pu-239 concentrations	35
7. Relative Pu-240 concentrations	36
8. Relative Pu-241 concentrations	37
9. Relative Pu-242 concentrations	38
10. Relative Am-241 concentrations	39
11. Relative Am-243 concentrations	40
12. Relative Np-237 concentrations	41
13. Relative Mo-95 concentrations	42
14. Relative Tc-99 concentrations	43
15. Relative Ru-101 concentrations	44
16. Relative Rh-103 concentrations	45
17. Relative Ag-109 concentrations	46
18. Relative Cs-133 concentrations	47
19. Relative Cs-135 concentrations	48
20. Relative Nd-143 concentrations	49
21. Relative Nd-145 concentrations	50
22. Relative Sm-147 concentrations	51
23. Relative Sm-149 concentrations	52
24. Relative Sm-150 concentrations	53
25. Relative Sm-151 concentrations	54
26. Relative Sm-152 concentrations	55
27. Relative Eu-153 concentrations	56
28. Relative Gd-155 concentrations	57
29. Relative Np-237 activities	58
30. Relative Am-241 activities	59
31. Relative Am-243 activities	60
32. Relative Tc-99 activities	61
33. Relative Cs-135 activities	62
34. Relative Am-243 concentrations with converted activities	63
35. Average agreement (all cases) by isotope for ORNL-Assm results	64
36. Average agreement (all cases) by isotope for AEA results	65
37. Average agreement (all cases) by isotope for AECL-ORIGEN results	66
38. Average agreement (all cases) by isotope for AECL-WIMS results	67
39. Average agreement (all cases) by isotope for Belgonucleaire results	68

40.	Average agreement (all cases) by isotope for BNFL results	69
41.	Average agreement (all cases) by isotope for CEA results	70
42.	Average agreement (all cases) by isotope for CSN results	71
43.	Average agreement (all cases) by isotope for ECN-new lib results	72
44.	Average agreement (all cases) by isotope for ECN-old lib results	73
45.	Average agreement (all cases) by isotope for GRS results	74
46.	Average agreement (all cases) by isotope for JAERI results	75
47.	Average agreement (all cases) by isotope for NUPEC/INS results	76
48.	Average agreement (all cases) by isotope for ORNL-27g results	77
49.	Average agreement (all cases) by isotope for ORNL-44g results	78
50.	Average agreement (all cases) by isotope for PNC results	79
51.	Average agreement (all cases) by isotope for PSI results	80
52.	Average agreement (all cases) by isotope for Riso results	81
53.	Average agreement (all cases) by isotope for Tohoku results	82
54.	Average agreement (all cases) by isotope for Toshiba-leakage results	83
55.	Average agreement (all cases) by isotope for Toshiba-poison results	84

LIST OF TABLES

Table	Page
1. Physical data for benchmark problem pin-cell calculation	2
2. Operating history data for benchmark problem pin-cell calculation	3
3. Specific power for the three benchmark cases	3
4. Initial fuel composition and number densities	3
5. Cycle 1 coolant number densities	4
6. Benchmark nuclides	4
7. Summary of participation organizations and codes used	6
8. Results for case A (27.35-GWd/MTU burnup) actinides (mg/g UO ₂)	16
9. Results for case B (37.12-GWd/MTU burnup) actinides (mg/g UO ₂)	17
10. Results for case C (44.34-GWd/MTU burnup) actinides (mg/g UO ₂)	18
11. Results for case A (27.35-GWd/MTU burnup) fission products (mg/g UO ₂)	19
12. Results for case B (37.12-GWd/MTU burnup) fission products (mg/g UO ₂)	20
13. Results for case C (44.34-GWd/MTU burnup) fission products (mg/g UO ₂)	21
14. Results for all highly active nuclides (mCi/g UO ₂)	22
15. Standard deviation of isotopic calculations by isotope and burnup	23
16. Revised averages and standard deviations for ²³⁸ Pu results	25
17. Comparison of ²⁴³ Am thermal capture cross sections	25
18. Revised averages and standard deviations for ¹⁰⁹ Ag results	26
19. Cross-section and fission yield data for ¹⁴⁹ Sm	27
20. Cross-section and fission yield data for ¹⁵¹ Sm	27
21. Comparison of ²³⁷ Np thermal capture cross sections	29
A.1. Reactivity values obtained with different concentration sets	89
A.2. Effect of individual isotopes for Case A (27.35 GWd/MTU)	90
A.3. Effect of individual isotopes for Case B (37.12 GWd/MTU)	91
A.4. Effect of individual isotopes for Case C (44.34 GWd/MTU)	92
A.5. Total impact on reactivity of the standard deviation of the isotope concentrations	93
A.6. Impact on reactivity of the standard deviation of each isotope concentration	94
B.1. Revised (11/15/95) results for PSI Phase I-B benchmark	99

ABSTRACT

Burnup credit is an ongoing technical concern for many countries that operate commercial nuclear power reactors. In a multinational cooperative effort to resolve burnup credit issues, a Burnup Credit Working Group has been formed under the auspices of the Nuclear Energy Agency of the Organization for Economic Cooperation and Development. This working group has established a set of well-defined calculational benchmarks designed to study significant aspects of burnup credit computational methods. These benchmarks are intended to provide a means for the intercomparison of computer codes, methods, and data applied in spent fuel analysis. The benchmarks have been divided into multiple phases, each phase focusing on a particular feature of burnup credit analysis. This report summarizes the results and findings of the Phase I-B benchmark, which was proposed to provide a comparison of the ability of different code systems and data libraries to perform depletion analysis for the prediction of spent fuel isotopic concentrations. Results included here represent 21 different sets of calculations submitted by 16 different organizations worldwide and are based on a limited set of nuclides determined to have the most important effect on the neutron multiplication factor of light-water-reactor spent fuel.

A comparison of all sets of results demonstrates that most methods are in agreement to within 10% in the ability to estimate the spent fuel concentrations of most actinides. All methods are within 11% agreement about the average for all fission products studied. Furthermore, most deviations are less than 10%, and many are less than 5%. The exceptions are ^{149}Sm , ^{151}Sm , and ^{155}Gd .

1. INTRODUCTION

In most countries, criticality analysis of light-water-reactor (LWR) fuel stored in racks and casks has assumed that the fuel is fresh with the maximum allowable initial enrichment. This assumption has led to the design of widely spaced and/or highly poisoned storage and transport arrays. If credit is assumed for fuel burnup, initial enrichment limitations can be raised in existing systems, and more compact and economical arrays can be designed. Such reliance on the reduced reactivity of spent fuel for criticality control is referred to as "burnup credit." However, before such an approach can be approved by licensing agencies, it is necessary to demonstrate that the available criticality safety calculational tools are appropriate for application to spent or partially burned fuel systems. Toward this end, a suite of calculational benchmarks related to burnup credit criticality analysis has been conceived and proposed by the Nuclear Energy Agency (NEA) of the Organization for Economic Cooperation and Development (OECD) and analyzed by numerous participants.

The goal of any criticality safety analysis based on burnup credit will be to demonstrate that an adequate margin of subcriticality is provided while taking credit for the reduced reactivity of spent fuel. In practice, determination of subcriticality using a burnup credit approach requires a two-step process: (1) determination of spent fuel composition using depletion analysis, and (2) calculation of the multiplication factor for the spent fuel system based on the predicted spent fuel composition. A series of benchmark problems have been established to analyze various aspects of burnup credit for light-water-reactor (LWR) fuel designs. This report summarizes the results of Burnup Credit Criticality Benchmark Phase I-B, which provides a comparison of the ability of various code systems and data libraries to predict spent fuel isotopic concentrations via depletion analysis. Analyses performed under Phase I-A of this program examined the effect of basic parameters (burnup, initial enrichment, cooling time, and the presence of fission products) on the ability to calculate k_{∞} for an infinite array of pressurized-water-reactor (PWR) spent fuel pins. Subsequent benchmark studies (Phase II) will engage criticality-related aspects of spent fuel analysis in more complicated configurations.

Chemical assay measurements of isotopic concentrations in spent fuel samples serve as a quantitative measure of the ability of any given code system to computationally predict spent fuel composition. Many such measurements have been performed in the United States at the Materials Characterization Center (MCC) of the Pacific Northwest Laboratories (PNL) under the U.S. Department of Energy (DOE) Office of Civilian Radioactive Waste Management program. In a specific set of measurements performed at MCC, spent fuel samples obtained from three different locations (and burnups) of a single fuel rod have yielded nuclide inventories for a large number of both actinides and fission products.¹ These fuel samples have been selected as a basis for Phase I-B benchmark calculations. However, because the purpose of the benchmark calculations is to determine the degree of consistency between different code systems and nuclear data, the problem specification has been simplified somewhat to provide an approximate representation of the fuel configuration during depletion. This simplification will allow a more straightforward and consistent comparison between the codes used by the various participants in this study. The specifications for the benchmark problem are described in the following section. References 1 through 3 provide detailed descriptions of the actual configuration of the test sample during its in-core exposure.

2. BENCHMARK SPECIFICATION

The purpose of this calculational benchmark problem is to compare nuclide concentrations computed by all participants for depletion in a simple pin-cell model. The fuel pin-cell description is given in Table 1. The fuel sample assay at MCC was from a Combustion Engineering 14×14 assembly design. For the purposes of this benchmark, actual pin dimensions were used but the fuel pin pitch was modified such that the fuel-to-moderator ratio matched that of the actual two-dimensional (2-D) assembly. The fuel sample was burned for four complete cycles; the length of the burn time and subsequent down time for each reactor cycle are given in Table 2. This benchmark consists of three cases, corresponding to fuel samples taken from three different axial locations in the reference fuel pin, each with a different total burnup. The specific power for each cycle and the final (cumulative) burnup are given in Table 3 for each of the three cases. Table 4 lists the initial isotopic concentrations to be used for the fuel material for all three cases. Table 5 provides the isotopic composition of the moderator for cycle 1. Note that boron concentrations given in Table 5 are for cycle 1 and should be modified by the cycle-specific relative boron concentrations given in Table 2 for subsequent cycles. Finally, Table 6 provides a list of those isotopes for which concentrations are desired at specified burnups and cooling times. The goal of this study is to compare the isotopic concentrations calculated by the study participants using various codes and data libraries.

Table 1. Physical data for benchmark problem pin-cell calculation

Parameter	Data
Type fuel pellet	UO ₂
Fuel density	10.045 g/cm ³
Rod pitch	1.5586 cm
Rod OD	1.118 cm
Rod ID	0.986 cm
Fuel diameter	0.9563 cm
Active fuel length	347.2 cm
Effective fuel temperature	841 K
Clad temperature	620 K
Clad material	Zircaloy-2 (97.91 wt % Zr, 1.59 wt % Sn, 0.5 wt % Fe)
Water temperature	558 K
Water density	0.7569 g/cm ³

Table 2. Operating history data for benchmark problem pin-cell calculation

Operating cycle	Burntime (days)	Downtime (days)	Boron concentration (ppm)	Boron concentration (% of cycle 1)
1	306.0	71.0	331.0	100.0
2	381.7	83.1	469.7	141.9
3	466.0	85.0	504.1	152.3
4	461.1	1870.0	492.5	148.8

Table 3. Specific power for the three benchmark cases

Operating cycle	Specific Power (kW/kgU)		
	Case A (final burnup = 27.35 GWd/MTU)	Case B (final burnup = 37.12 GWd/MTU)	Case C (final burnup = 44.34 GWd/MTU)
1	17.24	24.72	31.12
2	19.43	26.76	32.51
3	17.04	22.84	26.20
4	14.57	18.87	22.12

Table 4. Initial fuel composition and number densities

Nuclide	Number density (atoms/b-cm)
²³⁴ U	6.15165×10^{-6}
²³⁵ U	6.89220×10^{-4}
²³⁶ U	3.16265×10^{-6}
²³⁸ U	2.17104×10^{-2}
¹² C	9.13357×10^{-6}
¹⁴ N	1.04072×10^{-5}
¹⁶ O	4.48178×10^{-2}

Table 5. Cycle 1 coolant number densities

Nuclide	Number density (atoms/b-cm)
¹ H	5.06153×10^{-2}
¹⁶ O	2.53076×10^{-2}
¹⁰ B	2.75612×10^{-6}
¹¹ B	1.11890×10^{-5}

Table 6. Benchmark nuclides

Actinides	Fission products
²³⁴ U	⁹⁵ Mo
²³⁵ U	⁹⁹ Tc
²³⁶ U	¹⁰¹ Ru
²³⁸ U	¹⁰³ Rh
²³⁸ Pu	¹⁰⁹ Ag
²³⁹ Pu	¹³³ Cs
²⁴⁰ Pu	¹⁴⁷ Sm
²⁴¹ Pu	¹⁴⁹ Sm
²⁴² Pu	¹⁵⁰ Sm
²⁴¹ Am	¹⁵¹ Sm
²⁴³ Am	¹⁵² Sm
²³⁷ Np	¹⁴³ Nd
	¹⁴⁵ Nd
	¹⁵³ Eu
	¹⁵⁵ Gd

3. PARTICIPANTS AND ANALYSIS METHODS

Results included in this report were provided by 16 participating organizations, with a total of 21 sets of calculations. Table 7 summarizes the participants and method(s) used in their analyses. This summary is followed by a more detailed description of each analysis set, as provided by each participant with their results. The organization label given in Table 7 represents the abbreviation used to identify each set of calculations throughout the remainder of this report.

Table 7. Summary of participation organizations and codes used

Organization label	Organization	Code(s) used	Comments
1. AEA	Atomic Energy Authority, United Kingdom	LWRWIMS	
2a. AECL-ORIGEN	Atomic Energy of Canada, Ltd., Canada	WIMS-AECL, ORIGEN-S	Coupled WIMS-AECL/ ORIGEN-S calculation similar to SAS2H
2b. AECL-WIMS	Atomic Energy of Canada, Ltd., Canada	WIMS-AECL, ORIGEN-S	
3. Belgonucleaire	Belgonucleaire, Belgium	LWRWIMS	
4. BNFL	British Nuclear Fuels, Ltd., United Kingdom	FISPIN	
5. CEA	Commissariat a l'Energie Atomique, France	Apollo	
6. CSN	Consejo de Seguridad Nuclear, Spain	CASMO-3G	
7a. ECN-New Lib	Energieonderzoek Centrum Nederland, The Netherlands	ORIGEN-S	New ECN JEF2.2/EAF-3 library
7b. ECN-Old Lib	Energieonderzoek Centrum Nederland, The Netherlands	ORIGEN-S	Original ORIGEN-S library
8. GRS	Gesellschaft für Anlagen-und Reaktorsicherheit, Germany	HAMMER/ORIGEN (OREST)	
9. JAERI	Japan Atomic Energy Research Institute, Japan	UNITBURN	
10. NUPEC/INS	Institute for Nuclear Safety, NUPEC, Japan	ORIGEN2	
11a. ORNL-27g	Oak Ridge National Laboratory, USA	SAS2H/ORIGEN-S (SCALE 4.2)	SCALE 27-group ENDF/B-IV/ -V burnup library
11b. ORNL-44g	Oak Ridge National Laboratory, USA	SAS2H/ORIGEN-S (SCALE 4.2)	SCALE 44-group ENDF/B-V library
11c. ORNL-Assm	Oak Ridge National Laboratory, USA	SAS2H/ORIGEN-S (SCALE 4.2)	Based on experimental data rather than benchmark specification
12. PNC	PNC Tokai Works, Japan	SAS2H/ORIGEN-S (SCALE-4)	
13. PSI	Paul Scherrer Institute, Switzerland	ETOBX/BOXER (ELCOS)	
14. Risø	Risø National Laboratory, Denmark	CCCMO	
15. Tohoku	Tohoku University, Japan	SWAT	
16a. Toshiba-Leakage	Toshiba Corporation, Japan	TGBLA	Leakage control
16b. Toshiba-Poison	Toshiba Corporation, Japan	TGBLA	Poison control

AEA:

Date: 2 Feb 1993

Institute: Atomic Energy Authority, United Kingdom

Participants: N. T. Gulliford

Computer code: LWRWIMS (69 groups)

Data library: WIMS1986

Notes: Decay of ^{155}Eu to ^{155}Gd added 19th Feb 1993 (not standard in WIMS1986 library).

AECL-ORIGEN:

Date: 22 June 1993

Institute: Atomic Energy of Canada, Ltd., Canada

Participants: I. C. Gauld, J. V. Donnelly

Computer code: WIMS-AECL, ORIGEN-S

Data library: ENDF/B-5 fission product yields (SCALE 4.1). Library updated with WIMS and SCALE cross sections using modified SAS2 sequence of SCALE 4 (WIMS-AECL lattice cell code in place of XSDRNPM).

Notes:

1. The unspecified Zircaloy density was assumed to be 6.5 g/cm^3 . The gap was assumed to be oxygen at a density of 0.0014 g/cm^3 .
2. The WIMS-AECL calculation (collision probability mode) was performed as a k_{∞} calculation without any buckling corrections to the spectrum. Cross sections from WIMS-AECL are passed into ORIGEN-S, and the fuel flux is used to collapse additional multigroup data from the SCALE 27-group library.
3. Calculations with buckling (critical spectrum) gave better agreement with the measured data provided. However, since you indicated that this is a numerical benchmark, and not a comparison with the measured data, no buckling was used in the calculations presented.
4. The ORIGEN-S results are also sensitive to the addition of light elements due to the calculation of the Q value (recoverable MeV/fission) calculated by ORIGEN-S. When additional light elements were added to the ORIGEN case, in concentrations that might be expected in a real full-assembly model, the numbers improved due to the small increase in Q and a corresponding decrease in the flux. However, no adjustments in the light-element concentrations were made to better reflect what might be expected in a full assembly.

AECL-WIMS:

Date: 22 June 1993

Institute: Atomic Energy of Canada, Ltd., Canada

Participants: I. C. Gauld, J. V. Donnelly

Computer code: WIMS-AECL, ORIGEN-S

Data library: Lattice cell code; 89-group ENDF/B-V cross-section library. Additional multigroup cross sections for ORIGEN-S updating were obtained from SCALE 27-group burnup library (SCALE 4.1).

Notes: see Notes description in "AECL-ORIGEN" above.

Belgonucleaire:

Date: 19 Feb 1993

Institute: Belgonucleaire, Belgium

Participants: Th. Maldague, S. Tastenoy

Computer code: LWRWIMS, AEA Winfrith, UK

Data library: LWRWIMS version 1986, 69 energy groups

Notes: This library doesn't contain Cm isotopes, giving an underestimation of ^{238}Pu and ^{242}Pu .

BNFL:

Date: 21 October 1994

Institute: British Nuclear Fuels, Ltd., United Kingdom

Participants: P. R. Thorne, P. E. Broome, R. L. Bowden

Computer code: FISPIN6.3

Data library: Burnup-independent libraries: UKFPTR6, HEDEC1, PWRBIN4; burnup-dependent libraries: PWRBUG3A, PWRBUG4

Notes: The inventory calculations carried out in support of this benchmark exercise were performed using FISPIN with standard burnup-dependent library data. At BNFL Risley, we have a library set for each major commercial reactor type, the data of which have been derived from reactor calculations for a specific reactor using fuel of various enrichments. For PWR fuel inventory calculations, we use a set of libraries which are based upon the Bugey reactor at fuel enrichments of 2, 3, and 4 w/o $^{235}\text{U}/\text{U}$. Currently, an installed macro is run at the start of each FISPIN calculation in order to decide upon the appropriate burnup-dependent data for that case. If necessary, this macro will interpolate linearly between two bounding libraries in order to obtain the flux-weighted cross sections and neutron spectra for the FISPIN calculation.

The fuel considered in the Phase I-B calculations has an initial fuel enrichment of approximately 3.1 w/o $^{235}\text{U}/\text{U}$. Hence, the FISPIN calculations were performed using burnup-dependent data interpolated between the 3 and 4 w/o enriched libraries.

The use of standard burnup-dependent library data means that no reactor lattice calculation is performed for the inventory prediction. Hence, the physical data presented in the benchmark specification do not form part of the calculation. The irradiation histories specified for the three cases do, however, form part of the input to the FISPIN calculation.

CEA:

Date: 19 Feb 1993

Institute: Commissariat a l'Energie Atomique, France

Participants: MM. Santamarina, Maubert, Poullot, Albarede

Computer code: APOLLO

Data library: CEA-86 (99 multigroup library based on JEF -1 European file + internal CEA evaluations')

CSN:

Date: 22 Dec 1993

Institute: Consejo de Seguridad Nuclear, Spain

Participants: Jose M. Conde, Manuel Recio, Ana I. Alvarez

Computer code: CASMO-3G, Version 4.7

Data library: E4LTJB7 (70 energy groups, mostly from ENDF/B-IV with some data from ENDF/B-V and JEF-2, processed with NJOY).

ECN-New Lib:

Date: 9 Sept 1993

Institute: Energieonderzoek Centrum Nederland, The Netherlands

Participants: J. L. Kloosterman

Computer code: ORIGEN-S

Data library: New ECN library with about 275 nuclides updated based on the JEF2.2 file and cross sections of about 285 nuclides updated based on the EAF-3 library compiled at ECN.

ECN-Old Lib:

Date: 9 Sept 1993

Institute: Energieonderzoek Centrum Nederland, The Netherlands

Participants: J. L. Kloosterman

Computer code: ORIGEN-S

Data library: Original ORIGEN-S library

GRS:

Date: 2 Feb 1993

Institute: Gessellschaft für Anlagen- und Reaktorsicherheit, Germany

Participants: Bernhard Gmal, Walter Heinicke

Computer code: OREST, a HAMMER-ORIGEN coupling burnup code system, developed by U. Hesse, GRS. The code is available via the NEA Data Bank

Data library: Updated ORIGEN libraries. (See Notes below.)

Notes: Libraries of HAMMER: The original THERMOS and HAMLET libraries are used, but shortened for only the available OREST-isotopes. The THERMOS library was checked against other data. Greater differences of about 10% could be found for only 6 nuclides (O, Ni, ^{135}Xe , ^{240}Pu , ^{241}Pu , and ^{242}Pu). Only these nuclides had been updated, and better results for ^{242}Pu could be calculated, compared with a number of experiments.

Libraries of ORIGEN:

- LIB1 (light-element and structural-materials reaction and decay data);
- LIB2 (actinides and daughters reaction and decay data);
- LIB3 (fission products reaction and decay data);
- LIB4 (light-element and structural-materials photon data);
- LIB5 (actinides and daughters photon data); and
- LIB6 (fission products photon data)

are fully updated. Buildup of the 6 card image datasets is unchanged. The libraries are generated by the GRS code @LIBGEN from only one GRS overall dataset LIBMAST with all information. During updating of these libraries, most constraints had been directed to the following points:

- The libraries are “closed” because all isotopes of buildup and decay reactions are present. Especially for actinides, all decay chains are present.
- All decay energy entries are updated.
- The library for fission products is enlarged for short-living isotopes. Together with updated decay energies the post-irradiation fuel decay power is also described in the short range of seconds after shutdown.
- All cross sections are preweighted in LWR neutron spectra. Unknown resonance data are filled with the $1/v$ model.
- All photon libraries are updated by detailed gamma line libraries. Bremsstrahlung is included for all beta emitters.

JAERI:

Date: 3 Aug 1993

Institute: Japan Atomic Energy Research Institute, Japan

Participants: M. Takano, F. Masukawa, and T. Kaneko

Computer code: UNITBURN

Data library: Cross sections: MGCL (based on ENDF/B-IV, with Am from JENDL-2); Decay constants: JDDL (based on ENSDF); Fission yield and decay constants for fission products: FPGS.

NUPEC/INS:

Date: 27 Sept 1993

Institute: Institute for Nuclear Safety, NUPEC, Japan

Participants: Susumu Mitake

Computer code: ORIGEN2

Data library: One group neutron cross-section library based on JENDL-3.¹

Reference:

1. F. Masukawa, T. Nakagawa, and S. Iijima, "Spectrum-Averaged One-Group Cross Sections of Actinides Based on JENDL-3," J. Nucl. Sci. Technol. 27 (6), 572-576 (June 1990).

ORNL-Assm:

Date: 13 Oct 1993

Institute: Oak Ridge National Laboratory, USA

Participants: O. W. Hermann

Computer code: SAS2H/ORIGEN-S sequence of SCALE-4.2 code system using SAS2H assembly model. Input based on experimental data instead of OECD problem specs.

Data library: 27-group burnup library (ENDF/B-IV actinides and ENDF/B-V fission products); ENDF/B-V fission yields, ENDF/B-VI decay data.

Notes: These results were obtained from calculations performed in an effort to validate the SCALE SAS2 sequence against experimental measurements. Calculations were made using a model which more closely resembled the physical configuration of the fuel samples during irradiation than that assumed in the benchmark calculation.

ORNL-27g:

Date: 6 June 1993

Institute: Oak Ridge National Laboratory, USA

Participants: Stephen M. Bowman

Computer code: SAS2H/ORIGEN-S sequence of SCALE-4.2 code system using infinite pin-cell model. Input based on OECD Part I-B problem specs.

Data library: 27-group burnup library (ENDF/B-IV actinides and ENDF/B-V fission products); ENDF/B-V fission yields, ENDF/B-VI decay data.

ORNL-44g:

Date: 6 June 1993

Institute: Oak Ridge National Laboratory, USA

Participants: Stephen M. Bowman

Computer code: SAS2H/ORIGEN-S sequence of SCALE-4.2 code system using infinite pin-cell model. Input based on OECD Part I-B problem specs.

Data library: 44-group ENDF/B-V cross sections with ENDF/B-VI ^{154}Eu and ^{155}Eu ; ENDF/B-V fission yields, ENDF/B-VI decay data.

PNC:

Date: 16 April 1993

Institute: PNC Tokai Works, Japan

Participants: Ichiro Nojiri

Computer code: SAS2H/ORIGEN-S sequence of SCALE-4.

Data library: SCALE4 27GROUPNDF4 (ENDF/B-IV, ENDF/B-V); ENDF/B-IV fission product data base; ORNL master photon data base.

PSI:

Date: 7 Jan 1994*

Institute: Paul Scherrer Institute, Switzerland

Participants: Peter Grimm and Jean-Marie Paratte

Computer code: ETOBOX and BOXER codes of the ELCOS LWR neutronics package (developed at PSI).

Data library: The BOXLIB cross-section library for BOXER used in the present calculations contains cross sections for 34 actinide nuclides (from ^{232}Th through ^{248}Cm), 55 fission products considered explicitly, and two pseudo-fission products. The 55 fission products were chosen based on their contribution to the total fission product neutron absorption in LWR configurations; in addition, six gadolinium isotopes are included for burnable poison calculations. For some fission products that contribute little to the absorption, the resonance cross sections are given for infinite dilution only.

The source of cross-section data for all nuclides is JEF-1, except for ^{155}Gd , whose cross sections are taken from JENDL-2. The fission product yields are taken from JEF-2 for thermal fission and summed over the isobaric chains. The decay data for the fission products originate from the compilation in ref. 1. For the actinides, half-lives from ref. 2 are used.

References:

1. M. E. Meek and B. F. Rider, *Compilation of Fission Product Yields*, NEDO-12154, 74NED6, 1974.
2. W. Seelmann-Eggebert et al., *Karlsruhe Chart of the Nuclides, 5th Edition*, Kernforschungszentrum Karlsruhe, 1981.

*Revised results dated November 15, 1995, are provided in Appendix B.

Risø:

Date: 23 Dec 1993

Institute: Risø National Laboratory, Denmark

Participants: Frank Højerup

Computer code: CCCMO

Data library: Neutron cross sections: UKNDL (mostly); Fission yields and decay data: NEDO-12154-1 (Meek and Rider); Actinides: own compilation from various sources.

Tohoku:

Date: 7 Mar 1994

Institute: Tohoku University, Japan

Participants: Kenya Suyama, Tomohiko Iwasaki, Naohiro Hirakawa

Computer code: SWAT

Data library: SWAT Library (ref. 1) - based on JENDL-3, with fission products from ORIGEN-2 (82)

Reference:

1. K. Suyama, T. Iwasaki, and N. Hirakawa, "Analysis of Post-Irradiation Experiments in PWR Using New Nuclear Data Libraries," *J. Nucl. Sci. Technol.* **31(6)**, 596-608 (1994).

Toshiba-Leakage:

Date: 22 Feb 1993

Institute: Toshiba Corporation, Japan

Participants: Munenari Yamamoto

Computer code: TGBLA,¹⁻⁴ with leakage control option turned on.

Data library: Energy-group structure: GAM-type 68 groups for fast and epithermal range, THERMOS-type 30 groups for thermal range

Data source: ²³⁵U, ²³⁸U, ²³⁹Pu, ²⁴⁰Pu - ENDF/B-V
²⁴¹Pu, ²⁴²Pu - ENDF/B-IV

All other actinides - JENDL-3

Fission products - mostly ENDF/B-IV

Fission product chain: 45 explicit fission products plus 1 lumped pseudo-fission-product model.⁵ Note: ⁹⁵Mo is not treated as an explicit fission product in this fission-product model, while it has been taken into account as one of the major contributors to the pseudo-fission-product poisoning as described in ref. 5.

Fission product yield data: based on Rider and Meek compilation.⁶

Notes: The fact is that neutron balance condition (k_{eff}) is always just critical throughout the irradiation of fuel in an operating reactor. An ordinary pin-cell calculation, however, evaluates a so-called k_{∞} , of which neutron balance differs from the actual one in an operating reactor. The flux spectrum, therefore, is somewhat different between the two. This gap in flux spectrum more or less exerts influence on fuel burnup property. In the TGBLA code, several approximate treatments are available as an option to simulate the actual situation in a burnup calculation. In the present benchmark calculations, we made, in parallel, two sets of burnup calculations different in the option (i.e., "leakage" and "poison" control option). In the case of leakage control, $D_g B^2$ pseudo-absorption cross sections are adjusted by scaling B^2 (buckling) so as k_{eff} being unity, resulting in that three broad-group fluxes somewhat differ from those of an ordinary pin-cell calculation with zero leakage. In the case of poison control, on the other hand, $1/v_g$ [v_g = gth broad-group average velocity] is used in place of D_g .

References:

1. M. Yamamoto, H. Mizuta, K. Makino, R. T. Chiang, and S. P. Congdon, "Validation of the TGBLA BWR Bundle Design Methods," *Trans. Am. Nucl. Soc.* **43**, 698 (1982).
2. "Development and Validation of TGBLA Lattice Physics Methods," *Proc. Top. Mtg. on Reactor Physics and Shielding*, Chicago (1984).
3. "Recent Developments in TGBLA Lattice Physics Code," *Proc. Inter. Top. Mtg. on Advances in Reactor Physics, Mathematics, and Computation*, Paris (1987).
4. "New Physics Models Recently Incorporated in TGBLA," *Proc. Inter. Top. Mtg. on Advances in Mathematics, Computations, and Reactor Physics*, Pittsburgh (1991).
5. S. Iijima et al., *J. Nucl. Sci. Technol.* (1982).
6. B. F. Rider et al., NEDO-12154-2 (GE) (1977).

Toshiba-Poison:

Date: 22 Feb 1993

Institute: Toshiba Corporation, Japan

Participants: Munenari Yamamoto

Computer code: TGBLA with poison control option turned on.

Data library: see Data library description in "Toshiba-Leakage" above.

Notes: see Notes description in "Toshiba-Leakage" above.

4. RESULTS AND DISCUSSION

The calculated isotopic concentrations for all three benchmark cases are listed in Tables 8 through 14. Tables 8 through 10 list the results for actinides for cases A, B, and C, respectively; similarly, Tables 11 through 13 list the results for fission-product concentrations for these cases. Concentrations in Tables 8 through 13 are in units of mg per g UO₂. Table 14 provides the results for nuclides ²³⁷Np, ²⁴¹Am, ²⁴³Am, ⁹⁹Tc, and ¹³⁵Cs for all cases in units of mCi per g UO₂ (the isotopic abundances of these nuclides were specified in terms of activity in the measurements reported in ref. 1).

All tables provide the measured concentration for each nuclide where available. In addition, the tables include the ORNL-Assm concentrations, which were calculated based on the actual fuel configuration, rather than the somewhat simplified benchmark specifications. For each isotope, the average and standard deviation of the **calculated** concentrations are included. The standard deviation characterizes the level of agreement between the benchmark calculations for each isotope. Although it is possible to compare the average for all calculations with the measured concentration for each nuclide that has been chemically assayed, such a comparison may be misleading. Even though such differences may result from inadequacies in cross-section data, the differences may also result from differences between the benchmark depletion model and the actual configuration of the sample pin during reactor operation. Measurements were made for a specific fuel pellet located within a specific pin in an assembly; depletion codes and methods are generally tailored toward assembly-averaged behaviors. ORNL-Assm calculations, shown in the second row of each table, may illustrate differences between benchmark and actual conditions. Unlike the benchmark calculations, ORNL-Assm calculations were based on actual pin-lattice conditions for cross-section processing calculations; however, like the benchmark calculations, depletion calculations were performed using a pin-cell model created based on assembly-wide properties.

Figures 1 through 33 (shown at the end of this section) illustrate the relative agreement between results for each isotope studied in each sample. Results are plotted in column chart format, showing the percentage difference between each participant's calculated concentration and the average of all calculated concentrations for each of the three burnup cases. The measured concentrations are shown in the first set of columns (for cases A, B, and C, respectively) for all nuclides for which they are available. The second set represents the results of the ORNL-Assm calculations. The results for each of the benchmark calculations are shown in the remaining sets of columns for each participant.

Table 15 provides a summary of the standard deviation of the calculated isotopic concentration for each isotope considered in this benchmark. The standard deviation is expressed in terms of its percentage of the average calculated value for each isotope and illustrates the degree of consistency between the results provided by the various participants. A small standard deviation for a given isotope and burnup indicates consistency between the various codes and data applied in these analyses; conversely, a large deviation indicates poor agreement in the calculation of the inventory of a given nuclide. The point at which agreement is considered to change from "good" to "poor" is difficult to define; however, for the purposes of this study it is assumed that agreement within a 10% standard deviation is "good" and that isotopic concentration calculations

Table 8. Results for case A (27.35 GWd/MTU burnup) actinides (mg/g UO₂)

Nuclide	²³⁴ U	²³⁵ U	²³⁶ U	²³⁸ U	²³⁸ Pu	²³⁹ Pu	²⁴⁰ Pu	²⁴¹ Pu	²⁴² Pu	²⁴¹ Am	²⁴³ Am	²³⁷ Np
Measurement	1.60E-1	8.47E+0	3.14E+0	8.42E+2	1.01E-1	4.26E+0	1.71E+0	6.81E-1	2.88E-1	2.50E-1	4.62E-2	2.68E-1
ORNL-Assm	1.61E-1	8.01E+0	3.23E+0	8.37E+2	9.78E-2	4.28E+0	1.61E+0	7.09E-1	2.76E-1	2.370E-1	3.88E-2	3.15E-1
AEA	1.56E-1	8.22E+0	3.13E+0	8.37E+2	6.52E-2	4.20E+0	1.67E+0	6.77E-1	2.69E-1			2.61E-1
AECL-ORIGEN	1.75E-1	8.04E+0	3.30E+0	8.37E+2	8.25E-2	4.19E+0	1.69E+0	6.73E-1	2.95E-1			
AECL-WIMS	1.72E-1	8.18E+0	3.26E+0	8.37E+2	5.72E-2	4.21E+0	1.69E+0	6.52E-1	2.78E-1			
Belgonucleaire	1.57E-1	8.30E+0	3.12E+0	8.37E+2	6.26E-2	4.18E+0	1.71E+0	6.55E-1	2.55E-1	2.29E-1	3.62E-2	2.54E-1
BNFL	1.57E-1	8.66E+0	3.12E+0	8.37E+2	9.34E-2	4.69E+0	1.79E+0	7.33E-1	2.75E-1	2.59E-1	4.10E-2	2.52E-1
CEA	1.53E-1	8.18E+0	3.17E+0	8.37E+2	1.04E-1	4.19E+0	1.67E+0	6.71E-1	3.04E-1	2.40E-1	4.40E-2	3.06E-1
CSN	1.56E-1	8.10E+0	3.23E+0	8.41E+2	9.38E-2	4.04E+0	1.68E+0	6.38E-1	2.62E-1	2.26E-1	3.82E-2	2.73E-1
ECN-New Lib	1.61E-1	8.00E+0	3.13E+0	8.38E+2	7.80E-2	3.66E+0	1.86E+0	6.72E-1	2.80E-1			
ECN-Old Lib	1.33E-1	8.08E+0	3.54E+0	8.37E+2	9.78E-2	4.22E+0	1.69E+0	5.31E-1	2.00E-1			
GRS	1.50E-1	8.09E+0	3.15E+0	8.37E+2	9.31E-2	4.21E+0	1.80E+0	6.89E-1	3.19E-1			
JAERI	1.59E-1	8.35E+0	3.17E+0	8.37E+2	9.69E-2	4.39E+0	1.65E+0	6.83E-1	2.68E-1	2.43E-1	3.48E-2	3.39E-1
NUPEC/INS	1.63E-1	8.42E+0	3.19E+0	8.37E+2	9.41E-2	4.32E+0	1.77E+0	6.98E-1	2.80E-1			
ORNL-27g	1.61E-1	8.11E+0	3.22E+0	8.36E+2	9.87E-2	4.40E+0	1.62E+0	7.27E-1	2.78E-1	2.56E-1	4.67E-2	3.18E-1
ORNL-44g	1.57E-1	8.18E+0	3.21E+0	8.37E+2	9.28E-2	4.17E+0	1.71E+0	6.91E-1	3.12E-1	2.46E-1	5.16E-2	2.83E-1
PNC	1.63E-1	7.45E+0	3.26E+0	8.37E+2	8.43E-2	3.76E+0	1.57E+0	6.36E-1	2.78E-1			
PSI*	1.56E-1	8.38E+0	3.17E+0	8.37E+2	9.77E-2	4.38E+0	1.71E+0	6.59E-1	2.65E-1	2.34E-1	4.07E-2	2.88E-1
Riso	1.61E-1	8.35E+0	3.31E+0	8.36E+2	1.08E-1	4.25E+0	1.73E+0	6.20E-1	2.93E-1	2.43E-1	4.01E-2	2.98E-1
Tohoku	1.66E-1	8.15E+0	3.31E+0	8.37E+2	8.84E-2	4.40E+0	1.75E+0	6.54E-1	2.64E-1	2.33E-1	3.72E-2	2.93E-1
Toshiba-Leakage	1.58E-1	8.13E+0	3.20E+0	8.37E+2	1.00E-1	4.20E+0	1.70E+0	6.77E-1	2.67E-1	2.40E-1	3.83E-2	2.89E-1
Toshiba-Poison	1.56E-1	8.56E+0	3.18E+0	8.36E+2	1.08E-1	4.42E+0	1.76E+0	7.12E-1	2.74E-1	2.55E-1	3.99E-2	3.01E-1
Average	1.59E-1	8.19E+0	3.22E+0	8.37E+2	9.02E-2	4.23E+0	1.71E+0	6.69E-1	2.76E-1	2.42E-1	4.10E-2	2.91E-1
Std. Dev.	5.19%	2.98%	2.91%	0.12%	15.68%	5.16%	3.95%	6.45%	8.69%	4.22%	11.31%	8.61%

*Revised results dated November 15, 1995, are provided in Appendix B.

Table 9. Results for case B (37.12-GWd/MTU burnup) actinides (mg/g UO₂)

Nuclide	²³⁴ U	²³⁵ U	²³⁶ U	²³⁸ U	²³⁸ Pu	²³⁹ Pu	²⁴⁰ Pu	²⁴¹ Pu	²⁴² Pu	²⁴¹ Am	²⁴³ Am	²³⁷ Np
Measurement	1.400E-1	5.170E+0	3.530E+0	8.327E+2	1.893E-1	4.357E+0	2.239E+0	9.028E-1	5.761E-1	3.221E-1	1.271E-1	3.560E-1
ORNL-Assm	1.395E-1	4.731E+0	3.630E+0	8.298E+2	1.881E-1	4.424E+0	2.069E+0	9.345E-1	5.551E-1	3.041E-1	1.112E-1	4.574E-1
AEA	1.298E-1	4.868E+0	3.553E+0	8.303E+2	1.271E-1	4.298E+0	2.164E+0	8.901E-1	5.442E-1			3.752E-1
AECL-ORIGEN	1.570E-1	4.710E+0	3.720E+0	8.300E+2	1.600E-1	4.280E+0	2.170E+0	8.820E-1	5.880E-1			
AECL-WIMS	1.495E-1	4.831E+0	3.702E+0	8.304E+2	1.144E-1	4.312E+0	2.183E+0	8.603E-1	5.574E-1			
Belgonucleaire	1.312E-1	4.989E+0	3.547E+0	8.307E+2	1.212E-1	4.291E+0	2.213E+0	8.692E-1	5.153E-1	2.969E-1	1.028E-1	3.647E-1
BNFL	1.361E-1	5.418E+0	3.547E+0	8.292E+2	1.806E-1	4.877E+0	2.327E+0	9.846E-1	5.469E-1	3.418E-1	1.140E-1	3.619E-1
CEA	1.270E-1	4.806E+0	3.585E+0	8.301E+2	1.970E-1	4.252E+0	2.173E+0	8.850E-1	6.210E-1	3.080E-1	1.230E-1	4.350E-1
CSN	1.304E-1	4.660E+0	3.662E+0	8.360E+2	1.794E-1	4.051E+0	2.177E+0	8.312E-1	5.386E-1	2.880E-1	1.108E-1	3.959E-1
ECN-New Lib	1.390E-1	4.680E+0	3.530E+0	8.310E+2	1.580E-1	3.710E+0	2.170E+0	9.210E-1	6.100E-1			
ECN-Old Lib	1.080E-1	4.830E+0	3.930E+0	8.300E+2	1.960E-1	4.310E+0	2.040E+0	7.510E-1	4.200E-1			
GRS	1.270E-1	4.872E+0	3.526E+0	8.295E+2	1.792E-1	4.394E+0	2.347E+0	9.162E-1	6.347E-1	3.194E-1	9.637E-2	4.919E-1
JAERI	1.379E-1	5.510E+0	3.568E+0	8.301E+2	1.881E-1	4.567E+0	2.146E+0	9.134E-1	5.451E-1			
NUPEC/INS	1.429E-1	5.066E+0	3.576E+0	8.297E+2	1.844E-1	4.475E+0	2.249E+0	9.519E-1	5.482E-1			
ORNL-27g	1.399E-1	4.827E+0	3.617E+0	8.295E+2	1.894E-1	4.533E+0	2.079E+0	9.554E-1	5.564E-1	3.298E-1	1.279E-1	4.609E-1
ORNL-44g	1.362E-1	4.884E+0	3.620E+0	8.297E+2	1.785E-1	4.279E+0	2.172E+0	9.014E-1	6.213E-1	3.139E-1	1.391E-1	4.09E-1
PNC	1.403E-1	4.022E+0	3.675E+0	8.317E+2	1.618E-1	3.735E+0	1.996E+0	8.136E-1	5.761E-1			
PSI*	1.344E-1	5.032E+0	3.588E+0	8.299E+2	1.888E-1	4.511E+0	2.235E+0	8.807E-1	5.404E-1	3.060E-1	1.126E-1	4.194E-1
Riso	1.394E-1	4.944E+0	3.802E+0	8.297E+2	2.069E-1	4.301E+0	2.249E+0	8.247E-1	6.007E-1	3.153E-1	1.138E-1	4.208E-1
Tohoku	1.452E-1	4.855E+0	3.713E+0	8.303E+2	1.741E-1	4.557E+0	2.325E+0	8.681E-1	5.271E-1	3.027E-1	1.045E-1	4.346E-1
Toshiba-Leakage	1.363E-1	4.800E+0	3.597E+0	8.302E+2	1.942E-1	4.277E+0	2.189E+0	8.895E-1	5.431E-1	3.088E-1	1.049E-1	4.157E-1
Toshiba-Poison	1.363E-1	5.128E+0	3.613E+0	8.299E+2	1.993E-1	4.154E+0	2.300E+0	8.809E-1	5.552E-1	3.094E-1	1.032E-1	4.129E-1
Average	1.363E-1	4.879E+0	3.633E+0	8.304E+2	1.746E-1	4.314E+0	2.189E+0	8.859E-1	5.593E-1	3.119E-1	1.137E-1	4.183E-1
Std. Dev.	7.08%	6.01%	2.72%	0.17%	14.80%	6.08%	4.27%	5.97%	8.28%	4.35%	10.41%	8.86%

*Revised results dated November 15, 1995, are provided in Appendix B.

Table 10. Results for case C (44.34-GWd/MTU burnup) actinides (mg/g UO₂)

Nuclide	²³⁴ U	²³⁵ U	²³⁶ U	²³⁸ U	²³⁸ Pu	²³⁹ Pu	²⁴⁰ Pu	²⁴¹ Pu	²⁴² Pu	²⁴¹ Am	²⁴³ Am	²³⁷ Np
Measurement												
ORNL-Assm	1.200E-1	3.540E+0	3.690E+0	8.249E+2	2.688E-1	4.357E+0	2.543E+0	1.020E+0	8.401E-1	3.611E-1	2.154E-1	4.680E-1
AEA	1.256E-1	3.208E+0	3.752E+0	8.236E+2	2.692E-1	4.570E+0	2.328E+0	1.067E+0	7.857E-1	3.309E-1	1.924E-1	5.585E-1
AECL-ORIGEN	1.117E-1	3.171E+0	3.702E+0	8.245E+2	1.815E-1	4.288E+0	2.426E+0	9.892E-1	7.764E-1			4.497E-1
AECL-WIMS	1.440E-1	3.060E+0	3.870E+0	8.240E+2	2.260E-1	4.270E+0	2.420E+0	9.780E-1	8.300E-1			
Belgonucleaire	1.334E-1	3.133E+0	3.857E+0	8.246E+2	1.656E-1	4.307E+0	2.442E+0	9.600E-1	7.916E-1			
BNFL	1.135E-1	3.304E+0	3.701E+0	8.252E+2	1.728E-1	4.289E+0	2.484E+0	9.744E-1	7.367E-1	3.262E-1	1.774E-1	4.378E-1
CEA	1.224E-1	3.716E+0	3.708E+0	8.234E+2	2.549E-1	4.902E+0	2.626E+0	1.111E+0	7.747E-1	3.785E-1	1.937E-1	4.327E-1
CSN	1.090E-1	3.101E+0	3.723E+0	8.243E+2	2.750E-1	4.217E+0	2.437E+0	9.850E-1	8.990E-1	3.360E-1	2.090E-1	5.160E-1
ECN-New Lib	1.122E-1	2.934E+0	3.807E+0	8.316E+2	2.493E-1	3.984E+0	2.431E+0	9.157E-1	7.783E-1	3.102E-1	1.944E-1	4.769E-1
ECN-Old Lib	1.240E-1	3.040E+0	3.650E+0	8.250E+2	2.270E-1	3.710E+0	2.280E+0	1.030E+0	8.900E-1			
GRS	9.030E-2	3.200E+0	4.030E+0	8.240E+2	2.810E-1	4.320E+0	2.180E+0	8.560E-1	5.960E-1			
JAERI	1.125E-1	3.271E+0	3.641E+0	8.235E+2	2.513E-1	4.454E+0	2.640E+0	1.037E+0	9.103E-1			
NUPEC/INS	1.240E-1	3.381E+0	3.695E+0	8.243E+2	2.659E-1	4.604E+0	2.419E+0	1.031E+0	7.874E-1	3.540E-1	1.634E-1	5.934E-1
ORNL-27g	1.296E-1	3.380E+0	3.686E+0	8.238E+2	2.640E-1	4.500E+0	2.442E+0	1.100E+0	7.774E-1			
ORNL-44g	1.262E-1	3.177E+0	3.746E+0	8.237E+2	2.653E-1	4.541E+0	2.320E+0	1.063E+0	7.913E-1	3.597E-1	2.150E-1	5.552E-1
PNC	1.223E-1	3.216E+0	3.755E+0	8.239E+2	2.500E-1	4.283E+0	2.418E+0	9.989E-1	8.832E-1	3.411E-1	2.316E-1	4.914E-1
PSI*	1.249E-1	2.389E+0	3.796E+0	8.256E+2	2.253E-1	3.659E+0	2.208E+0	8.816E-1	8.347E-1			
Riso	1.205E-1	3.332E+0	3.730E+0	8.240E+2	2.657E-1	4.526E+0	2.208E+0	8.816E-1	7.808E-1	3.388E-1	1.902E-1	5.078E-1
Tohoku	1.288E-1	3.625E+0	3.959E+0	8.255E+2	2.664E-1	4.267E+0	2.326E+0	9.944E-1	7.808E-1	3.367E-1	1.724E-1	4.812E-1
Toshiba-Leakage	1.311E-1	3.167E+0	3.842E+0	8.243E+2	2.509E-1	4.586E+0	2.450E+0	9.004E-1	7.943E-1	3.367E-1	1.724E-1	4.812E-1
Toshiba-Poison	1.223E-1	3.120E+0	3.726E+0	8.244E+2	2.722E-1	4.257E+0	2.661E+0	9.855E-1	7.604E-1	3.373E-1	1.831E-1	5.314E-1
Average	1.233E-1	3.293E+0	3.781E+0	8.246E+2	2.704E-1	3.826E+0	2.448E+0	9.888E-1	7.820E-1	3.364E-1	1.767E-1	4.973E-1
Std. Dev.	1.215E-1	3.201E+0	3.769E+0	8.247E+2	2.452E-1	4.303E+0	2.437E+0	9.892E-1	7.985E-1	3.403E-1	1.917E-1	5.005E-1
	8.99%	8.12%	2.60%	0.21%	13.86%	7.12%	5.27%	6.86%	8.39%	5.29%	10.40%	9.42%

*Revised results dated November 15, 1995, are provided in Appendix B.

Table 11. Results for case A (27.35-GWd/MTU burnup) fission products (mg/g UO₂)

Nuclide	⁹⁹ Mo	⁹⁹ Tc	¹⁰⁰ Ru	¹⁰⁰ Rh	¹⁰⁰ Ag	¹³⁷ Cs	¹³⁷ Cs	¹⁴⁷ Nd	¹⁴⁷ Nd	¹⁴⁸ Nd	¹⁴⁸ Nd	¹⁴⁹ Sm	¹⁴⁹ Sm	¹⁵⁰ Sm	¹⁵⁰ Sm	¹⁵¹ Sm	¹⁵² Sm	¹⁵² Sm	¹⁵⁴ Eu	¹⁵⁴ Eu	¹⁵⁴ Gd	
Measurement																						
ORNL-Assm	5.711E-1	5.874E-1	5.657E-1	3.503E-1	6.060E-2	8.500E-1	3.600E-1	6.130E-1	5.100E-1	5.131E-1	6.208E-1	1.859E-1	2.070E-1	2.171E-3	2.001E-1	1.013E-2	7.900E-2	8.700E-2	7.443E-2	7.900E-2	4.524E-3	
AEA	5.793E-1	6.904E-1	5.612E-1	3.304E-1	5.303E-2	8.602E-1	3.959E-1	6.319E-1	5.029E-1	5.080E-1	6.319E-1	1.728E-1	2.001E-1	2.383E-3	2.010E-1	1.413E-2	9.710E-2	9.710E-2	6.845E-2	6.845E-2	1.507E-3	
AECL-ORIGEN	5.720E-1		5.630E-1	3.520E-1	5.910E-2	8.650E-1	3.520E-1	6.140E-1	5.080E-1	5.080E-1	6.140E-1	1.860E-1	2.010E-1	1.910E-3	1.933E-1		9.700E-2	9.700E-2	6.860E-2	6.860E-2	4.310E-3	
AECL-WIMS	5.590E-1		5.548E-1	3.492E-1	5.933E-2	8.489E-1	3.492E-1	6.049E-1	5.041E-1	5.041E-1	6.049E-1	1.854E-1	1.933E-1	1.899E-3	1.975E-1		9.641E-2	9.641E-2	7.765E-2	7.765E-2	3.631E-3	
Belgonucleaire	5.741E-1		5.550E-1	3.270E-1	5.199E-2	8.368E-1	3.270E-1	6.270E-1	4.984E-1	4.984E-1	6.270E-1	1.720E-1	1.975E-1	2.363E-3	1.975E-1		9.605E-2	9.605E-2	6.730E-2	6.730E-2		
BNFL	5.667E-1		5.629E-1	3.426E-1	4.238E-2	8.640E-1	3.426E-1	6.395E-1	5.063E-1	5.063E-1	6.395E-1	1.758E-1	1.969E-1	2.811E-3	1.969E-1		7.947E-2	7.947E-2	8.921E-2	8.921E-2	5.424E-3	
CEA	5.590E-1		5.680E-1	3.520E-1	5.400E-2	8.510E-1	3.520E-1	6.400E-1	5.060E-1	5.060E-1	6.400E-1	1.860E-1	1.930E-1	2.000E-3	1.930E-1		8.800E-2	8.800E-2	8.400E-2	8.400E-2	2.000E-3	
CSN				3.030E-1	4.161E-2	8.312E-1	3.772E-1	6.162E-1	4.986E-1	4.986E-1	6.162E-1	1.847E-1	1.930E-1	1.865E-3	1.930E-1		8.831E-2	8.831E-2	7.841E-2	7.841E-2	5.427E-3	
ECN-New Lib																						
ECN-Old Lib																						
GRS	5.679E-1		5.750E-1	3.570E-1	5.364E-2	8.573E-1	3.570E-1	6.196E-1	5.103E-1	5.103E-1	6.196E-1	2.146E-1	2.146E-1	2.079E-3	2.146E-1		8.298E-2	8.298E-2	8.413E-2	8.413E-2	4.024E-3	
JABRI		5.648E-1		3.625E-1		8.475E-1		6.231E-1	5.151E-1	5.151E-1	6.231E-1	1.982E-1	1.982E-1	2.079E-3	1.982E-1		9.364E-2	9.364E-2	7.563E-2	7.563E-2		
NUPEC/INS	5.591E-1	5.723E-1	5.640E-1	3.476E-1	5.385E-2	8.420E-1	3.476E-1	6.040E-1	5.036E-1	5.036E-1	6.040E-1	1.564E-1	1.725E-1	1.626E-3	1.725E-1		9.608E-2	9.608E-2	7.441E-2	7.441E-2	4.389E-3	
ORNL-27g	5.704E-1	5.873E-1	5.658E-1	3.520E-1	6.095E-2	8.602E-1	3.520E-1	6.225E-1	5.127E-1	5.127E-1	6.225E-1	1.860E-1	2.032E-1	2.210E-3	2.032E-1		9.714E-2	9.714E-2	7.474E-2	7.474E-2	4.554E-3	
ORNL-44g	5.694E-1	5.893E-1	5.648E-1	3.591E-1	6.164E-2	8.636E-1	3.591E-1	6.187E-1	5.101E-1	5.101E-1	6.187E-1	1.882E-1	2.019E-1	2.030E-3	2.019E-1		9.960E-2	9.960E-2	8.015E-2	8.015E-2	1.864E-3	
PNC																						
PSI*	5.642E-1	5.909E-1	5.750E-1	3.594E-1	5.138E-2	8.363E-1	3.728E-1	6.174E-1	5.114E-1	5.114E-1	6.174E-1	1.932E-1	2.028E-1	1.968E-3	2.028E-1		8.439E-2	8.439E-2	8.517E-2	8.517E-2	2.431E-3	
Riso	5.593E-1	5.943E-1	5.559E-1	3.699E-1	4.753E-2	8.820E-1	3.954E-1	6.792E-1	5.119E-1	5.119E-1	6.792E-1	1.862E-1	1.913E-1	2.196E-3	1.913E-1		1.073E-1	1.073E-1	7.498E-2	7.498E-2	5.762E-3	
Tohoku	5.601E-1	5.804E-1	5.630E-1	3.463E-1	5.261E-2	8.515E-1	3.463E-1	6.118E-1	5.046E-1	5.046E-1	6.118E-1	1.570E-1	1.713E-1	1.628E-3	1.713E-1		9.582E-2	9.582E-2	7.381E-2	7.381E-2	4.323E-3	
Toshiba-Leakage	6.064E-1	6.064E-1	5.621E-1	3.605E-1	5.584E-2	8.540E-1	3.754E-1	6.100E-1	5.021E-1	5.021E-1	6.100E-1	1.871E-1	1.907E-1	1.860E-3	1.907E-1		9.694E-2	9.694E-2	7.303E-2	7.303E-2	3.896E-3	
Toshiba-Poison	6.060E-1	6.060E-1	5.630E-1	3.657E-1	5.774E-2	8.530E-1	3.924E-1	6.167E-1	5.003E-1	5.003E-1	6.167E-1	1.861E-1	1.913E-1	1.913E-3	1.913E-1		9.744E-2	9.744E-2	7.387E-2	7.387E-2	3.997E-3	
Average	5.666E-1	5.985E-1	5.637E-1	3.492E-1	5.396E-2	8.415E-1	3.821E-1	6.232E-1	5.066E-1	5.066E-1	6.232E-1	1.806E-1	1.953E-1	2.054E-3	1.953E-1		9.394E-2	9.394E-2	7.655E-2	7.655E-2	3.879E-3	
Std. Dev.	1.17%	5.17%	1.03%	4.57%	11.03%	4.87%	2.94%	2.76%	1.02%	1.02%	2.76%	6.03%	5.30%	14.14%	5.30%	22.41%	7.20%	7.20%	7.90%	7.90%	33.45%	

*Revised results dated November 15, 1995, are provided in Appendix B.

Table 12. Results for case B (37.12-GWd/MTU burnup) fission products (mg/g UO₂)

Nuclide	⁹⁵ Mo	⁹⁹ Tc	¹⁰¹ Ru	¹⁰³ Rh	¹⁰⁶ Ag	¹³⁷ Cs	¹³⁷ Cs	¹⁴³ Nd	¹⁴³ Nd	¹⁴⁷ Sm	¹⁴⁹ Sm	¹⁵⁰ Sm	¹⁵¹ Sm	¹⁵² Sm	¹⁵³ Eu	¹⁵⁷ Gd
Measurement																
ORNL-Asm	7.383E-1	7.620E-1	7.635E-1	4.442E-1	9.197E-2	1.090E+0	4.000E-1	7.160E-1	6.530E-1	2.079E-1	3.000E-3	2.710E-1	1.149E-2	1.040E-1	1.090E-1	7.852E-3
AEA	7.545E-1	7.995E-1	7.627E-1	4.248E-1	8.217E-2	1.110E+0	4.317E-1	7.237E-1	6.548E-1	1.907E-1	2.375E-3	2.830E-1	1.571E-2	1.258E-1	1.095E-1	2.538E-3
AECL-ORIGEN	7.400E-1	7.590E-1	7.590E-1	4.460E-1	8.900E-2	1.096E+0	7.100E-1	6.432E-1	6.402E-1	2.070E-1	2.546E-3	2.831E-1	1.230E-1	1.261E-1	1.045E-1	7.450E-3
AECL-WIMS	7.214E-1	7.485E-1	7.485E-1	4.436E-1	9.057E-2	1.110E+0	7.013E-1	6.426E-1	6.406E-1	2.077E-1	2.081E-3	2.800E-1	1.230E-1	1.230E-1	9.960E-2	7.450E-3
Belgonucleaire	7.444E-1	7.883E-1	7.502E-1	4.190E-1	8.006E-2	1.081E+0	7.445E-1	6.351E-1	6.351E-1	1.899E-1	2.518E-3	2.777E-1	1.557E-2	1.243E-1	1.186E-1	6.360E-3
BNFL	7.355E-1	8.372E-1	7.619E-1	4.280E-1	6.504E-2	1.113E+0	7.540E-1	6.430E-1	6.430E-1	1.924E-1	3.092E-3	2.810E-1	7.990E-3	9.761E-2	1.309E-1	9.168E-3
CEA	7.220E-1	7.500E-1	7.670E-1	4.450E-1	8.200E-2	1.099E+0	7.400E-1	6.450E-1	6.450E-1	2.090E-1	2.000E-3	2.710E-1	9.000E-3	1.090E-1	1.270E-1	4.000E-3
CSN		3.785E-1			6.401E-2	1.071E+0	3.967E-1	7.146E-1	6.326E-1	2.077E-1	1.989E-3	2.706E-1	8.997E-3	1.107E-1	1.152E-1	8.940E-3
ECN-New Lib																
ECN-Old Lib																
GRS	7.309E-1		7.743E-1	4.513E-1	8.122E-2	1.101E+0		7.232E-1	6.476E-1					1.018E-1	1.247E-1	7.022E-3
JAERI		7.327E-1		4.686E-1		1.093E+0		7.312E-1	6.600E-1					1.202E-1	1.120E-1	
NUPEC/TNS	7.250E-1	7.437E-1	7.634E-1	4.337E-1	8.120E-2	1.081E+0	7.046E-1	6.428E-1	6.428E-1	1.659E-1	2.267E-3		1.161E-2	1.197E-1	1.085E-1	7.596E-3
ORNL-27g	7.377E-1	7.620E-1	7.635E-1	4.463E-1	9.241E-2	1.111E+0	7.275E-1	6.547E-1	6.547E-1	2.082E-1	1.736E-3		1.052E-2	1.197E-1	1.099E-1	7.903E-3
ORNL-44g	7.364E-1	7.663E-1	7.612E-1	4.570E-1	9.369E-2	1.117E+0	7.212E-1	6.500E-1	6.500E-1	2.119E-1	2.225E-3		1.169E-2	1.256E-1	1.099E-1	3.023E-3
PNC																
PSI	7.296E-1	7.712E-1	7.787E-1	4.611E-1	8.003E-2	1.081E+0	4.072E-1	7.231E-1	6.545E-1	2.201E-1	2.163E-3		8.614E-3	1.054E-1	1.272E-1	4.054E-3
Risø	7.262E-1	7.797E-1	7.511E-1	4.771E-1	7.314E-2	8.784E-1	4.297E-1	8.254E-1	6.555E-1	2.092E-1	2.347E-3		1.237E-2	1.416E-1	1.165E-1	1.028E-2
Tohoku	7.238E-1	7.548E-1	7.598E-1	4.321E-1	7.958E-2	1.094E+0	4.070E-1	7.113E-1	6.421E-1	1.659E-1	1.738E-3		1.047E-2	1.191E-1	1.075E-1	7.466E-3
Toshiba-Leakage		7.965E-1	7.557E-1	4.599E-1	8.602E-2	1.096E+0	4.077E-1	7.050E-1	6.346E-1	2.099E-1	2.016E-3		8.997E-3	1.225E-1	1.073E-1	6.681E-3
Toshiba-Poison		7.984E-1	7.578E-1	4.688E-1	8.811E-2	1.101E+0	4.238E-1	7.142E-1	6.360E-1	2.131E-1	1.952E-3		8.839E-3	1.255E-1	1.070E-1	6.478E-3
Average	7.333E-1	7.745E-1	7.611E-1	4.436E-1	8.237E-2	1.085E+0	4.148E-1	7.292E-1	6.454E-1	2.010E-1	2.208E-3		1.092E-2	1.195E-1	1.139E-1	6.676E-3
Std. Dev.	1.30%	3.57%	1.05%	5.15%	4.90%	3.24%	3.93%	1.25%	7.95%	15.01%	7.07%		21.72%	8.19%	33.28%	

*Revised results dated November 15, 1995, are provided in Appendix B.

Table 13. Results for case C (44.34-GWd/MTU burnup) fission products (mg/g UO₂)

Nuclide	⁹⁵ Mo	⁹⁹ Tc	¹⁰¹ Ru	¹⁰³ Rh	¹⁰⁹ Ag	¹³³ Cs	¹³⁵ Cs	¹⁴³ Nd	¹⁴⁵ Nd	¹⁴⁷ Sm	¹⁴⁹ Sm	¹⁵⁰ Sm	¹⁵¹ Sm	¹⁵² Sm	¹⁵³ Eu	¹⁵⁵ Gd
Measurement																
ORNL-Assm	8.502E-1	8.773E-1	9.061E-1	5.012E-1	1.147E-1	1.240E+0	4.300E-1	7.630E-1	7.440E-1	2.139E-1	4.700E-3	3.610E-1	1.287E-2	1.210E-1	1.480E-1	1.074E-2
AEA	8.742E-1	9.299E-1	9.106E-1	4.831E-1	1.042E-1	1.273E+0	4.605E-1	7.763E-1	7.464E-1	1.951E-1	2.601E-3	3.450E-1	1.682E-2	1.443E-1	1.344E-1	3.379E-3
AECL-ORIGEN	8.550E-1		8.990E-1	5.010E-1	1.110E-1	1.280E+0		8.083E-1	7.339E-1	2.130E-1	2.200E-3	3.370E-1	1.682E-2	1.448E-1	1.305E-1	9.960E-3
AECL-WIMS	8.301E-1		8.886E-1	4.995E-1	1.137E-1	1.265E+0		7.480E-1	7.310E-1	2.148E-1	2.230E-3	3.292E-1	1.667E-2	1.409E-1	1.485E-1	8.672E-3
Belgonucleaire	8.602E-1	9.144E-1	8.925E-1	4.761E-1	1.012E-1	1.242E+0		8.010E-1	7.232E-1	1.946E-1	2.642E-3	3.363E-1	1.667E-2	1.424E-1	1.273E-1	
BNFL	8.508E-1	9.861E-1	9.063E-1	4.767E-1	8.826E-2	1.277E+0		8.086E-1	7.312E-1	1.967E-1	3.286E-3	3.439E-1	8.102E-3	1.077E-1	1.596E-1	1.207E-2
CEA	8.300E-1	8.660E-1	9.100E-1	4.990E-1	1.030E-1	1.261E+0		7.800E-1	7.350E-1	2.160E-1	2.000E-3	3.280E-1	1.000E-2	1.220E-1	1.370E-1	5.000E-3
CSN			4.208E-1		8.004E-2	1.226E+0	3.977E-1	7.505E-1	7.170E-1	2.150E-1	2.094E-3	3.267E-1	9.520E-3	1.249E-1	1.403E-1	1.150E-2
ECN-New Lib																
ECN-Old Lib																
GRS	8.406E-1		9.191E-1	5.068E-1	1.013E-1	1.258E+0		7.717E-1	7.366E-1			3.980E-1		1.145E-1	1.537E-1	9.515E-3
JAERI		8.449E-1		5.349E-1		1.254E+0		7.803E-1	7.560E-1		2.422E-3	3.370E-1	1.261E-2	1.377E-1	1.375E-1	
NUPEC/INS	8.372E-1	8.582E-1	9.087E-1	4.823E-1	1.017E-1	1.235E+0		7.494E-1	7.330E-1	1.660E-1	1.844E-3	2.751E-1	1.136E-2	1.338E-1	1.314E-1	1.019E-2
ORNL-27g	8.510E-1	8.791E-1	9.069E-1	5.021E-1	1.155E-1	1.276E+0		7.740E-1	7.474E-1	2.156E-1	2.572E-3	3.440E-1	1.268E-2	1.447E-1	1.345E-1	1.061E-2
ORNL-44g	8.492E-1	8.856E-1	9.032E-1	5.154E-1	1.175E-1	1.286E+0		7.654E-1	7.408E-1	2.203E-1	2.378E-3	3.404E-1	1.288E-2	1.480E-1	1.522E-1	3.924E-3
PNC																
PSI*	8.406E-1	8.933E-1	9.265E-1	5.231E-1	1.017E-1	1.242E+0	4.267E-1	7.703E-1	7.478E-1	2.302E-1	2.322E-3	3.578E-1	9.291E-3	1.186E-1	1.569E-1	5.597E-3
Riso	8.092E-1	8.728E-1	8.545E-1	5.262E-1	8.718E-2	9.723E-1	4.404E-1	8.839E-1	7.246E-1	2.143E-1	2.492E-3	3.096E-1	1.300E-2	1.587E-1	1.396E-1	1.318E-2
Tohoku	8.381E-1	8.749E-1	9.079E-1	4.819E-1	1.002E-1	1.259E+0	4.357E-1	7.510E-1	7.337E-1	1.655E-1	1.842E-3	2.735E-1	1.128E-2	1.334E-1	1.306E-1	1.007E-2
Toshiba-Leakage		9.269E-1	8.949E-1	5.195E-1	1.089E-1	1.253E+0	4.251E-1	7.423E-1	7.179E-1	2.173E-1	2.140E-3	3.174E-1	9.653E-3	1.384E-1	1.306E-1	8.898E-3
Toshiba-Poison		9.316E-1	8.985E-1	5.310E-1	1.112E-1	1.265E+0	4.363E-1	7.452E-1	7.227E-1	2.244E-1	1.973E-3	3.181E-1	8.944E-3	1.441E-1	1.293E-1	8.286E-3
Average	8.440E-1	8.958E-1	9.021EW-1	4.0989E-1	1.036E-1	1.244E+0	4.318E-1	7.748E-1	7.339E-1	2.070E-1	2.336E-3	3.311E-1	1.171E-2	1.355E-1	1.397E-1	8.849E-3
Std. Dev.	1.85%	4.21%	1.76%	5.40%	10.21%	5.60%	4.40%	4.51%	1.46%	9.12%	15.61%	8.50%	22.31%	9.68%	8.52%	32.97%

*Revised results dated November 15, 1995, are provided in Appendix B.

Table 14. Results for all highly active nuclides (mCi/g UO₂)

Nuclide	²³⁷ Np 27.35 GWd/MTU	²⁴¹ Am 27.35 GWd/MTU	²⁴⁰ Am 27.35 GWd/MTU	⁹⁹ Tc 27.35 GWd/MTU	¹³⁵ Cs 27.35 GWd/MTU	²³⁷ Np 37.12 GWd/MTU	²⁴¹ Am 37.12 GWd/MTU	²⁴⁰ Am 37.12 GWd/MTU	⁹⁹ Tc 37.12 GWd/MTU	¹³⁵ Cs 37.12 GWd/MTU	²³⁷ Np 44.34 GWd/MTU	²⁴¹ Am 44.34 GWd/MTU	²⁴⁰ Am 44.34 GWd/MTU	⁹⁹ Tc 44.34 GWd/MTU	¹³⁵ Cs 44.34 GWd/MTU
Measurement	1.890E-4	8.560E-1		9.590E-3	4.160E-4	2.510E-4	1.180E+0		1.230E-2	4.590E-4	3.310E-4	1.310E+0		1.350E-2	
ORNL-Assm	2.226E-4	8.583E-1		1.005E-2		3.224E-4	1.105E+0		1.303E-2		3.937E-4	1.238E+0		1.501E-2	4.950E-4
AEA															
AECL-ORIGEN	1.690E-4	8.000E-1	9.780E-3	1.000E-2		2.490E-4	1.020E+0	2.740E-2	1.300E-2		3.010E-4	1.110E+0	4.670E-2	1.510E-2	
AECL-WIMS	1.662E-4	7.754E-1	9.137E-3	9.969E-3		2.446E-4	1.000E+0	2.575E-2	1.296E-2		2.970E-4	1.094E+0	4.417E-2	1.495E-2	
Belgonucleaire	1.795E-4	7.865E-1	7.227E-3	1.024E-2		2.572E-4	1.020E+0	2.049E-2	1.337E-2		3.087E-4	1.120E+0	3.538E-2	1.551E-2	
BNFL	1.782E-4	8.921E-1	8.212E-3	1.066E-2		2.894E-4	1.331E+0	2.583E-2	1.611E-2		3.460E-4	1.474E+0	4.392E-2	1.898E-2	
CEA	2.150E-4	8.193E-1		9.911E-3		3.050E-4	1.051E+0		1.286E-2		3.620E-4	1.147E+0		1.485E-2	
CSN	1.927E-4	7.790E-1	7.632E-3			2.792E-4	9.889E-1	2.210E-2			3.363E-4	1.065E+0	3.877E-2		
ECN-New Lib	1.600E-4	7.970E-1		1.030E-2	4.280E-4	2.380E-4	1.070E+0		1.350E-2	4.630E-4	2.910E-4	1.170E+0		1.560E-2	4.830E-4
ECN-Old Lib	2.260E-4	6.050E-1	8.951E-3	1.050E-2	3.930E-4	3.340E-4	8.380E-1	2.408E-2	1.390E-2	4.250E-4	4.050E-4	9.380E-1		1.620E-2	4.430E-4
GRS	2.096E-4	8.019E-1	6.941E-3	1.003E-2		3.058E-4	1.039E+0		1.296E-2		3.695E-4	1.153E+0	4.016E-2	1.491E-2	
JAERI	2.395E-4	8.371E-1	8.823E-3	9.623E-3		3.469E-4	1.097E+0	1.922E-2	1.248E-2		4.185E-4	1.216E+0	3.258E-2	1.439E-2	
NUPEC/INS	2.083E-4	8.448E-1				3.122E-4	1.113E+0	2.464E-2			3.830E-4	1.259E+0	4.245E-2		
ORNL-27g	2.246E-4	8.808E-1		1.005E-2		3.249E-4	1.131E+0		1.304E-2		3.914E-4	1.234E+0		1.504E-2	
ORNL-44g	2.000E-4	8.438E-1		1.008E-2		2.887E-4	1.077E+0		1.311E-2		3.464E-4	1.170E+0		1.515E-2	
PNC	2.011E-4	7.485E-1	8.196E-3	1.051E-2	4.204E-4	2.918E-4	9.300E-1	2.344E-2	1.384E-2	4.446E-4	3.508E-4	9.826E-1	4.053E-2	1.618E-2	4.552E-4
PSI*	2.035E-4	8.055E-1	8.142E-3	1.018E-2	4.942E-4	2.958E-4	1.051E+0	2.248E-2	1.328E-2	5.399E-4	3.581E-4	1.164E+0	3.798E-2	1.539E-2	5.657E-4
Riso	2.109E-4	7.881E-1	7.430E-3	1.010E-2	4.584E-4	2.970E-4	1.023E+0	2.108E-2	1.325E-2	4.954E-4	3.396E-4	1.092E+0	3.195E-2	1.483E-2	5.076E-4
Tohoku	2.069E-4	8.014E-1	7.422E-3	9.840E-3	4.240E-4	3.063E-4	1.039E+0	2.082E-2	1.280E-2	4.686E-4	3.746E-4	1.158E+0	3.650E-2	1.483E-2	5.017E-4
Toshiba-Leakage	2.040E-4	8.248E-1	7.649E-3	1.030E-2	3.318E-4	2.931E-4	1.058E+0	2.096E-2	1.353E-2	3.604E-4	3.506E-4	1.153E+0	3.529E-2	1.574E-2	3.757E-4
Toshiba-Poison	2.125E-4	8.763E-1	7.970E-3	1.029E-2	3.468E-4	2.911E-4	1.060E+0	2.062E-2	1.356E-2	3.746E-4	3.363E-4	1.089E+0	3.391E-2	1.582E-2	3.856E-4
Average	2.015E-4	8.083E-1	8.108E-3	1.015E-2	4.121E-4	2.936E-4	1.052E+0	2.278E-2	1.337E-2	4.464E-4	3.530E-4	1.151E+0	43.859E-2	1.547E-2	4.647E-4
Std. Dev.	10.62%	7.58%	10.04%	2.52%	13.11%	9.93%	8.84%	10.78%	5.81%	13.36%	10.14%	9.55%	11.91%	6.49%	13.73%

*Revised results dated November 15, 1995, are provided in Appendix B.

Table 15. Standard deviation of isotopic calculations by isotope and burnup

	No. of calculations	Case A	Case B	Case C	Average
²³⁴ U	21	5.19	7.08	8.99	7.09
²³⁵ U	21	2.98	6.01	8.12	5.70
²³⁶ U	21	2.91	2.72	2.60	2.74
²³⁸ U	21	0.12	0.17	0.21	0.16
²³⁸ Pu	21	15.68	14.80	13.86	14.78
²³⁹ Pu	21	5.16	6.08	7.12	6.12
²⁴⁰ Pu	21	3.95	4.27	5.27	4.49
²⁴¹ Pu	21	6.45	5.97	6.86	6.43
²⁴² Pu	21	8.69	8.28	8.39	8.45
²⁴¹ Am	14	4.22	4.35	5.29	4.62
²⁴³ Am	14	11.31	10.41	10.40	10.71
²³⁷ Np	14	8.61	8.86	9.42	8.96
⁹⁵ Mo	14	1.17	1.30	1.85	1.44
⁹⁹ Tc	14	5.17	3.57	4.21	4.32
¹⁰¹ Ru	16	1.03	1.05	1.76	1.28
¹⁰³ Rh	18	4.57	5.15	5.40	5.04
¹⁰⁹ Ag	17	11.03	10.61	10.21	10.62
¹³³ Cs	18	4.87	4.90	5.60	5.12
¹³⁵ Cs	4	2.49	2.98	3.63	3.03
¹⁴³ Nd	18	2.76	3.93	4.51	3.73
¹⁴⁵ Nd	18	1.02	1.25	1.46	1.25
¹⁴⁷ Sm	16	6.03	7.95	9.12	7.70
¹⁴⁹ Sm	17	14.14	15.01	15.61	14.92
¹⁵⁰ Sm	18	5.30	7.07	8.50	6.96
¹⁵¹ Sm	15	22.41	21.72	22.31	22.15
¹⁵² Sm	18	7.20	9.01	9.68	8.63
¹⁵³ Eu	18	7.90	8.19	8.52	8.21
¹⁵⁵ Gd	16	33.45	33.28	32.97	33.23
²³⁷ Np*	20	10.62	9.93	10.14	10.23
²⁴¹ Am*	20	7.58	8.84	9.55	8.66
²⁴³ Am*	14	10.04	10.78	11.91	10.91
⁹⁹ Tc*	18	2.52	5.81	6.49	4.94
¹³⁵ Cs*	8	13.11	13.36	13.73	13.40

*Concentrations for these isotopes were calculated in units of mCi/g UO₂.

with a standard deviation of more than 10% indicate poor agreement between participants' results. Based on this criterion, calculational approaches and/or data are inadequate for the following eight isotopes: ^{238}Pu , ^{243}Am , ^{109}Ag , ^{149}Sm , ^{151}Sm , ^{155}Gd , ^{237}Np , and ^{135}Cs . (Of these isotopes, the latter two are found to be in good agreement for calculations performed to calculate concentrations in terms of mg/g UO_2 fuel, but in poor agreement for activities calculated in units of mCi/g UO_2 fuel.) Possible reasons for the poor agreement in the calculated concentrations of these eight isotopes are discussed in the following paragraphs.

^{238}Pu : As can be seen in Fig. 5, the results for most participants are reasonable, with the largest outliers being the results of the AEA, AECL-WIMS, and Belgonucleaire calculations. All three of these analyses were based on the LWRWIMS data library. As was noted by Belgonucleaire, this library does not contain curium isotopes. Since a significant portion of ^{238}Pu production is due to the α -decay of ^{242}Cm , this results in an underprediction of ^{238}Pu , as is observed for the three sets of results mentioned above. Excluding these three results from the average, new averages closer to the measured concentration are obtained, with significantly improved standard deviations. The revised averaged concentrations and standard deviations are listed in Table 16. Thus with the exception of the LWRWIMS-based calculations, the agreement for ^{238}Pu is considered to be good.

^{243}Am : Calculations for both the concentration and activity of ^{243}Am show a standard deviation on the order of 11%. For calculations of ^{243}Am concentrations (Fig. 11), CEA and the three ORNL calculations appear to be outliers; however, based on activity calculations for the same isotope (Fig. 31), AECL-ORIGEN, AECL-WIMS, GRS, and NUPEC/INS are high relative to the remaining cases. Figure 34 shows the relative computed concentrations for the three burnup cases with reported activities converted to concentrations for results in which no concentrations were available. This compilation provides a broader range of results for comparing trends. It is not clear why there is such a large discrepancy between results nor, with the lack of a measured concentration or activity for this isotope, is it known which group of results (if either) is closer to reality. There appears to be a group of results that are 5 to 15% above the average (ORNL-Assm, AECL-ORIGEN, AECL-WIMS, CEA, GRS, ORNL-27g, ORNL-44g, and PNC). These results are all based on ORIGEN/ORIGEN-S, WIMS, or a combination of the two. The remaining sets of results are roughly 5 to 15% below the average. None of these calculations were ORIGEN-based; however, both AEA and Belgonucleaire calculations were WIMS-based. Thus the cause of the discrepancy might be found by investigating the difference between the AECL-WIMS calculation, which is high, and the AEA and/or Belgonucleaire calculation, both of which are low.

Unfortunately, additional data requested to try to resolve differences were not provided by all participants, and definite conclusions cannot be drawn. However, data provided by responding participants indicate that disagreement may result from variations in capture cross sections used by the various participants. Thermal capture cross sections provided by each responding participant are listed in Table 17.

Table 16. Revised averages and standard deviations for ^{238}Pu results

	Average concentration (mg/g UO_2)	Standard deviation (%)
Case A	0.09504	8.52
Case B	0.1835	7.46
Case C	0.2572	6.58

Table 17. Comparison of ^{243}Am thermal capture cross sections

Participant	Thermal cross section (barns)	Participant	Thermal cross section (barns)
AEA	68	BNFL	40
NUPEC/INS	51	ORNL-27g	52
ORNL-44g	40	PSI	74

^{109}Ag : Figure 17 shows that there is relatively good agreement between computed results, with the exception of 2 to 3 sets; BNFL and CSN results are the most significant outliers. Average concentrations computed without these sets of results have a significantly lower deviation, as shown in Table 18. These results suggest that ^{109}Ag results are in good agreement with one another, with the exception of two inconsistent sets of results. Unfortunately, measured concentrations for this isotope are not available for comparison.

Note that BNFL depletion calculations were based on a standard assembly design and were interpolated from tabulated values for specific burnups and enrichments. Thus these calculations were not a true representation of the benchmark calculations. Although BNFL results are for the most part consistent with other participants' results, they tend to overpredict plutonium concentrations for most plutonium isotopes (especially ^{239}Pu), indicating a possible difference in the operating spectrum computed in the BNFL model. An error in plutonium production would result in an error in the prediction of fission-product concentrations; however, an overprediction in ^{239}Pu should result in an overprediction in ^{109}Ag , rather than the underprediction observed.

Table 18. Revised averages and standard deviations for ^{109}Ag results

	Average concentration (mg/g UO_2)	Standard deviation (%)
Case A	0.05892	7.05
Case B	0.08570	6.98
Case C	0.1053	7.61

^{149}Sm : There is clearly broad disagreement between participants' results for this nuclide, as illustrated in Fig. 23. BNFL appears to be an outlier; however, it is at the same time in closest agreement with the measured concentrations. In addition, there appears to be a problem in the measurement of this nuclide concentration; the measured concentration for the 44.34-GWd/MTU case is significantly and unexpectedly higher than that of the other two lower burnup cases. From data provided by a limited set of participants, discrepancies are noted between direct fission yields used, although cumulative fission yields and cross sections are relatively consistent. These data are listed in Table 19. However, trends noted for specific participants are inconsistent with these data. For example, AEA data include a larger thermal capture cross section and smaller direct fission yields than those of other participants; these data should result in an underprediction of ^{149}Sm concentrations. However, the results shown in Fig. 23 show that AEA tends to overpredict ^{149}Sm relative to many of the other participants. In addition, with the exception of BNFL, cumulative yields of mass 149 are consistent among participants. Thus inconsistencies in ^{149}Sm predictions are more likely to result from inconsistent cross-section data for parent isotopes (i.e., ^{149}Pm , ^{149}Nd , and ^{149}Pr).

^{151}Sm : As with ^{149}Sm , considerable disagreement is observed in concentrations predicted for this isotope, as shown in Fig. 25; however, in this case there is no experimental measurement with which one can compare the calculated results. Of the 15 sets of results available, AEA, Belgonucleaire, and perhaps BNFL results appear to be outliers; however, even with the exclusion of these results there is a greater than 10% standard deviation in the remaining results. The error in ^{151}Sm is not a direct result of error in ^{149}Sm concentrations ($^{149}\text{Sm} + n \geq ^{150}\text{Sm} + n \geq ^{151}\text{Sm}$) since no such large variation is seen in the intermediate ^{150}Sm concentrations.

Available fission yield and cross-section data are listed in Table 20. As with ^{149}Sm , discrepancies are noted between direct fission yields used, although cumulative fission yields are for the most part consistent. Thermal capture cross sections reported by AEA and PSI are roughly three to four times the values reported by others. Again, however, some trends noted for specific participants are inconsistent with these data. It is likely that some of the discrepancies between participants result from inconsistencies in ^{151}Sm data; it is equally likely that discrepancies result from inconsistent cross-section data for parent isotopes.

Table 19. Cross-section and fission yield data for ^{149}Sm

	AEA	CEA	BNFL	PSI	Tohoku	ORNL-27	ORNL-44
Thermal capture cross section (b)	6.15E+04	-	4.50E+04	4.16E+04	-	4.35E+04	4.70E+04
Direct Fission							
Yields							
^{235}U	4.47E-12	2.31E-09	1.04E-09	4.50E-12	6.53E-11	1.11E-10	1.11E-10
^{238}U	3.03E-15	1.83E-11	-	3.04E-16	4.18E-12	1.39E-13	1.39E-13
^{239}Pu	3.73E-10	3.50E-08	-	3.75E-10	1.91E-10	2.68E-09	2.68E-09
^{241}Pu	3.39E-12	1.98E-09	5.30E-09	3.37E-12	3.48E-11	-	-
Cumulative Fission yields							
^{235}U	1.05E-02	1.07E-02	2.42E-03	1.05E-02	1.09E-02	1.03E-02	1.03E-02
^{238}U	1.66E-02	1.62E-02	1.04E-03	1.68E-02	1.57E-02	1.61E-02	1.61E-02
^{239}Pu	1.25E-02	1.23E-02	3.81E-03	1.25E-02	1.27E-02	1.24E-02	1.24E-02
^{241}Pu	1.46E-02	1.47E-02	5.63E-03	1.45E-02	1.46E-02	1.45E-02	1.45E-02

Table 20. Cross-section and fission yield data for ^{151}Sm

	AEA	CEA	BNFL	PSI	Tohoku	ORNL-27	ORNL-44
Thermal capture cross section (b)	1.25E+04	-	4.38E+03	1.53E+04	-	4.03E+03	3.93E+03
Direct Fission							
Yields							
^{235}U	7.18E-09	3.42E-07	1.65E-07	-	3.80E-08	7.20E-08	7.20E-08
^{238}U	1.99E-11	1.02E-08	1.67E-09	-	3.22E-06	5.13E-10	5.13E-10
^{239}Pu	2.91E-07	4.20E-06	1.59E-07	-	2.47E-07	1.12E-06	1.12E-06
^{241}Pu	7.54E-09	4.87E-07	1.12E-06	-	-	-	-
Cumulative Fission yields							
^{235}U	4.16E-03	4.16E-03	3.12E-03	4.17E-03	4.22E-03	4.08E-03	4.08E-03
^{238}U	8.09E-03	8.05E-03	3.31E-03	8.10E-03	8.50E-03	8.01E-03	8.01E-03
^{239}Pu	7.62E-03	7.55E-03	6.37E-03	7.63E-03	7.83E-03	7.77E-03	7.77E-03
^{241}Pu	8.55E-03	9.11E-03	7.33E-03	8.40E-03	9.08E-03	9.12E-03	9.12E-03

^{155}Gd : By far the largest disagreement for nuclide concentrations is seen for ^{155}Gd . Relative to the average computed concentration, BNFL, CSN, and Risø are 40 to 50% high, AEA, CEA, ORNL-44g, and PSI are 40 to 60% low, and the remainder range from 5% lower to 15% higher than the average. Because mass spectroscopy results for mass chain 155 contain both ^{155}Gd and ^{155}Eu , it is not possible to experimentally determine the mass of ^{155}Gd in spent fuel directly, unless time is allowed for most ^{155}Eu to decay (with a 4.7-year half-life, such a wait is not practical). However, it is possible to calculate the concentrations of both ^{155}Gd and ^{155}Eu and compare the sum of the concentrations of the two nuclides. Such an approach was used at ORNL in other

burnup credit evaluations; these comparisons demonstrated that calculations based on the SCALE 27-group burnup library resulted in an almost 100% overprediction of the sum of ^{155}Gd and ^{155}Eu concentrations relative to assay measurements. Further investigation determined that the source of this discrepancy was an inadequate representation of ^{155}Eu cross sections, specifically, resonance data. A more recent evaluation, available in the ENDF/B-VI distribution and included in the SCALE 44-group library, has been demonstrated³ to provide improved agreement with measured data, although the new library resulted in a roughly 25% underprediction of the combined masses. Thus the best estimate of the measured concentration of ^{155}Gd is about 25% below the average shown in Fig. 28.

Resonance integral information would help to confirm the implication above that differences result from inadequate resonance data. However, insufficient data were provided by participants to investigate differences between results. Nevertheless, the significant differences between ORNL-27g and ORNL-44g results are believed to be a consequence of the differences between resonance data. Resonance integrals are 1825 and 23,200 for the 27-group and 44-group libraries, respectively.

^{237}Np : Although the ^{237}Np concentrations given in Tables 8 through 10 and Fig. 12 are in slightly better statistical agreement ($\pm 9\%$) than the activities given in Table 14 and Fig. 29 ($\pm 10\%$), this appears to be purely a function of the distribution of participants who submitted results in each format. Results submitted in terms of both concentration and activity are consistent. The reason for the disagreement among participants' results is likely to be due to cross-section data. Thermal capture cross sections are given in Table 21 for several participants. Note that the results of the top four upper outliers in Fig. 29 (ORNL-Assm, ECN-Old Lib, JAERI, and ORNL-27g) were calculated based on ENDF/B-IV actinide data. The remaining calculations, which are in better agreement with one another and with measured data, were based on ENDF/B-V, JEF-2, and JENDL-3 (exception: PNC results were ENDF/B-IV-based). Note that the predicted concentrations improve significantly in going from the ENDF-IV actinides in the SCALE 27-group library (ORNL-27g) to the ENDF/B-V actinides in the SCALE 44-group library (ORNL-44g). Only the cross-section libraries changed between these two sets of calculations. Although cross-section data for all participants were not available, data provided by responding participants support the assertion that differences are due to variations in capture cross sections used by the various participants. Thermal capture cross sections provided by each responding participant are listed below.

^{135}Cs : As was similarly observed for ^{237}Np , the ^{135}Cs concentrations given in Tables 11 through 13 and Fig. 19 are in better statistical agreement ($\pm 3\%$) than the activities given in Table 14 and Fig. 33 ($\pm 13\%$). However, in this case the statistical variations between the results of the two sets of data are significantly different. In this case, the difference can be traced to conversion factors relating activities to concentrations. Although the conversion factors were not explicitly supplied, they can be inferred from the ratio of the reported activity to the reported concentration for a specific sample and for a given participant's results. Five participants supplied both concentrations and activities for ^{135}Cs : Toshiba-Leakage, Toshiba-Poison, PSI, Risø, and Tohoku. The conversion factors for both sets of Toshiba results are significantly different than those

Table 21. Comparison of ^{237}Np thermal-capture cross sections

Participant	Thermal cross section (barns)	Participant	Thermal cross section (barns)
AEA	159	BNFL	132
NUPEC/INS	38	ORNL-27g	77
ORNL-44g	89	PSI	89

determined from PSI, Risø, and Tohoku results. Since the last three sets of results are more consistent with one another, it is likely that the problem lies in conversion factors used by Toshiba. However, there is a lack of consistency even among the remaining three participants. Because the results for calculated isotopic concentrations have a small standard deviation and are in relatively close agreement with measured concentrations, it may be argued that the only weakness in the ability to calculate ^{135}Cs inventory lies in decay-rate data. However, because ^{135}Cs concentration results were supplied by only seven participants, it is not possible to generalize this statement for all of the various codes and data sources used in this benchmark.

Figures 35 through 55 provide a summary of the agreement between each participant's calculations and the average of all participants' results for each isotope included in the benchmark study. Rather than attempt to show the relative agreement for each of the three cases studied, these plots show the average agreement for all three cases. "Agreement" is used in the sense given in the earlier figures [i.e., $(C/A-1)*100\%$], where C is a participant's calculated concentration for a given isotope, and A is the average of all participants' calculations for the same isotope. It must be emphasized that these figures do not show the agreement with the "correct" solution since this is not known in this benchmark; rather, the figures illustrate the consistency of each participant's codes and data relative to the other participants' results.

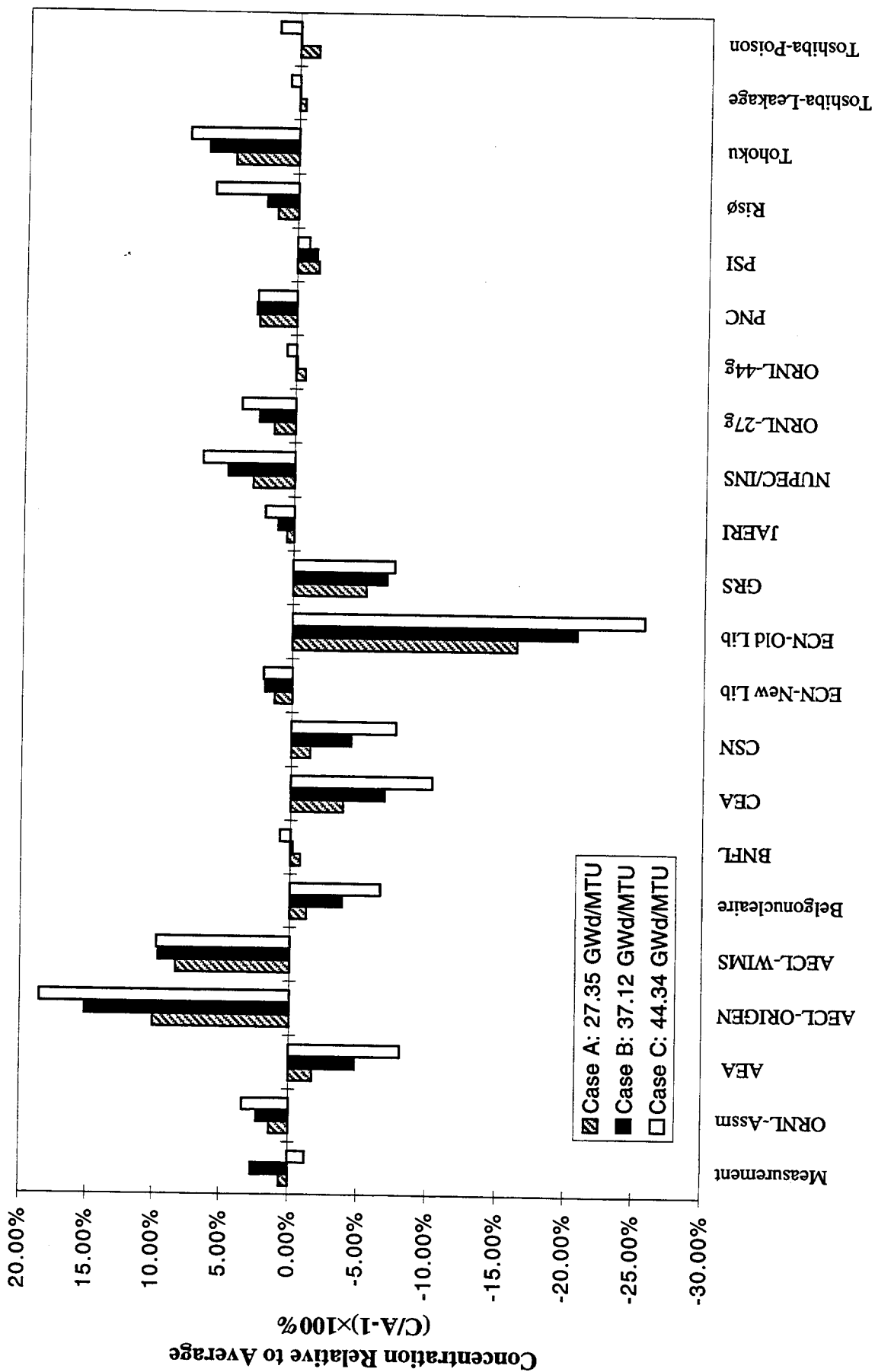


Fig. 1. Relative U-234 concentrations.

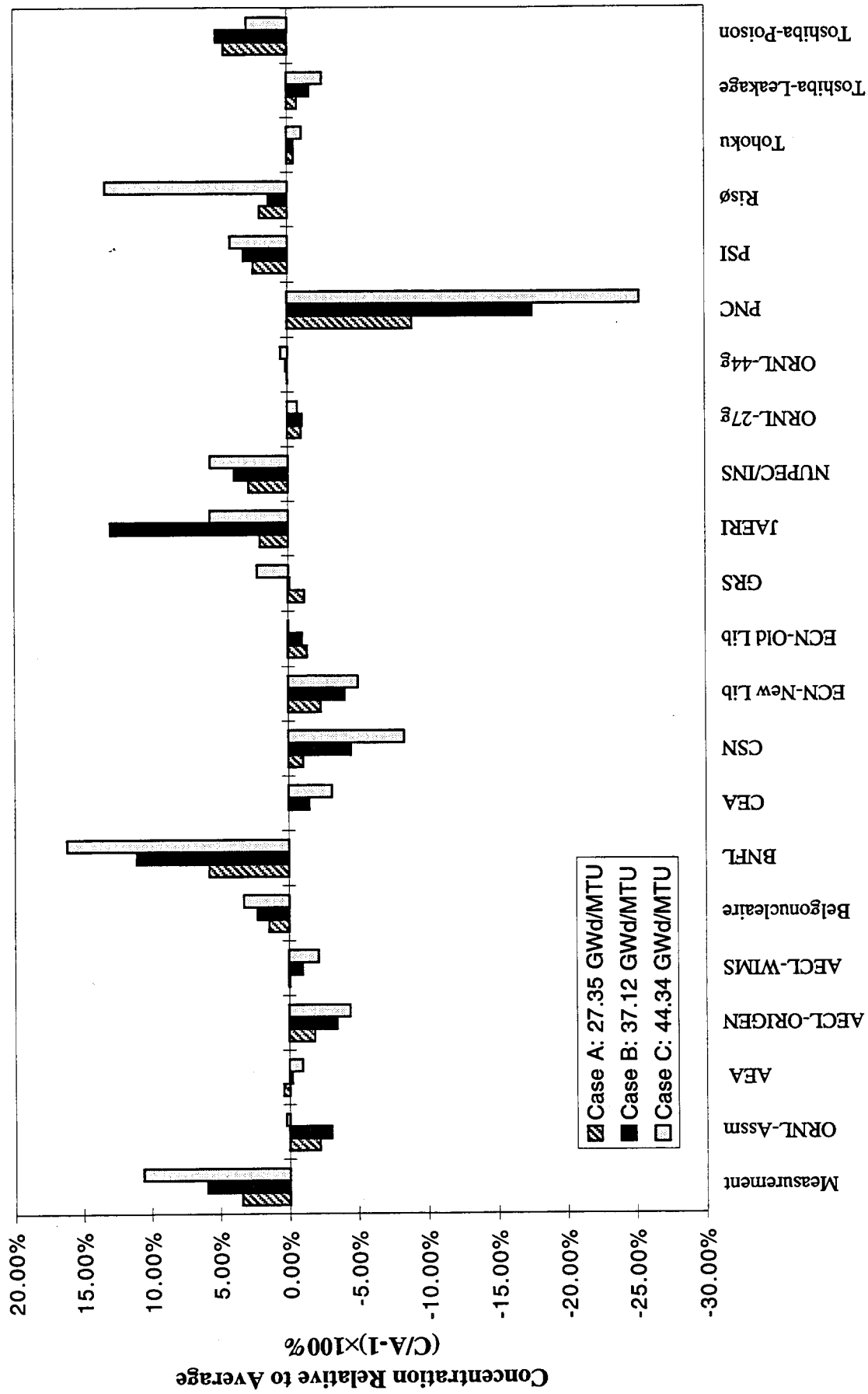


Fig. 2. Relative U-235 concentrations.

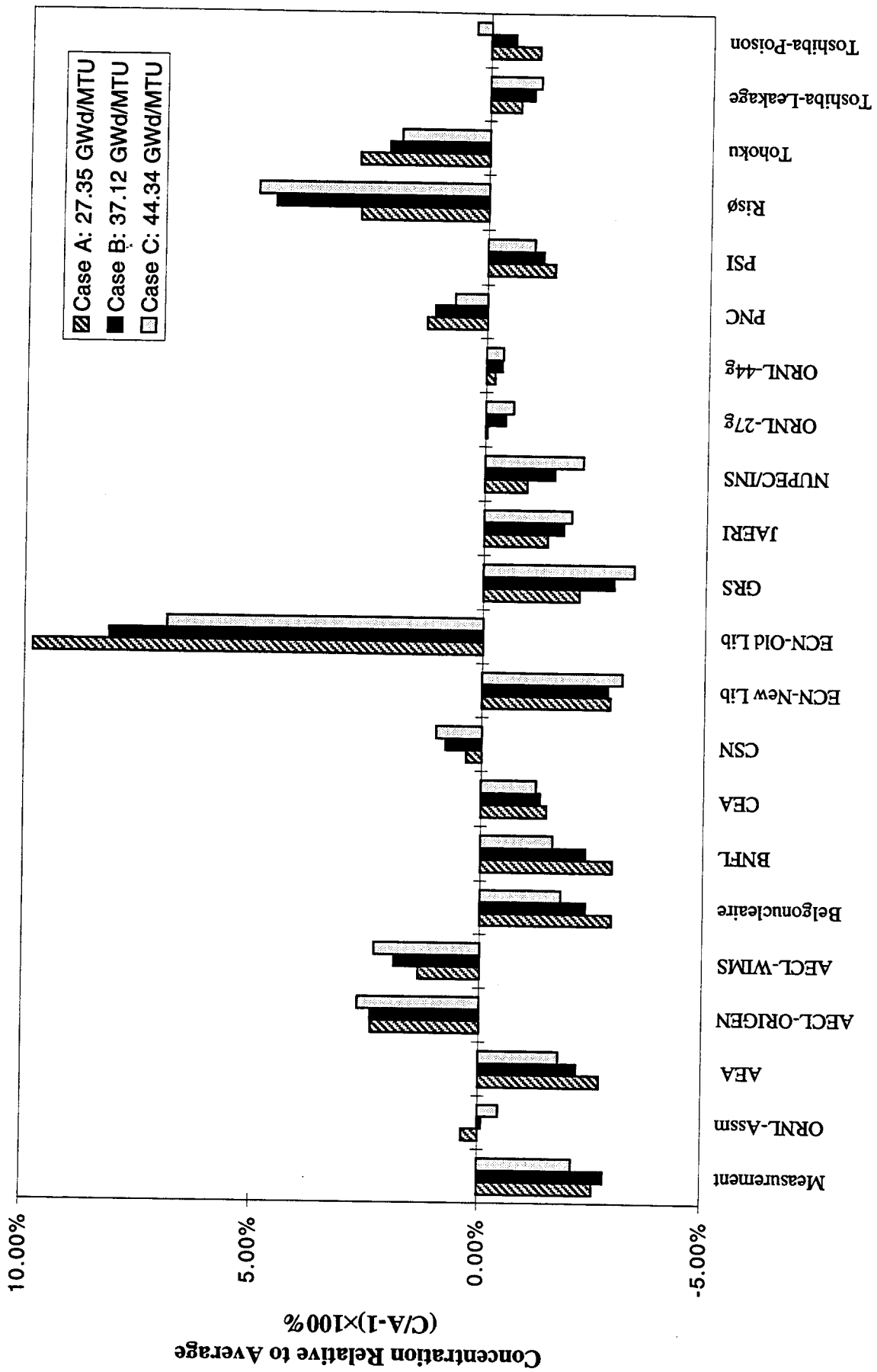


Fig. 3. Relative U-236 concentrations.

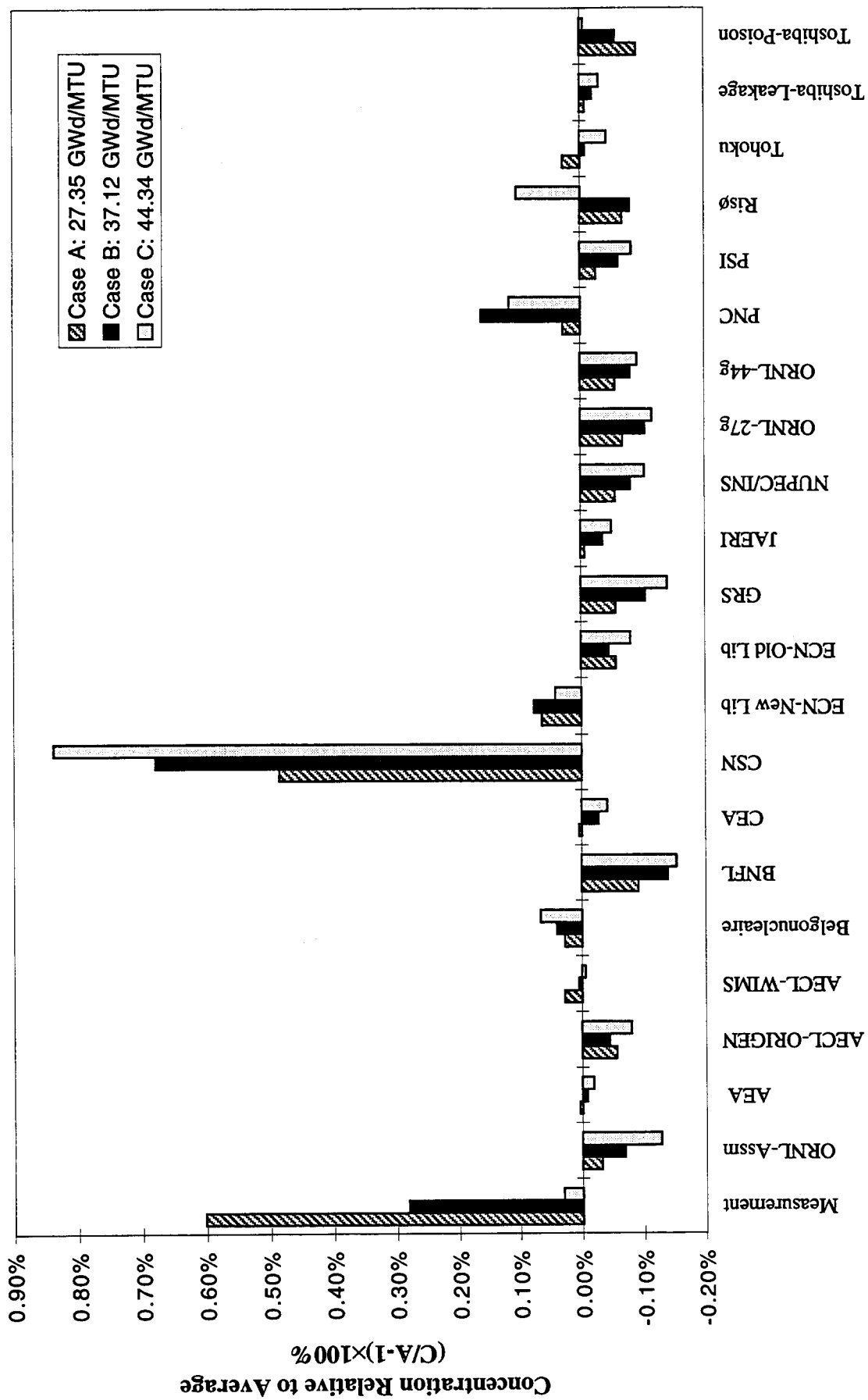


Fig. 4. Relative U-238 concentrations.

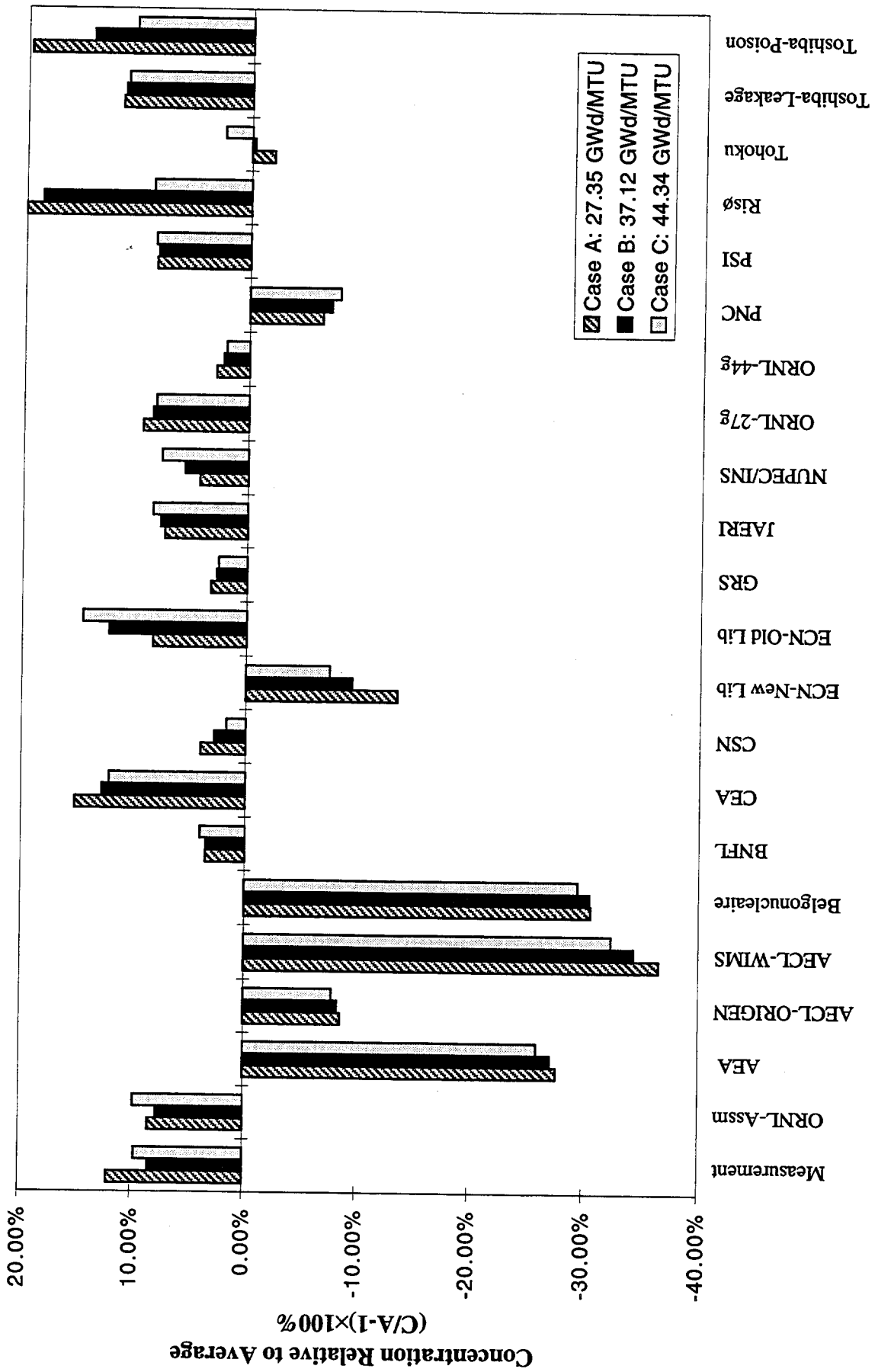


Fig. 5. Relative Pu-238 concentrations.

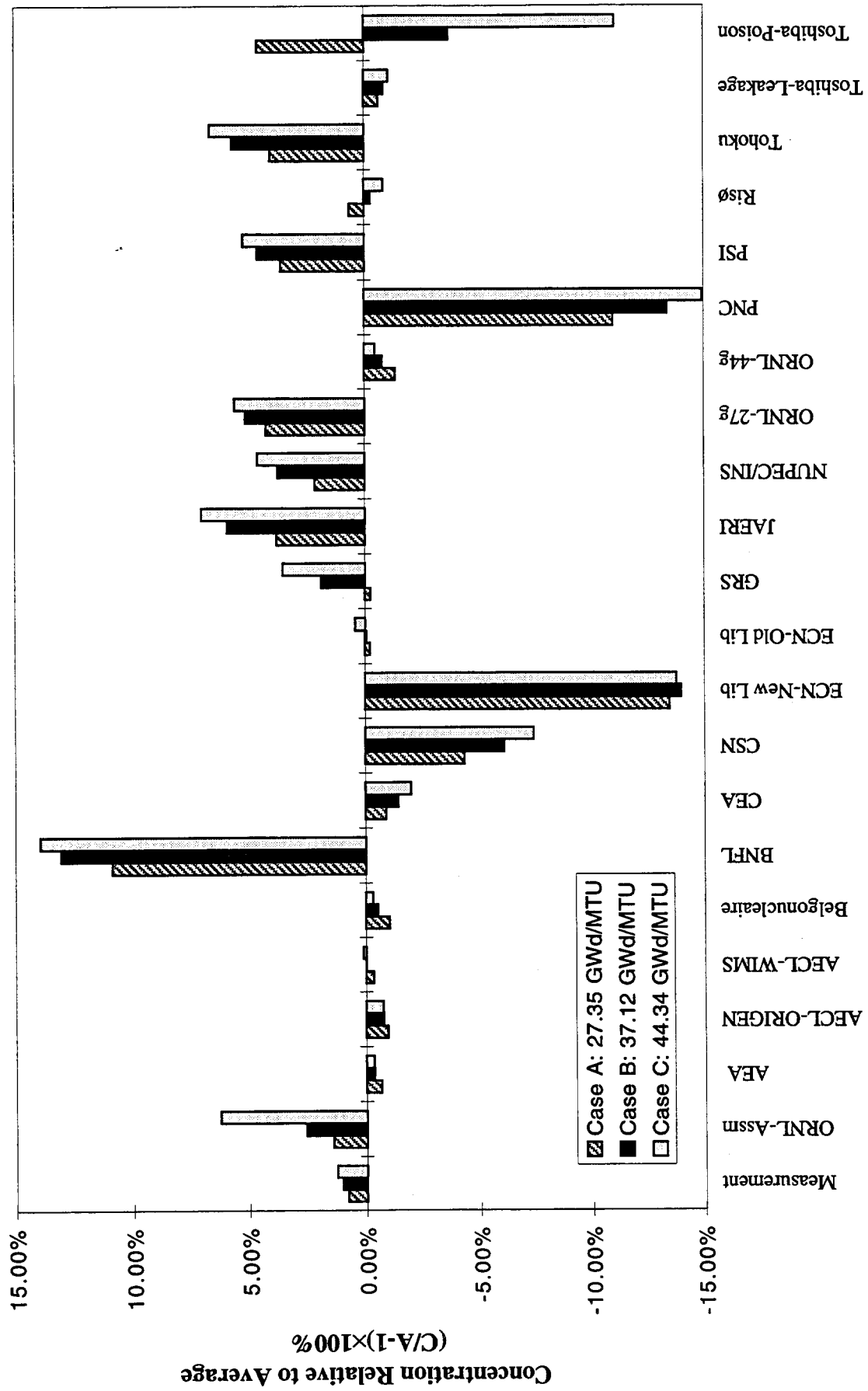


Fig. 6. Relative Pu-239 concentrations.

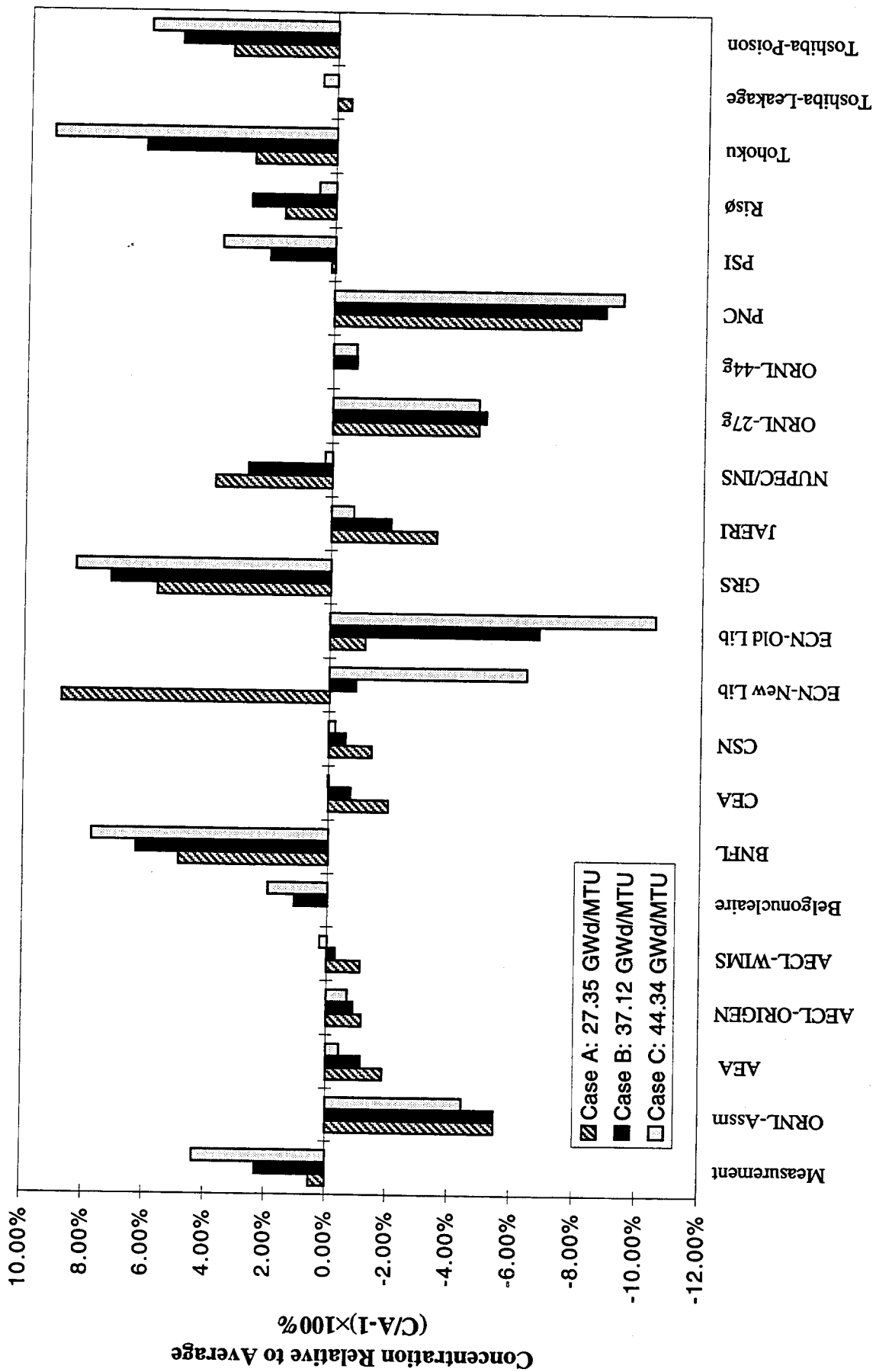


Fig. 7. Relative Pu-240 concentrations.

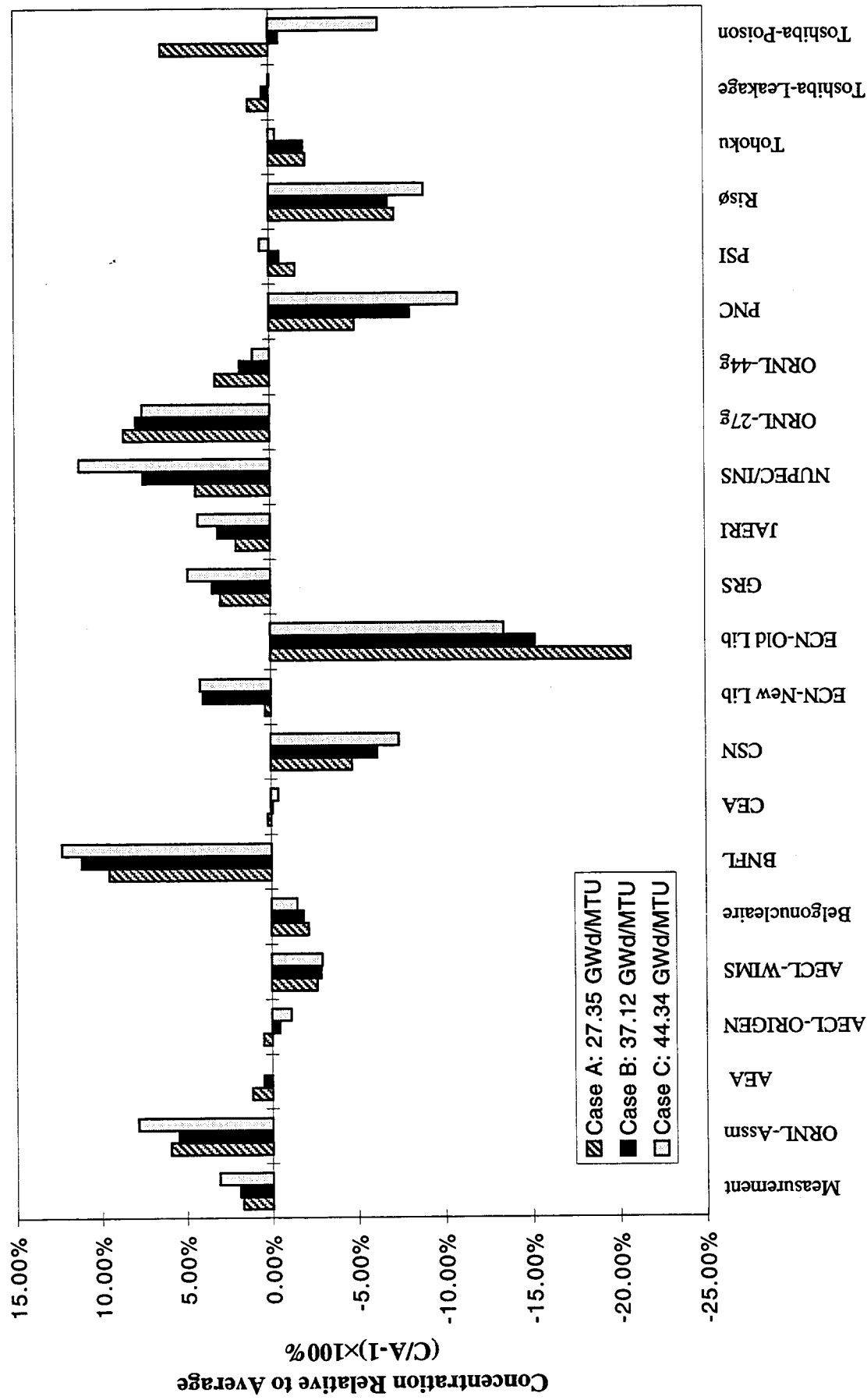


Fig. 8. Relative Pu-241 concentrations.

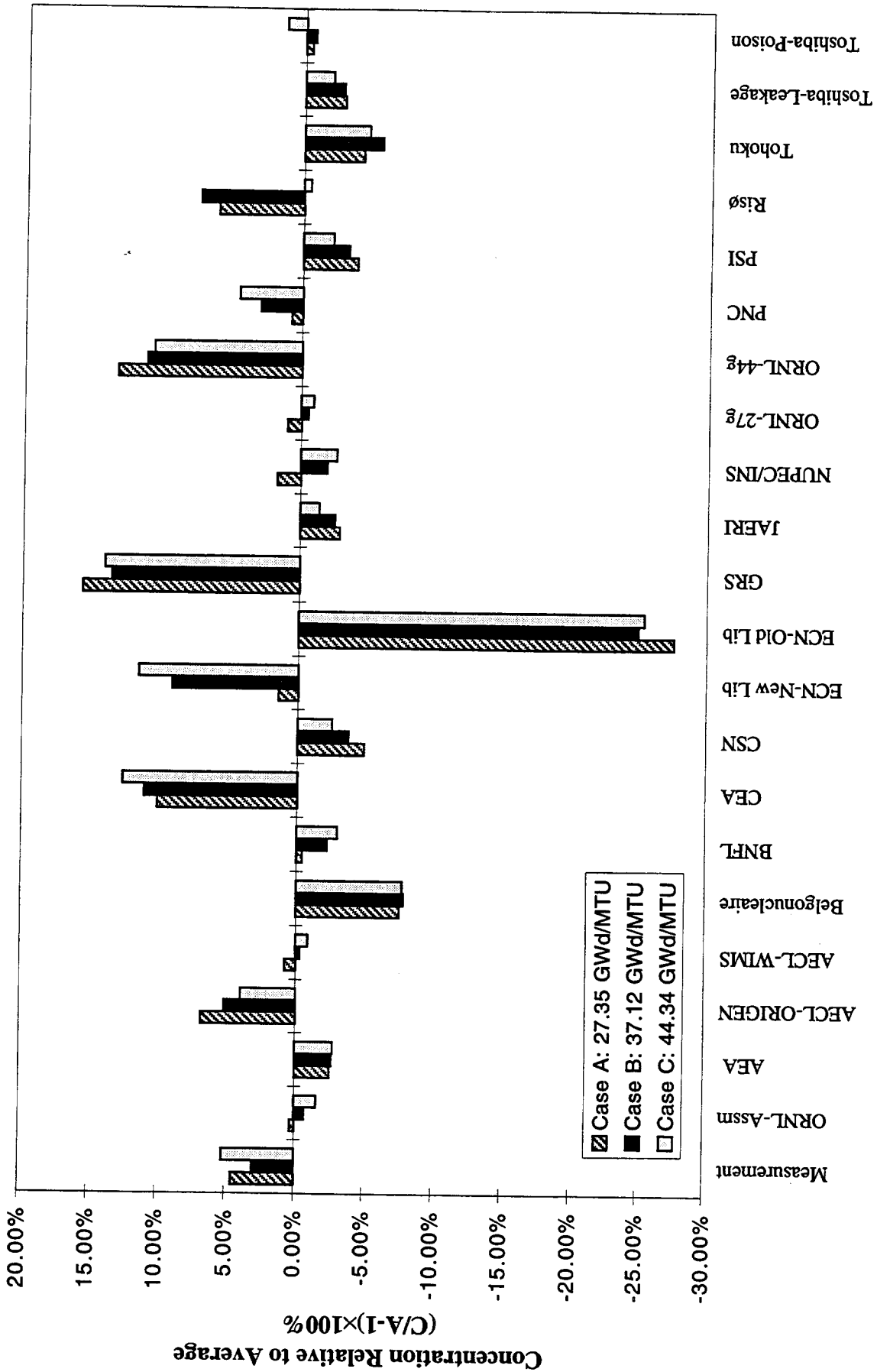


Fig. 9. Relative Pu-242 concentrations.

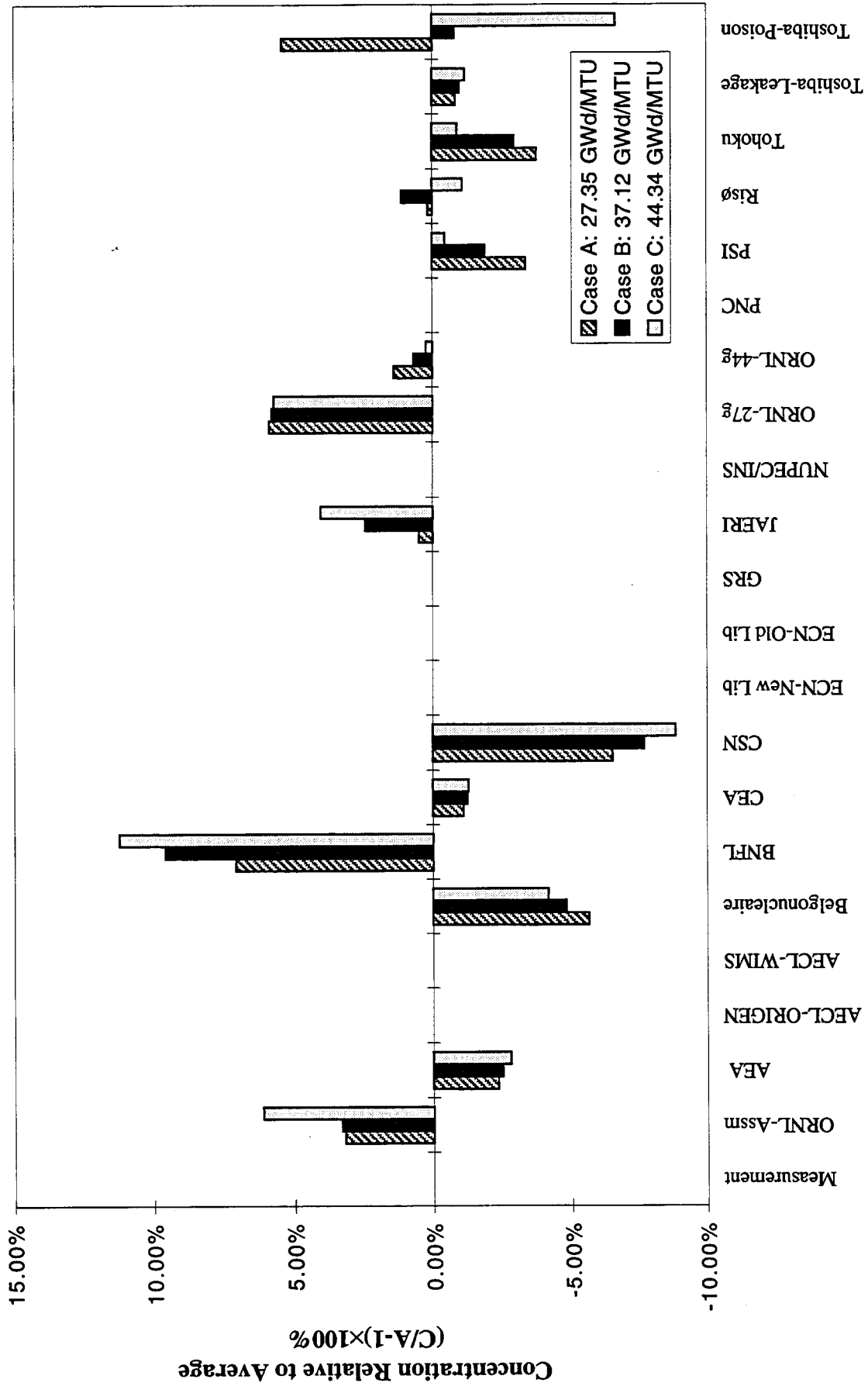


Fig. 10. Relative Am-241 concentrations.

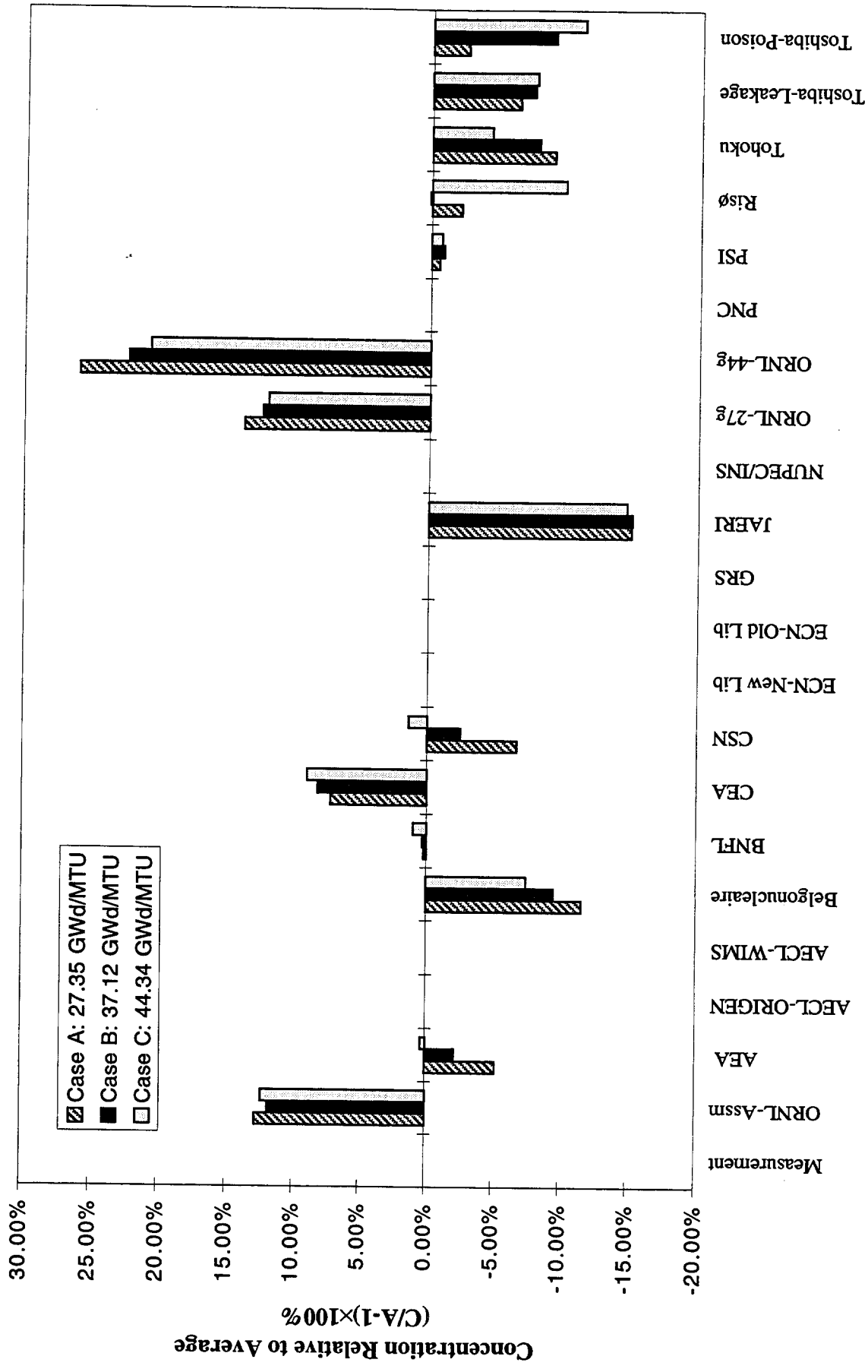


Fig. 11. Relative Am-243 concentrations.

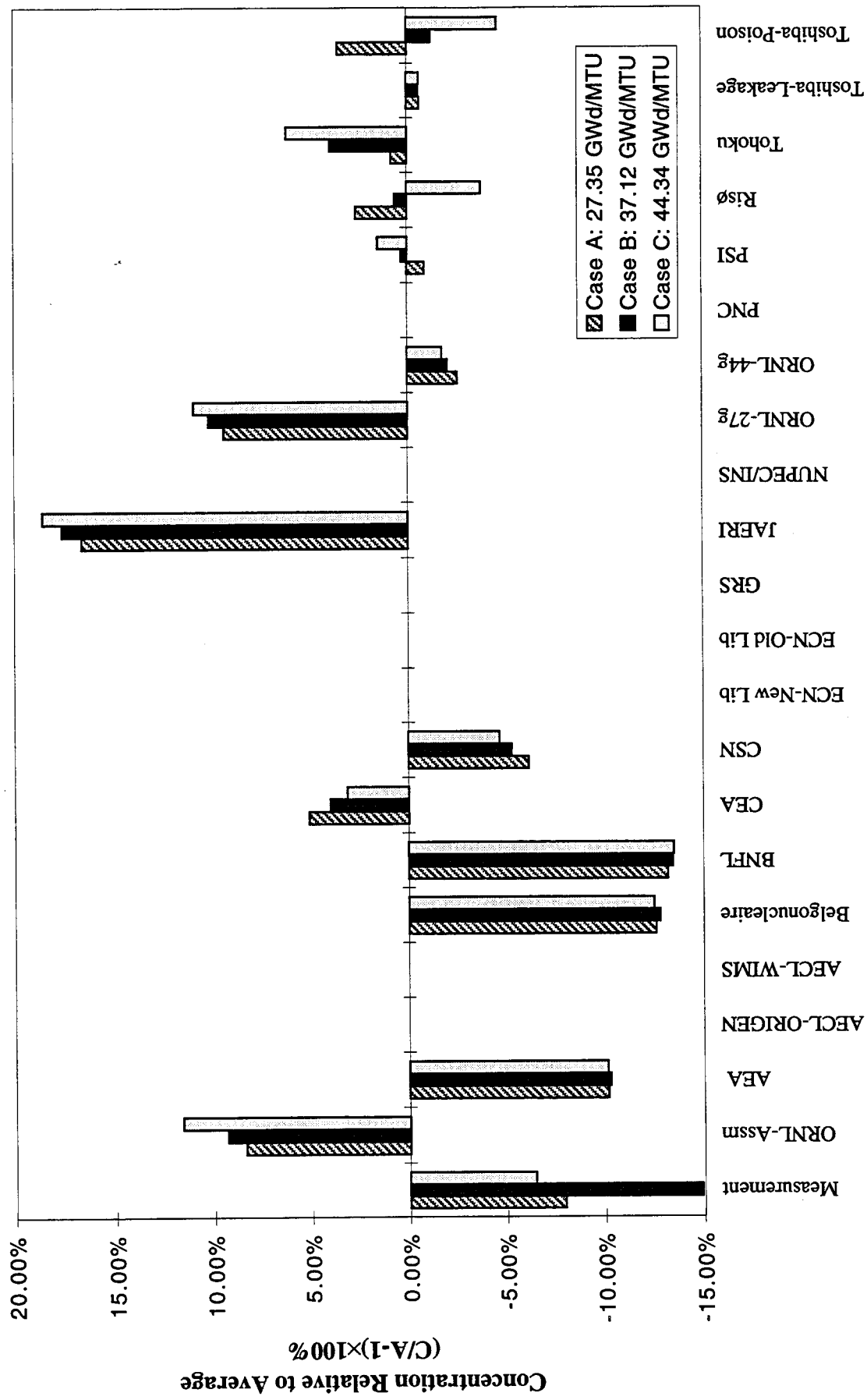


Fig. 12. Relative Np-237 concentrations.

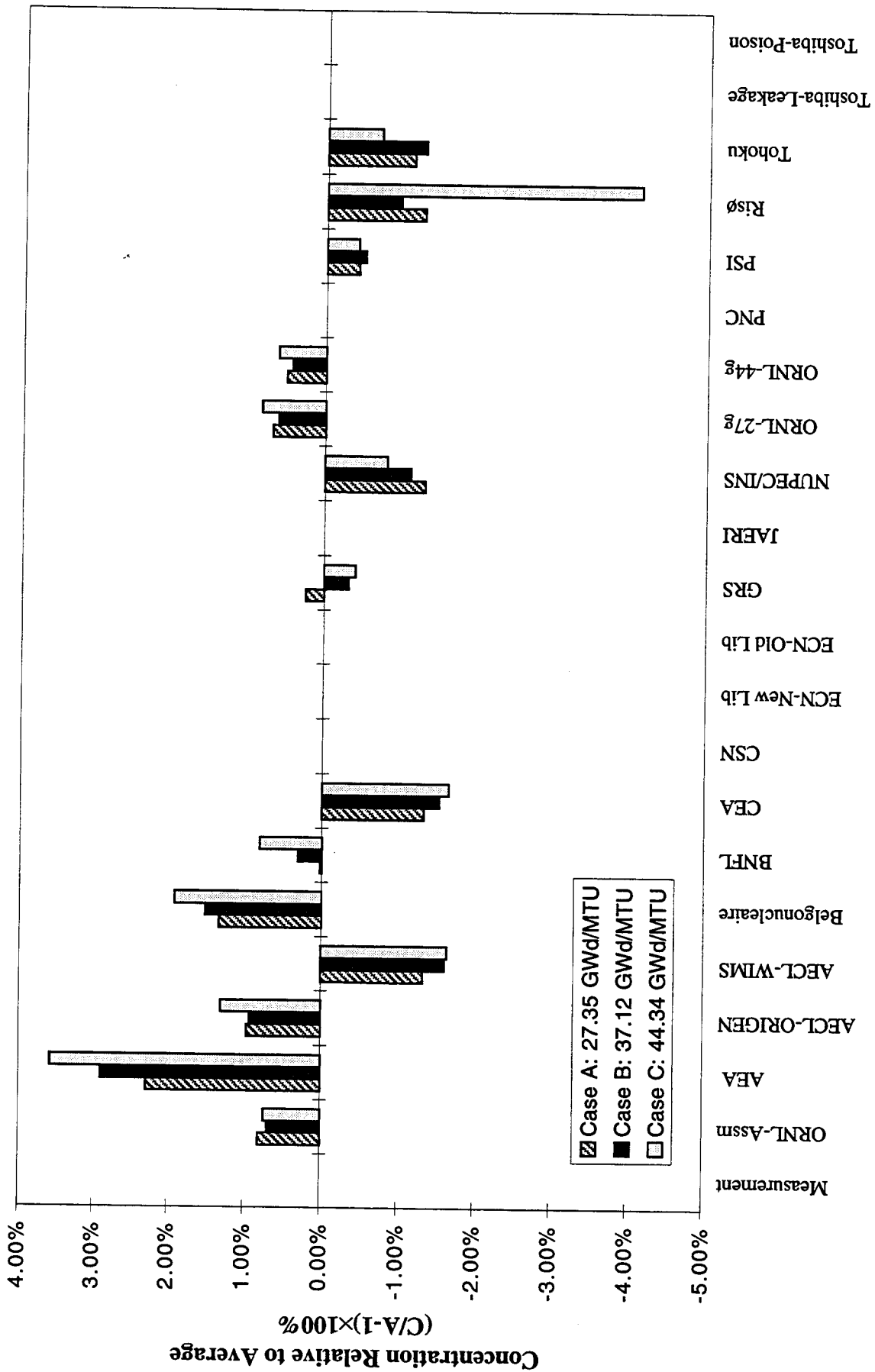


Fig. 13. Relative Mo-95 concentrations.

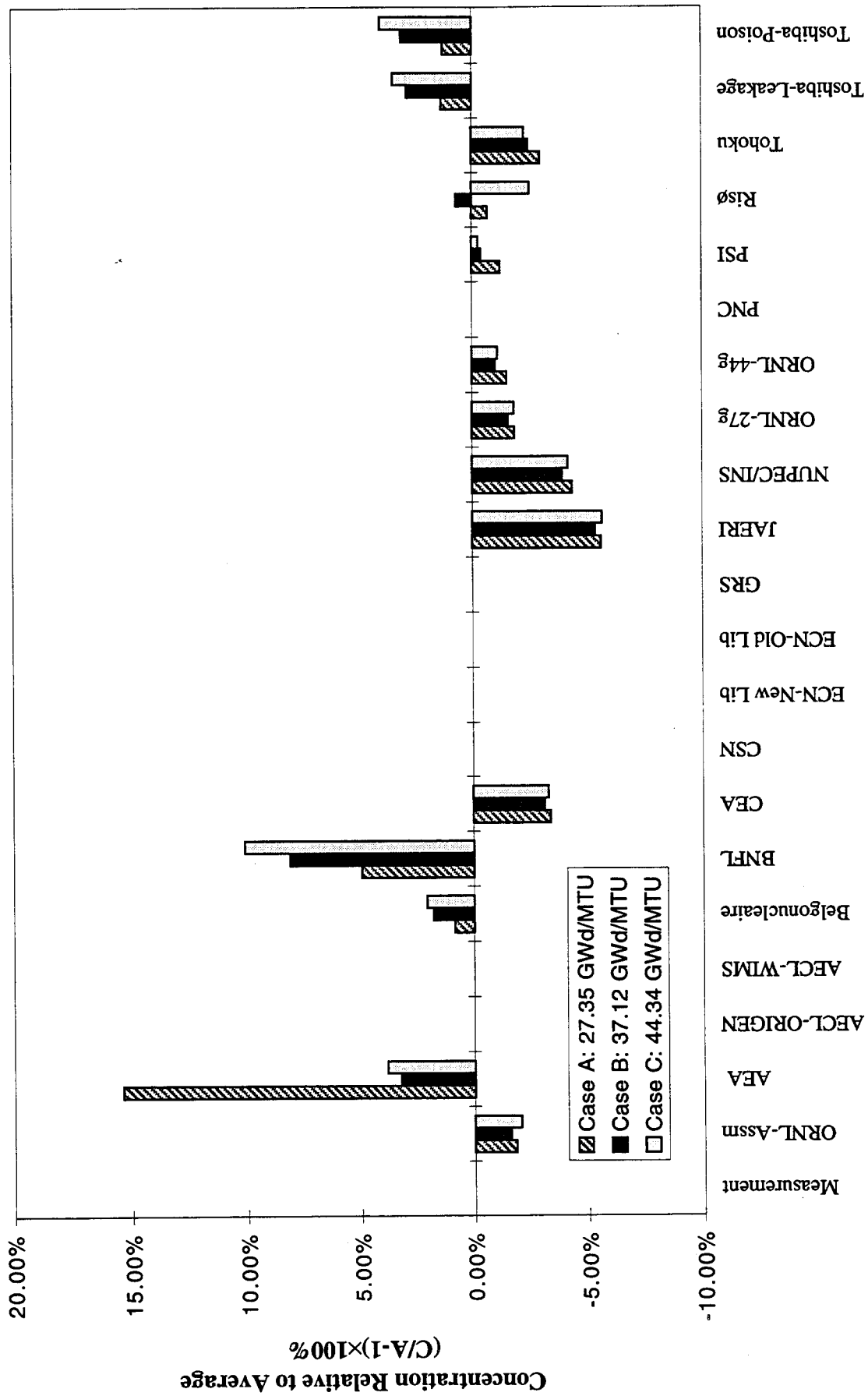


Fig. 14. Relative Tc-99 concentrations.

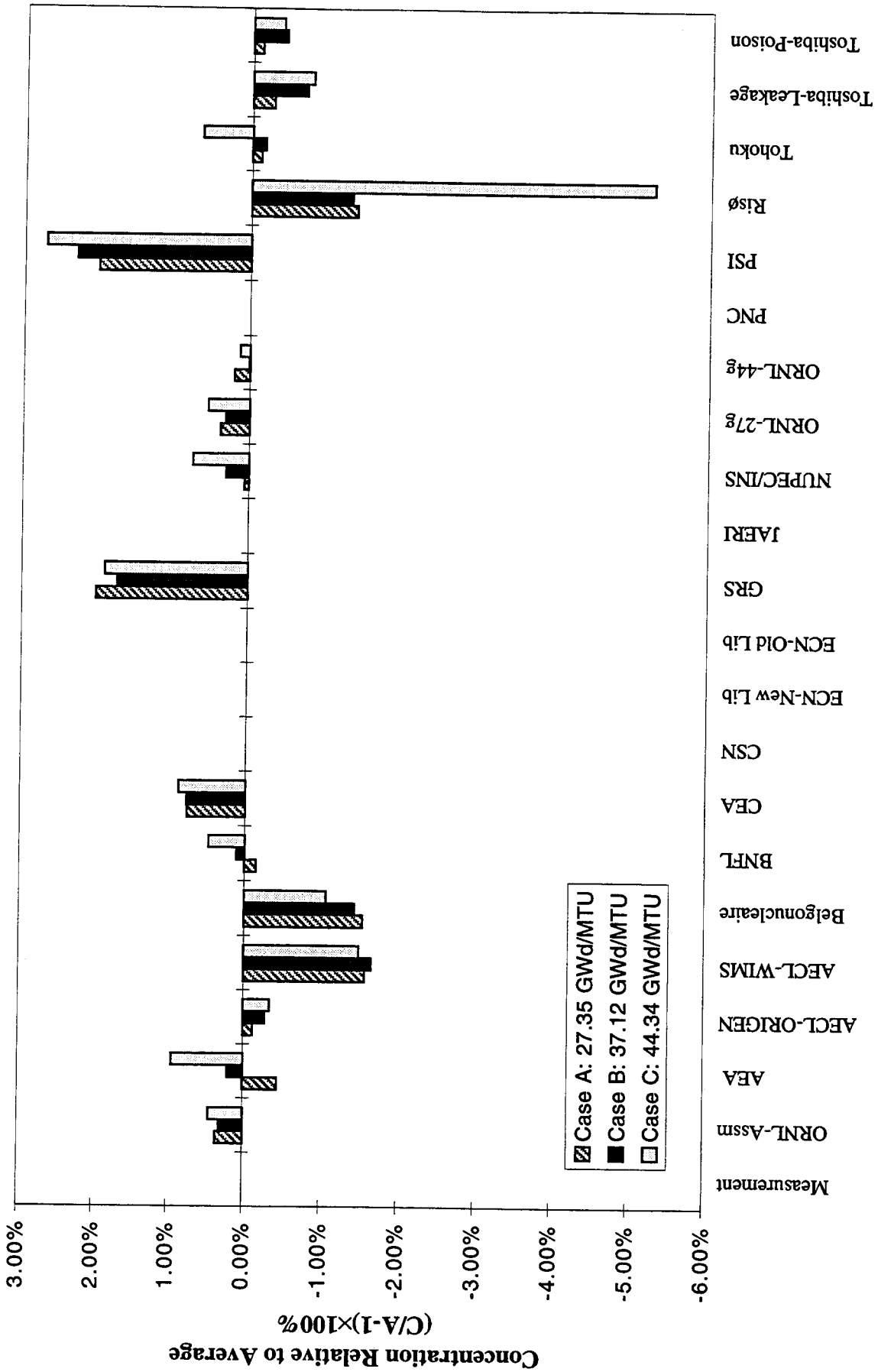


Fig. 15. Relative Ru-101 concentrations.

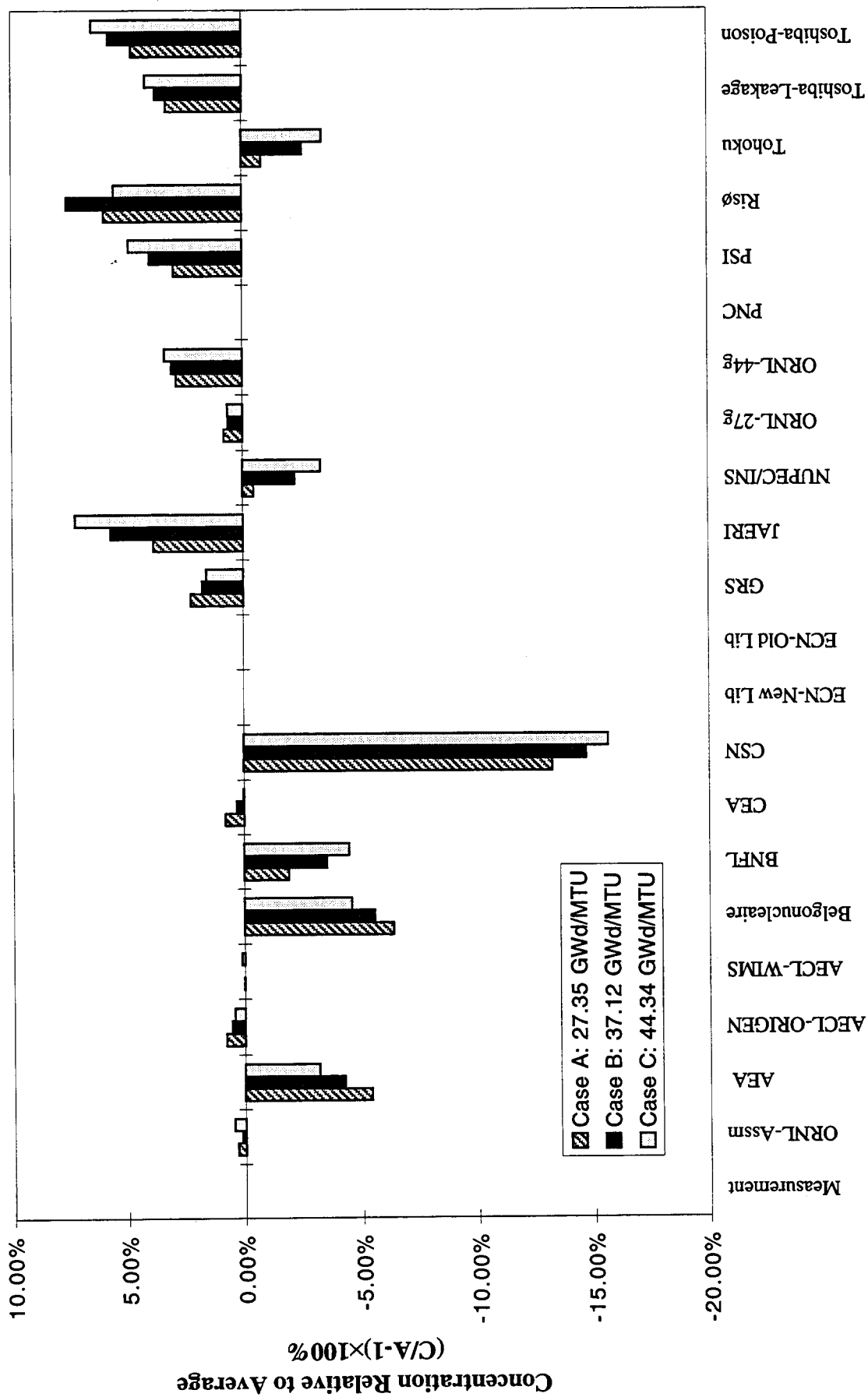


Fig. 16. Relative Rh-103 concentrations.

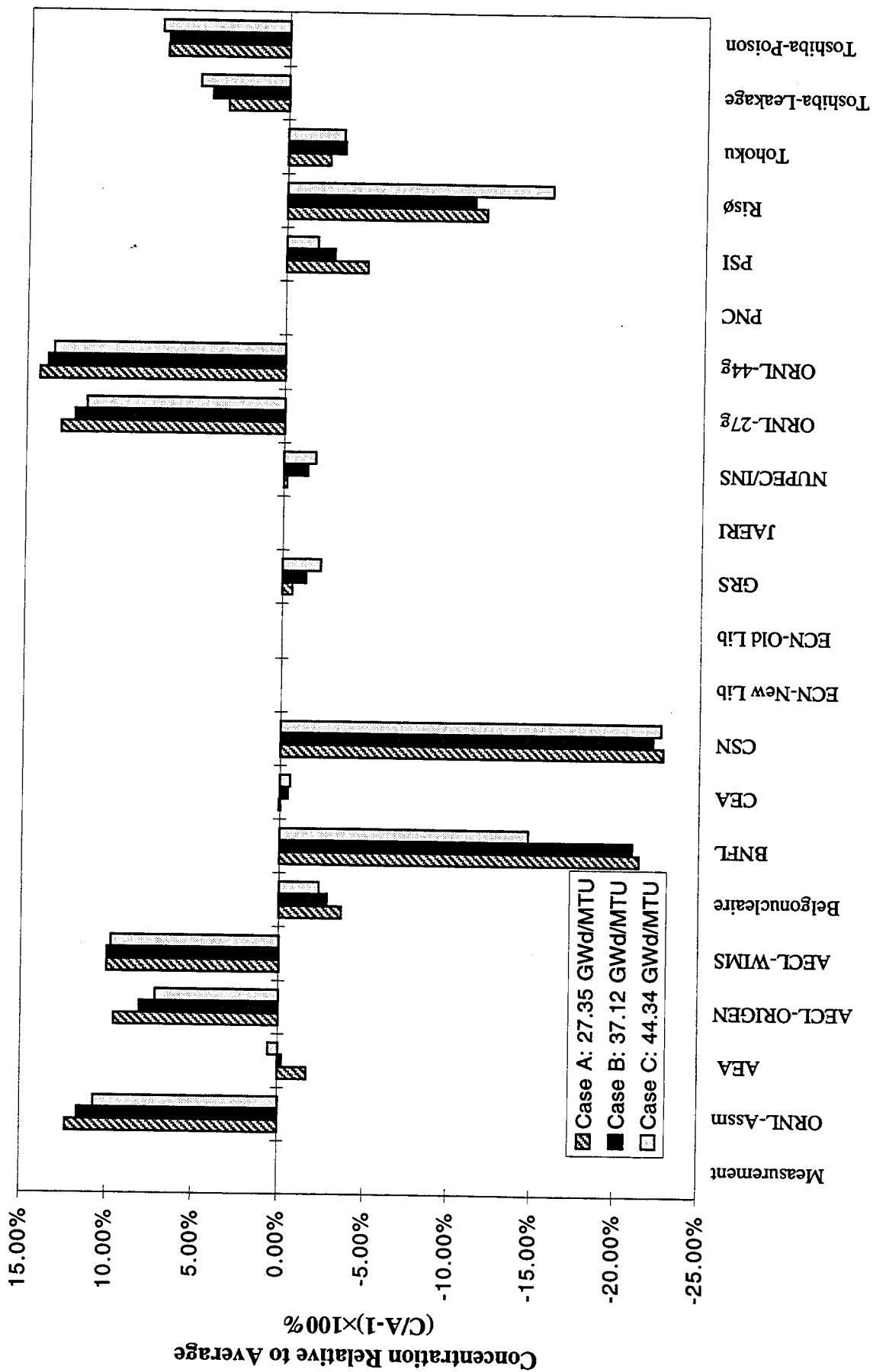


Fig. 17. Relative Ag-109 concentrations.

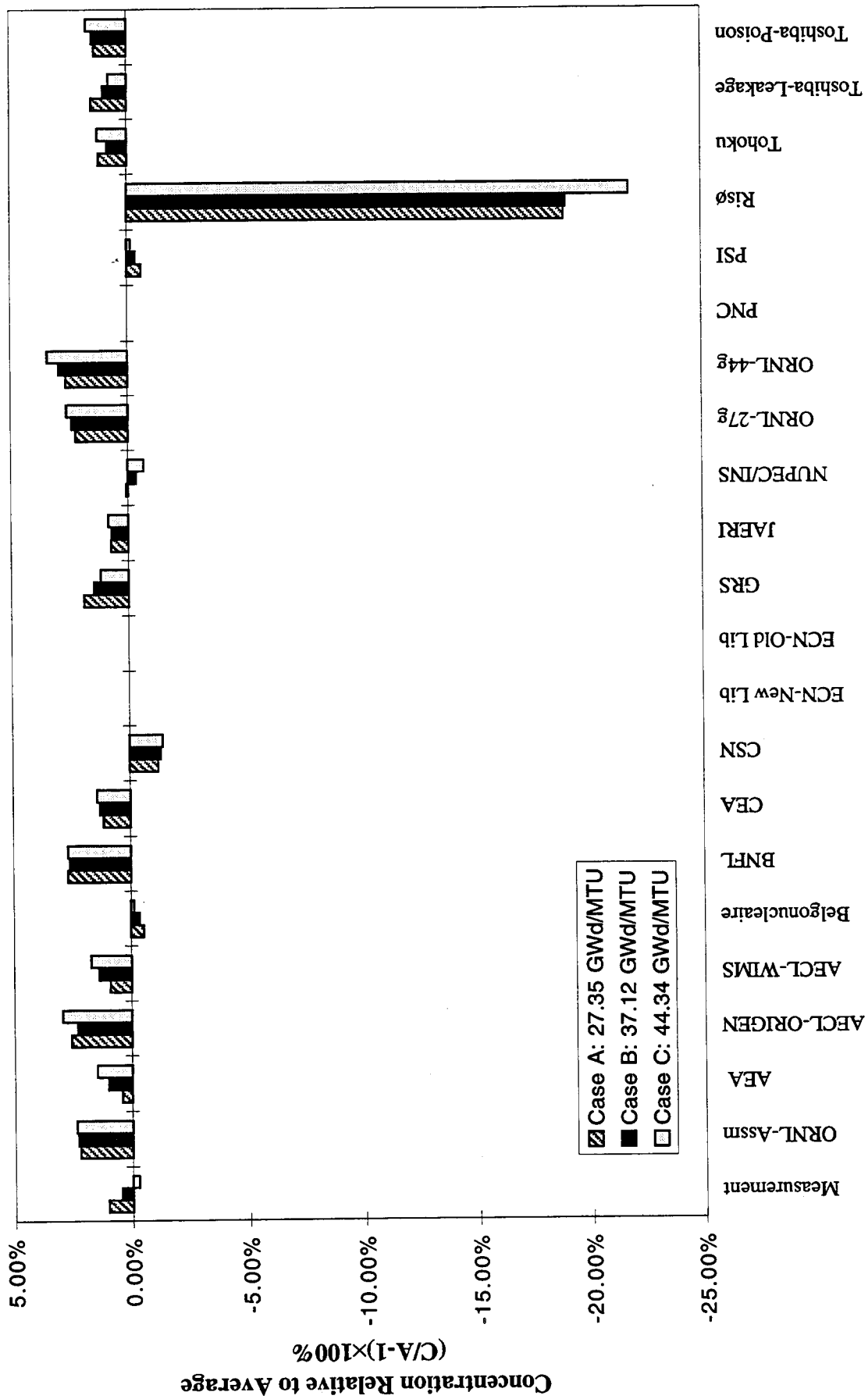


Fig. 18. Relative Cs-133 concentrations.

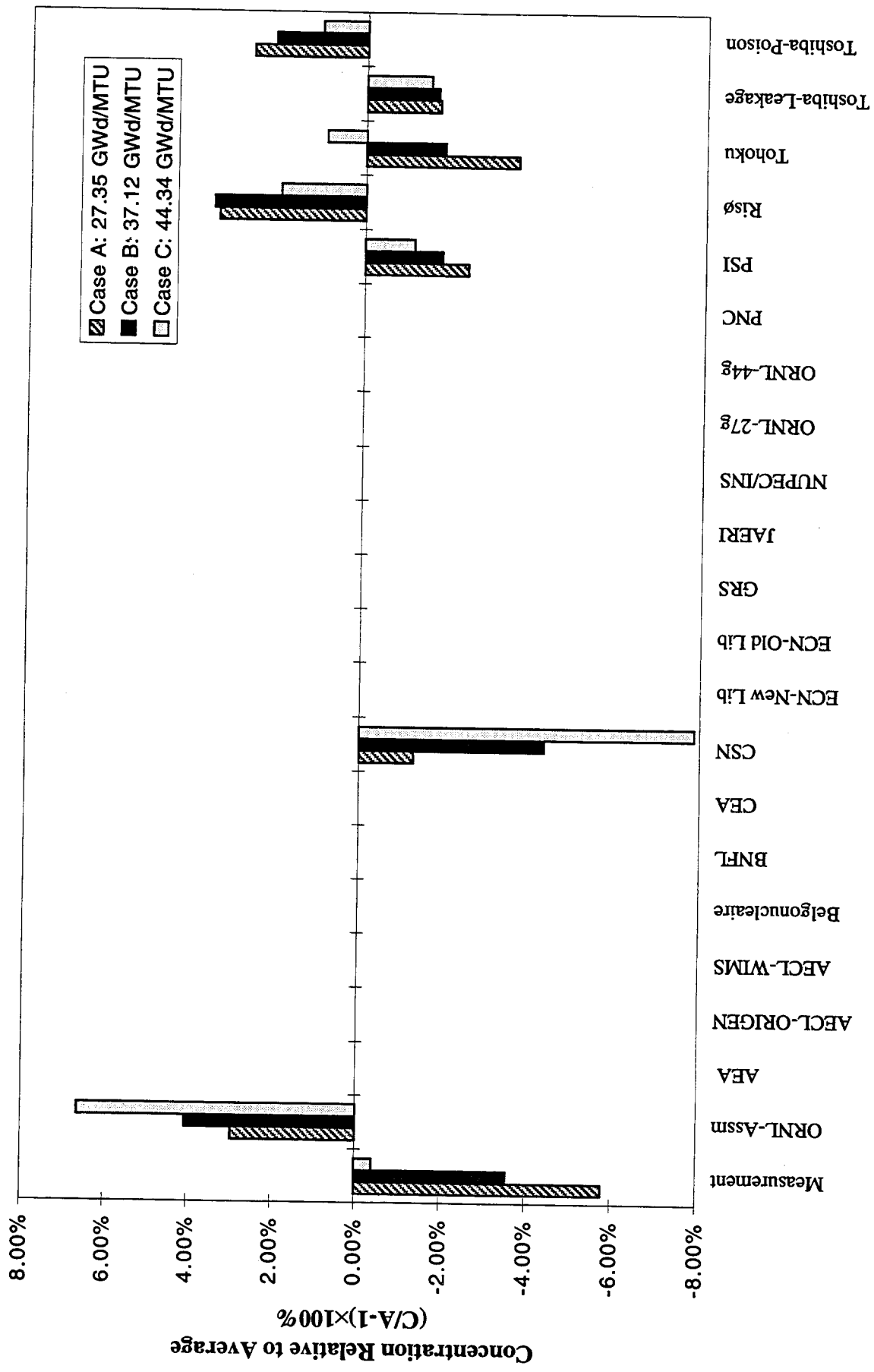


Fig. 19. Relative Cs-135 concentrations.

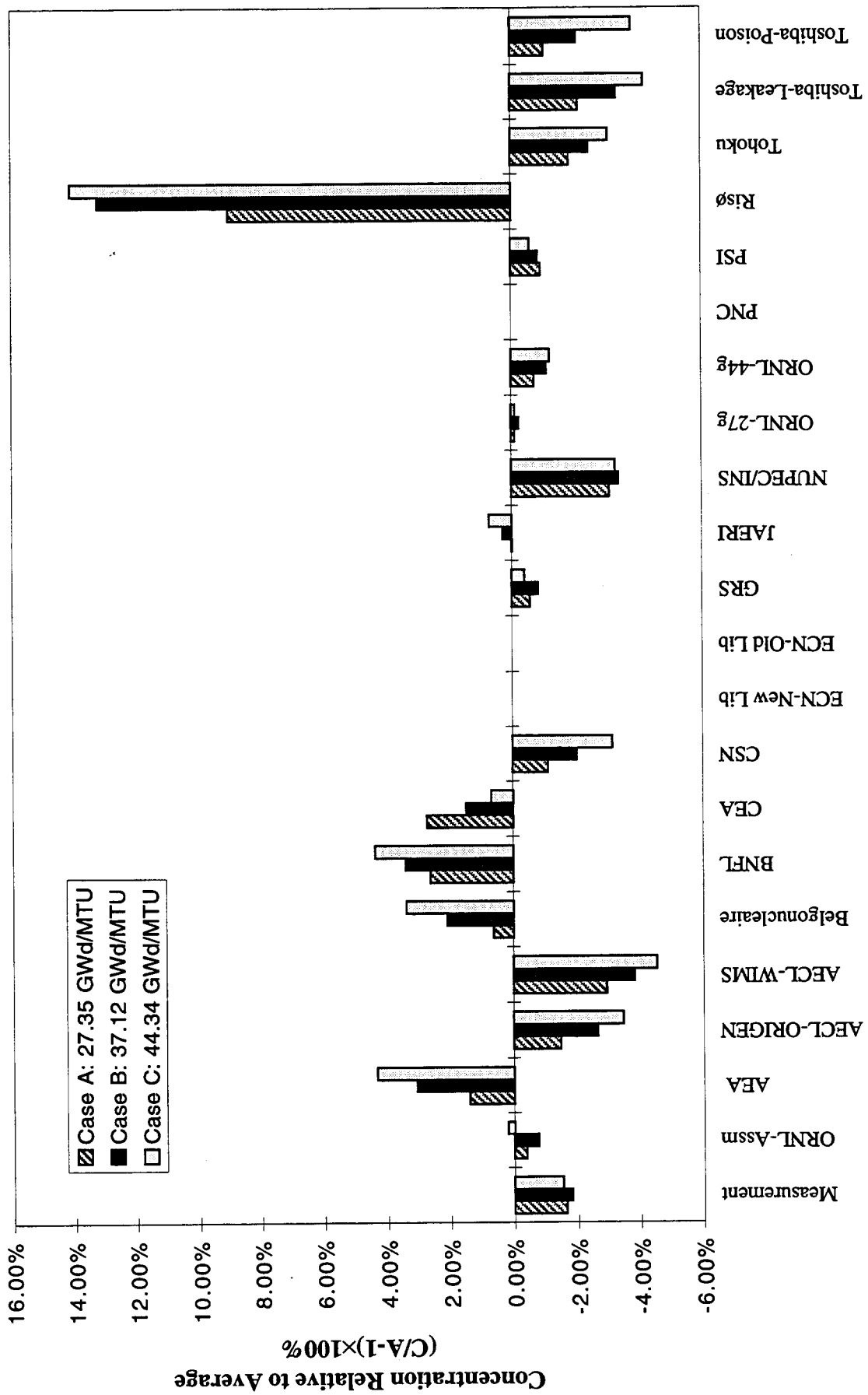


Fig. 20. Relative Nd-143 concentrations.

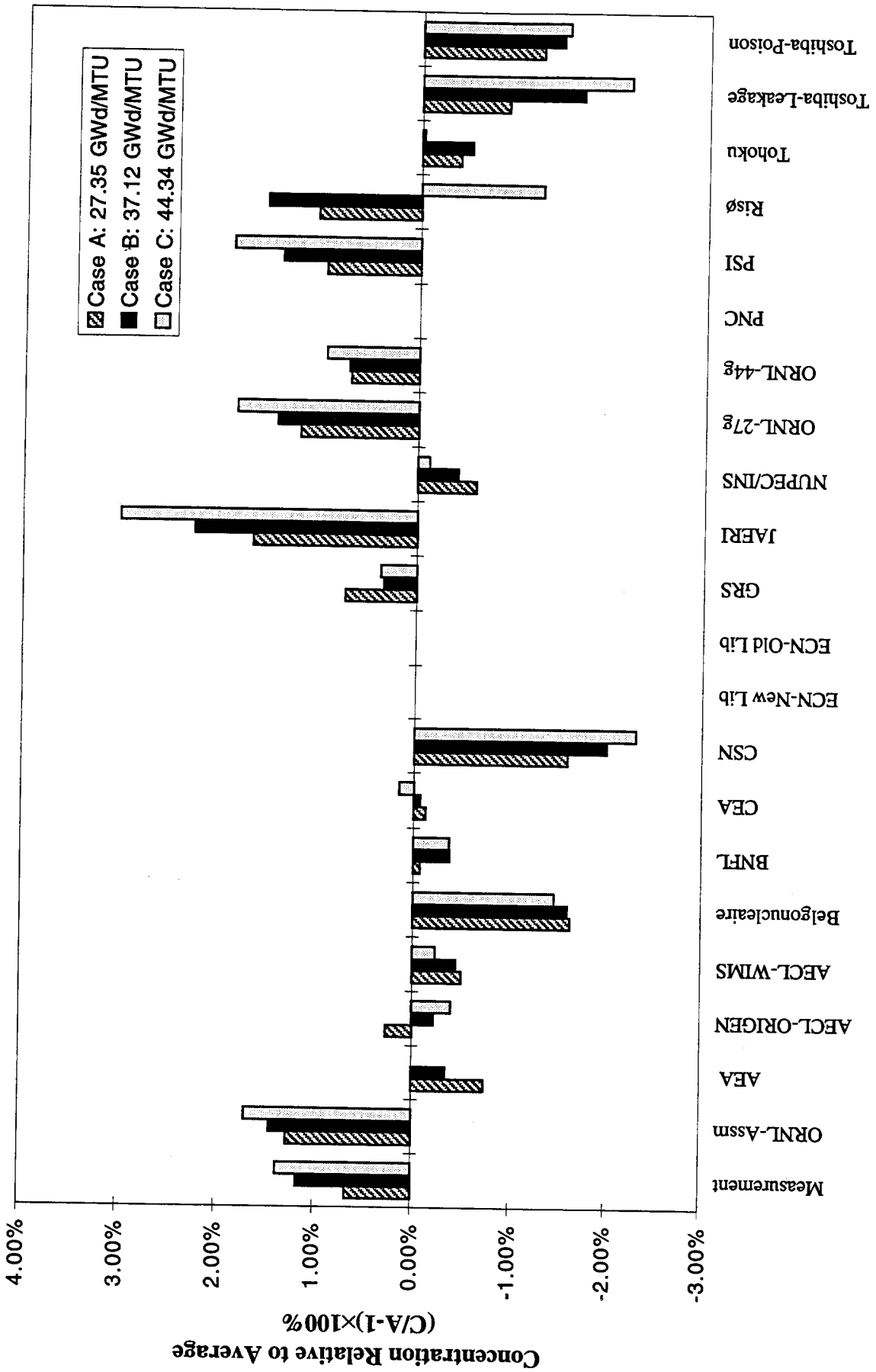


Fig. 21. Relative Nd-145 concentrations.

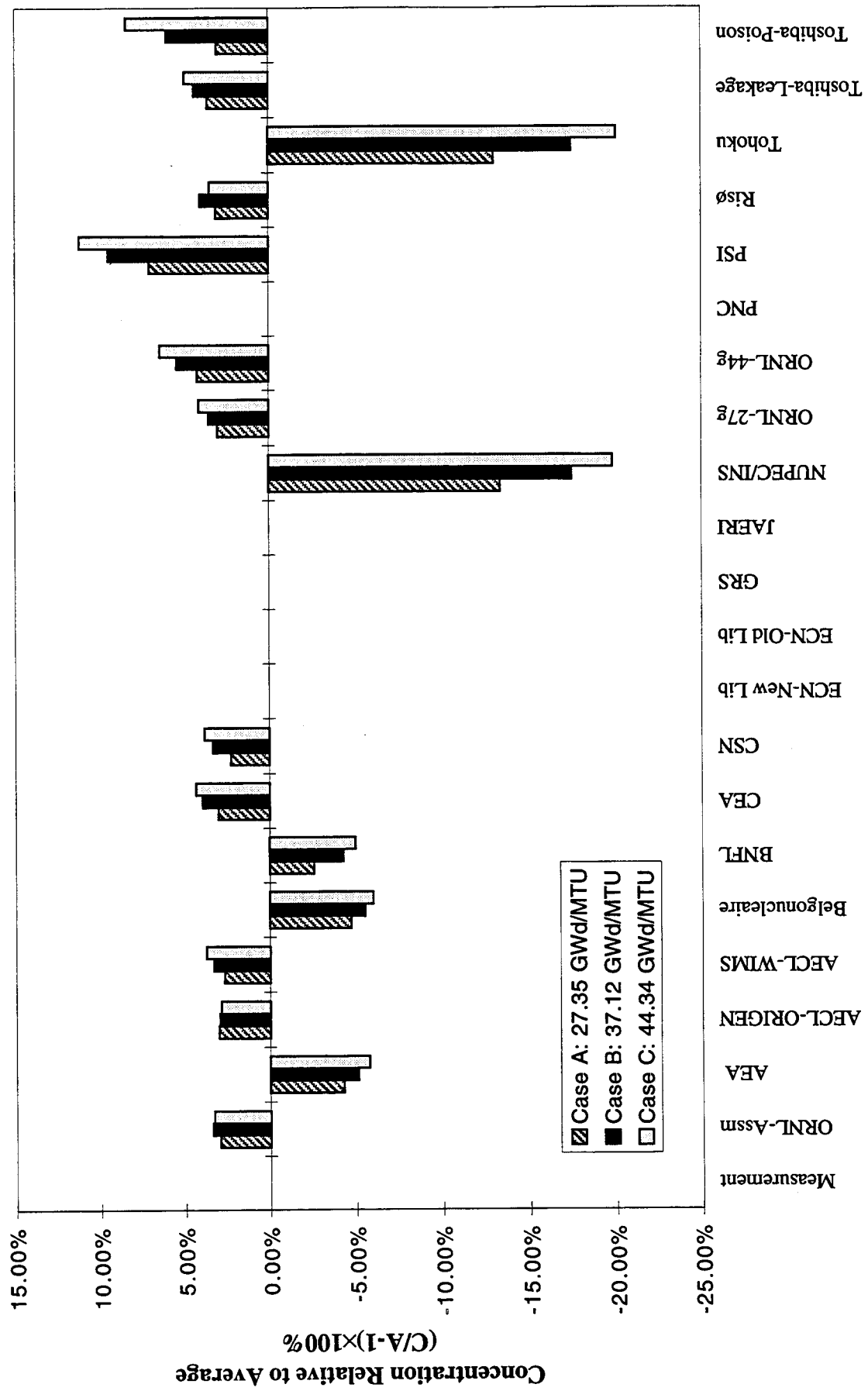


Fig. 22. Relative Sm-147 concentrations.

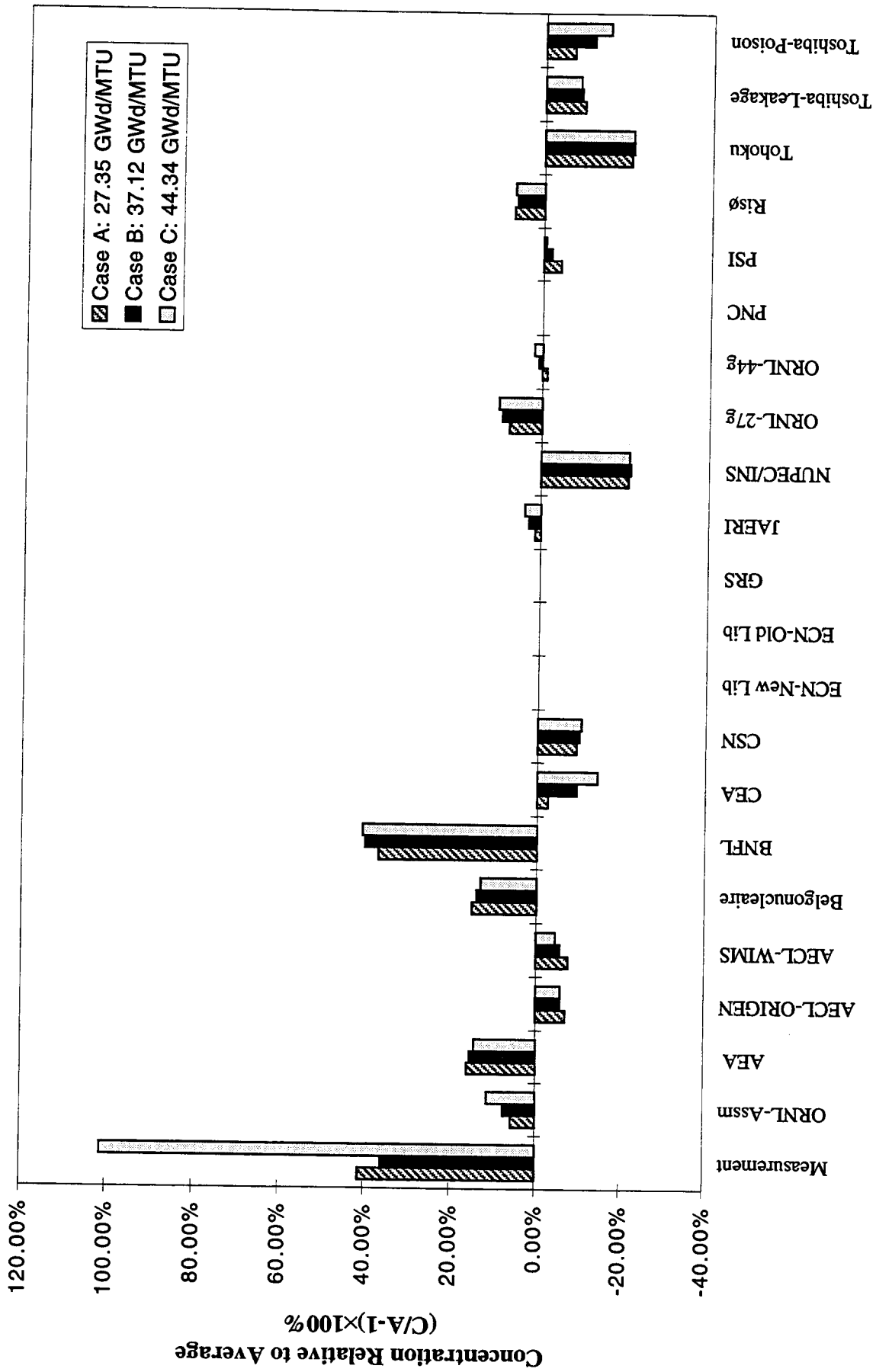


Fig. 23. Relative Sm-149 concentrations.

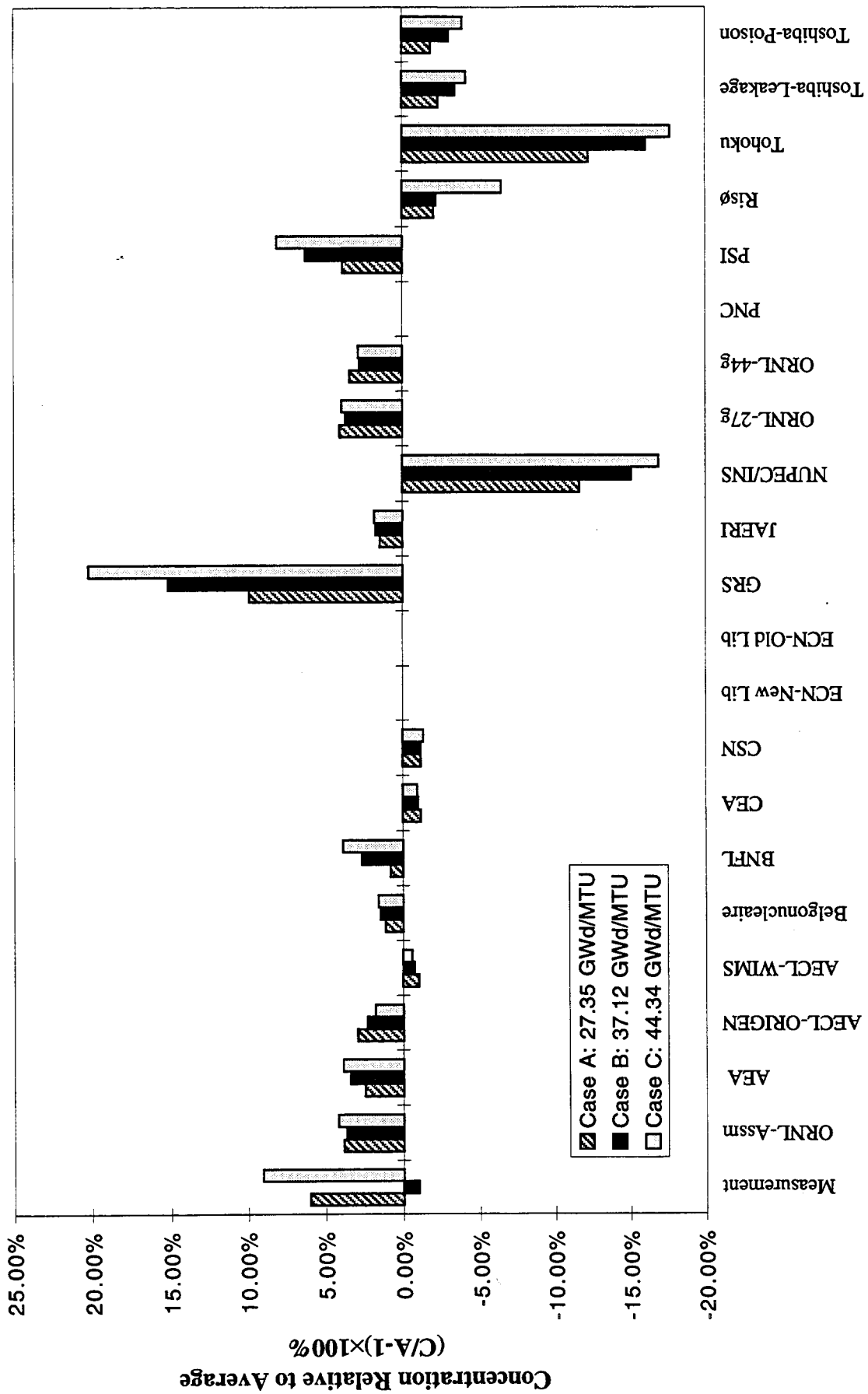


Fig. 24. Relative Sm-150 concentrations.

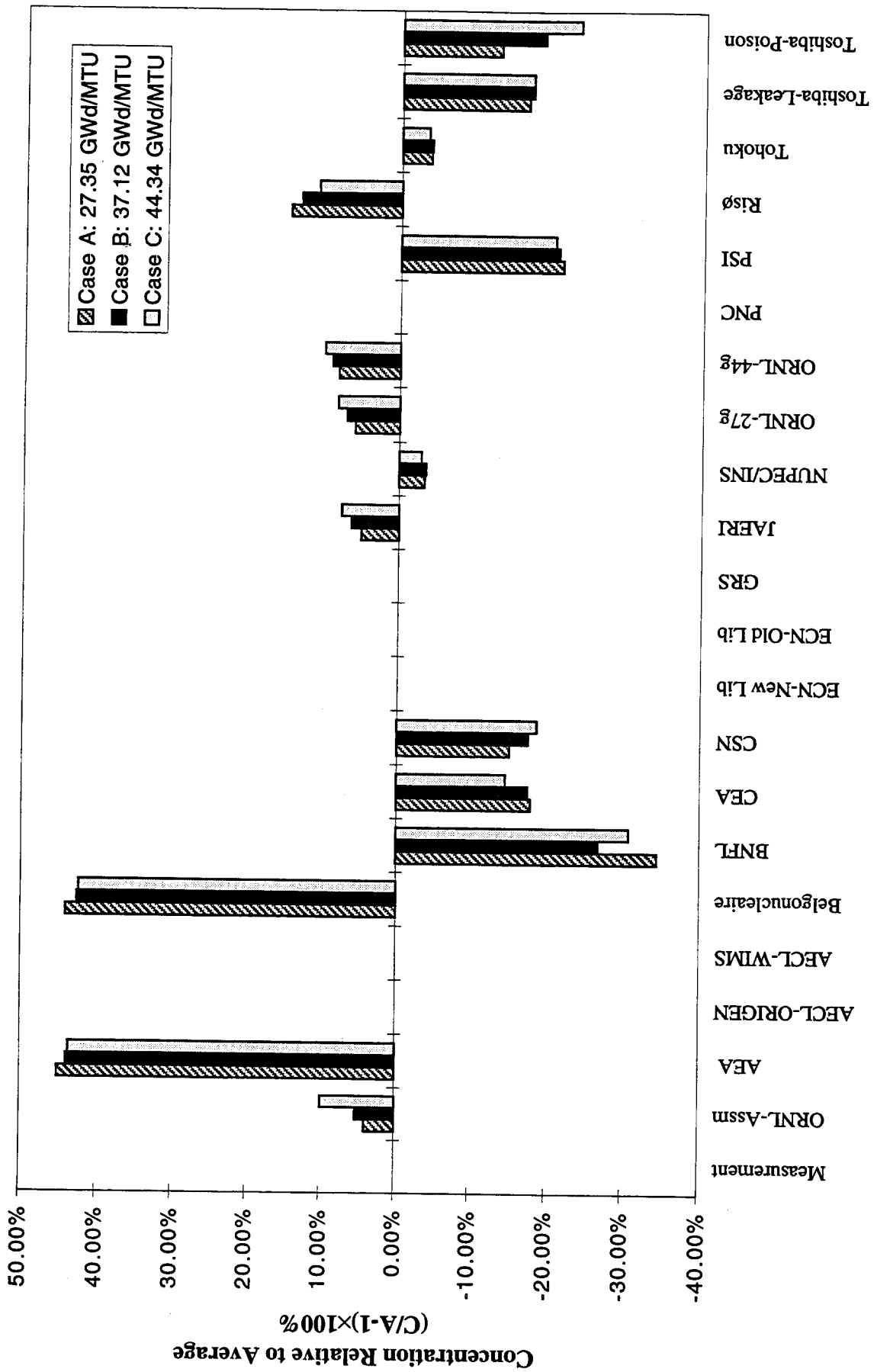


Fig. 25. Relative Sm-151 concentrations.

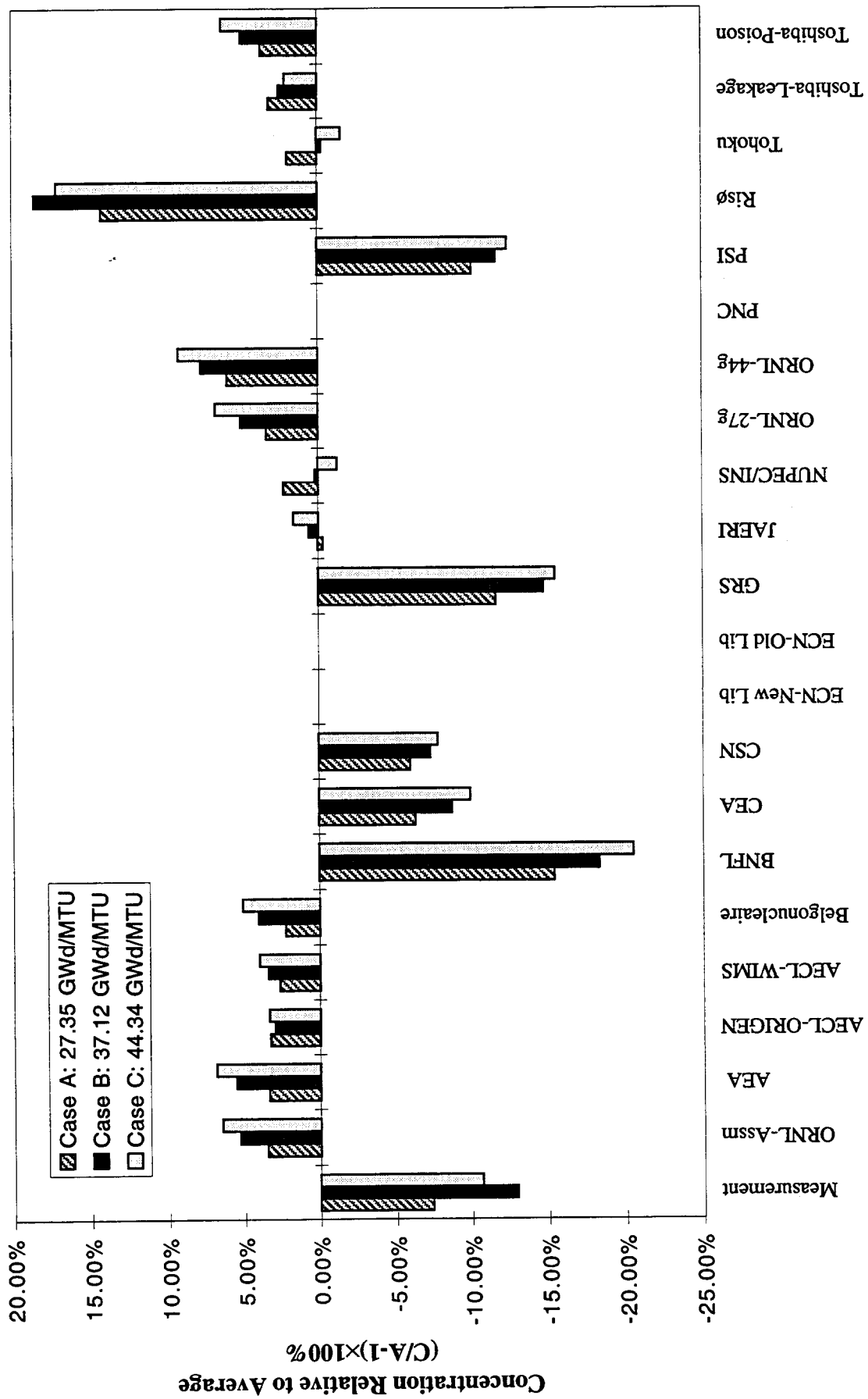


Fig. 26. Relative Sm-152 concentrations.

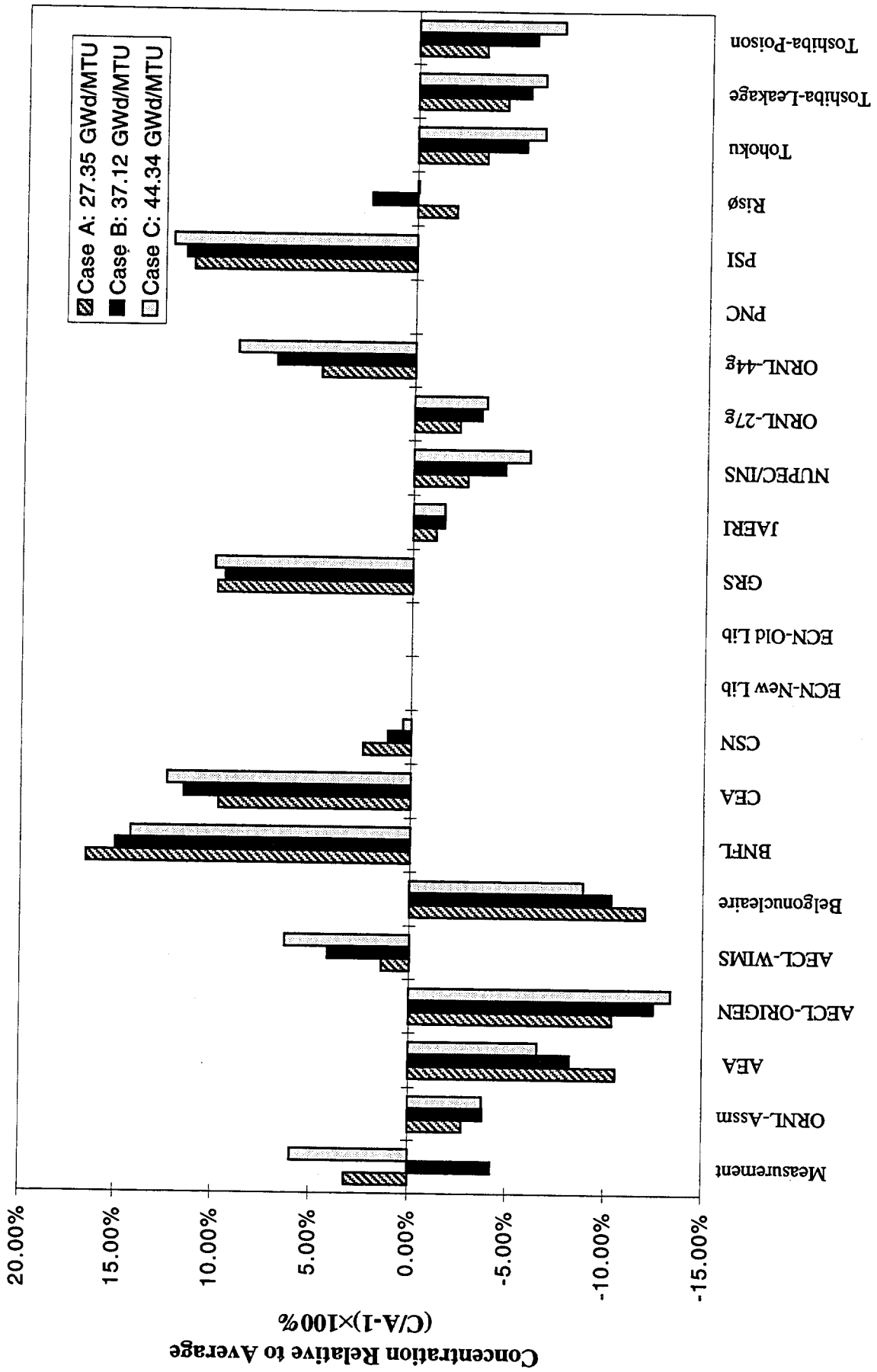


Fig. 27. Relative Eu-153 concentrations.

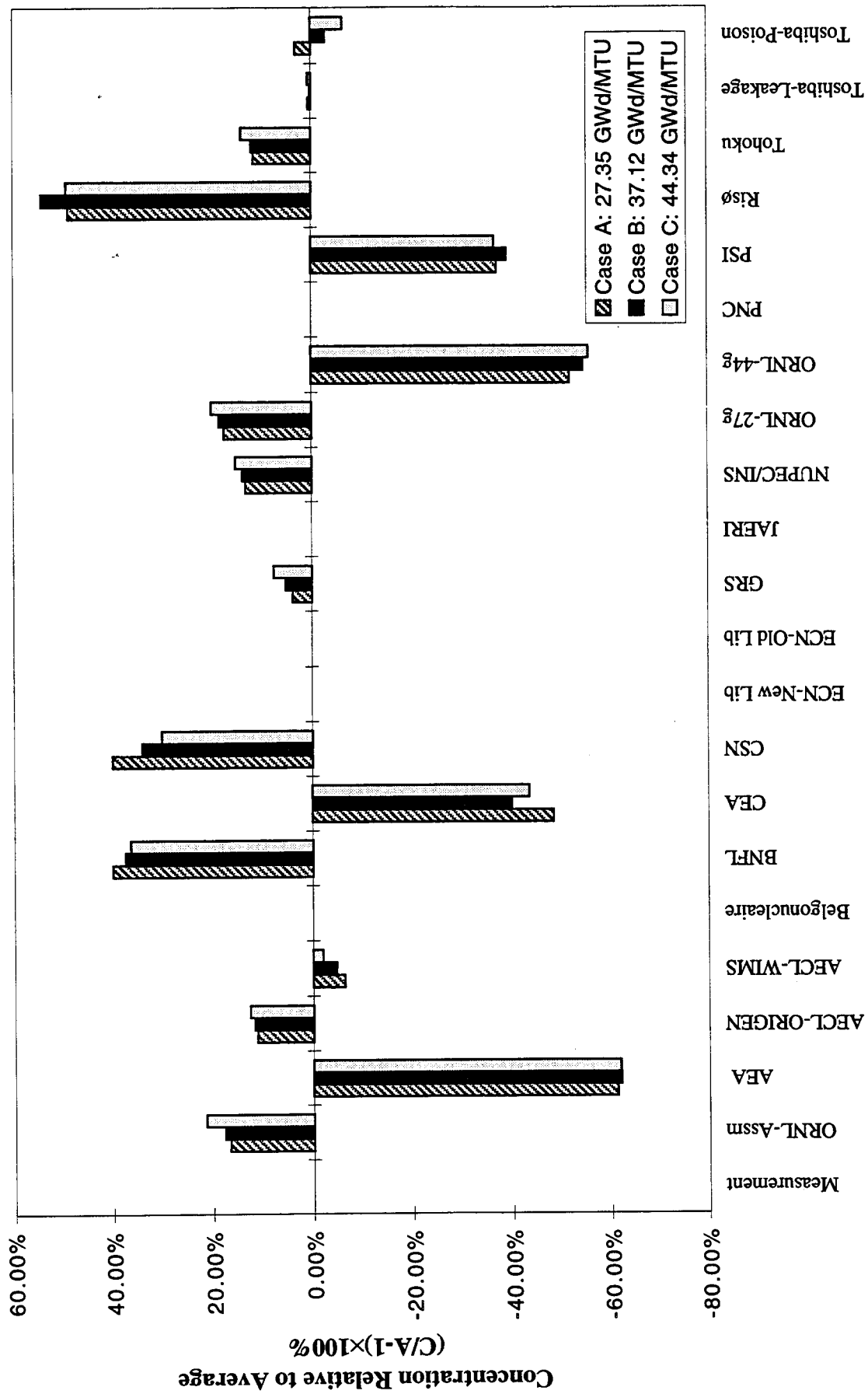


Fig. 28. Relative Gd-155 concentrations.

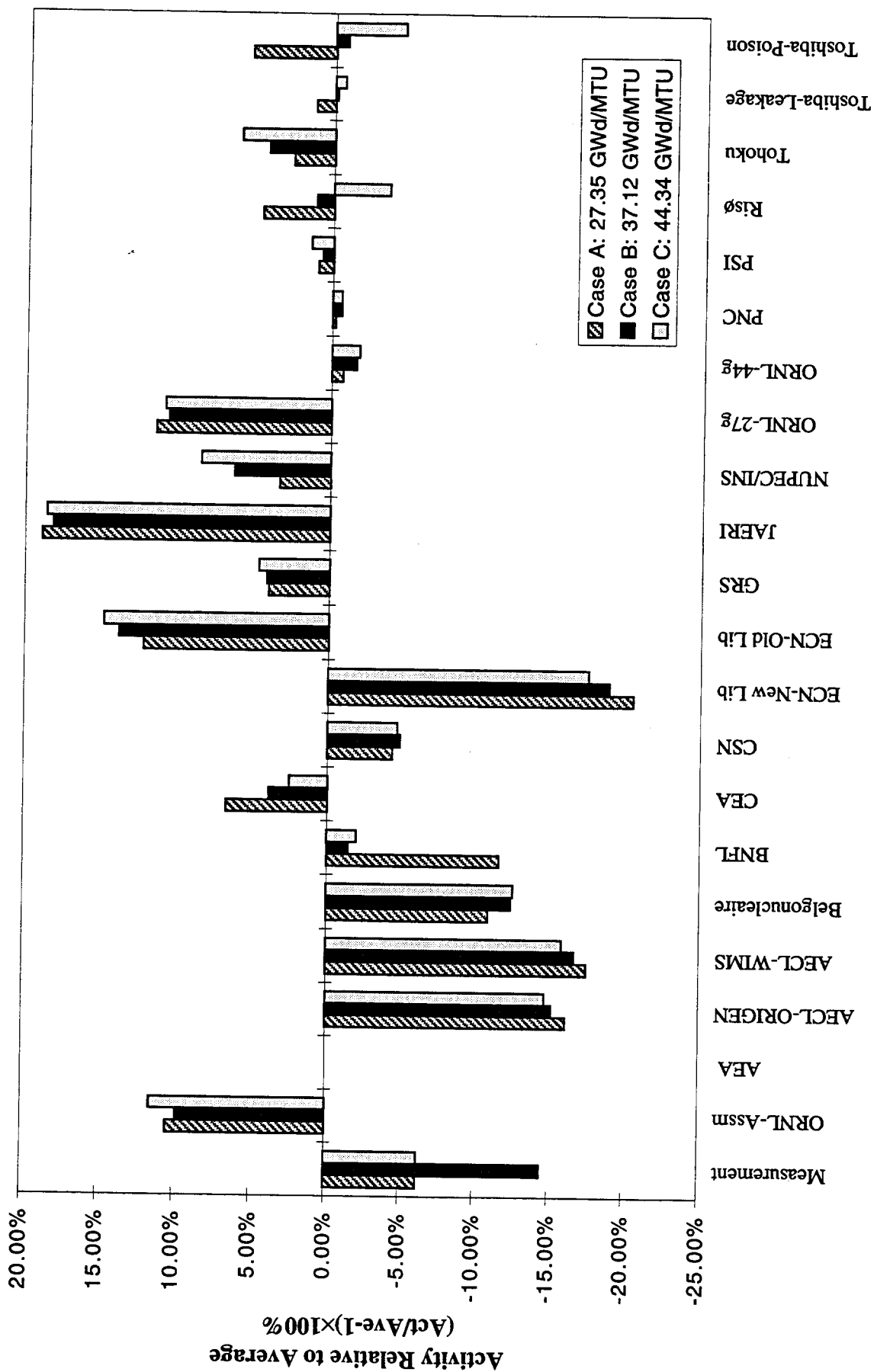


Fig. 29. Relative Np-237 activities.

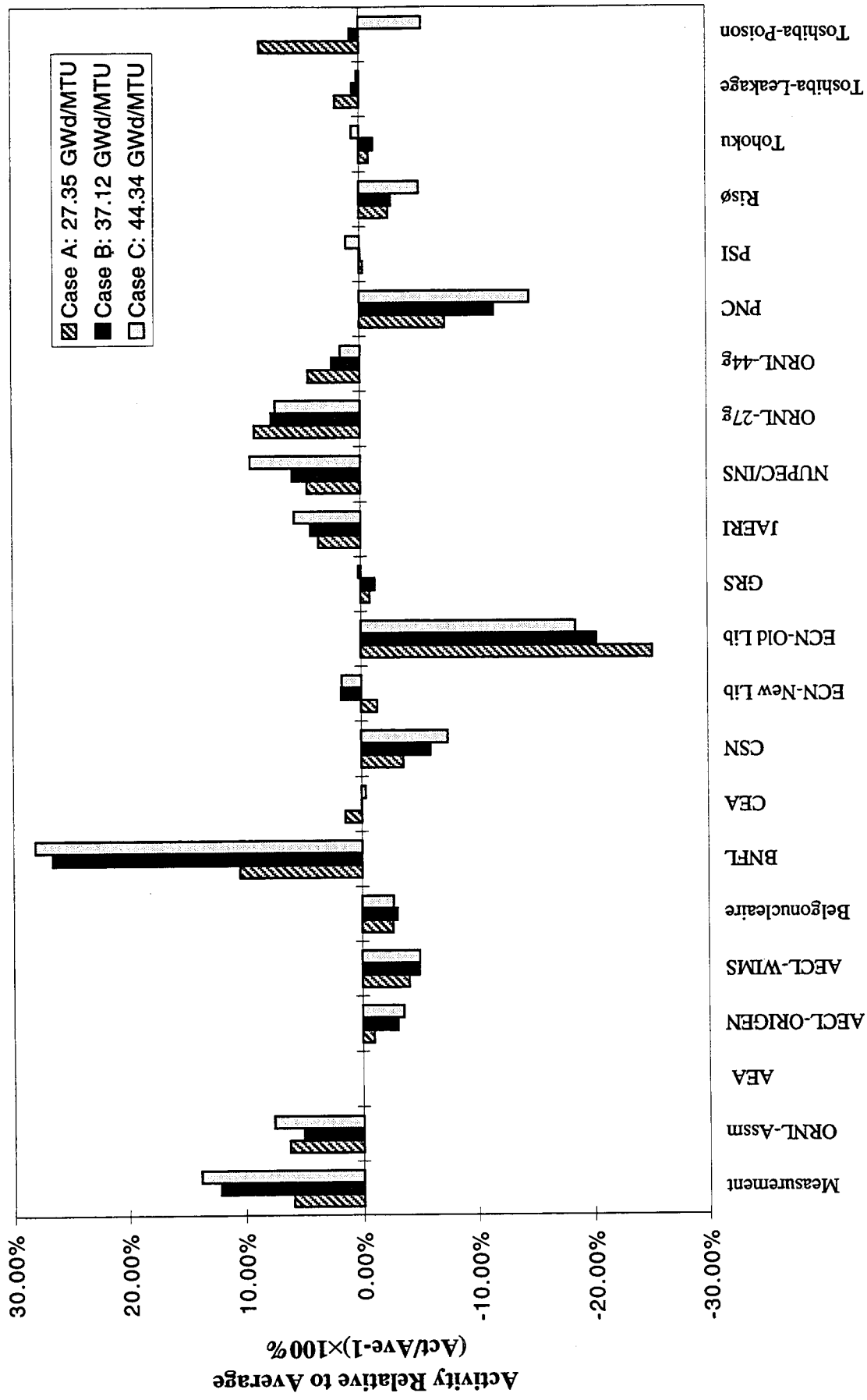


Fig. 30. Relative Am-241 activities.

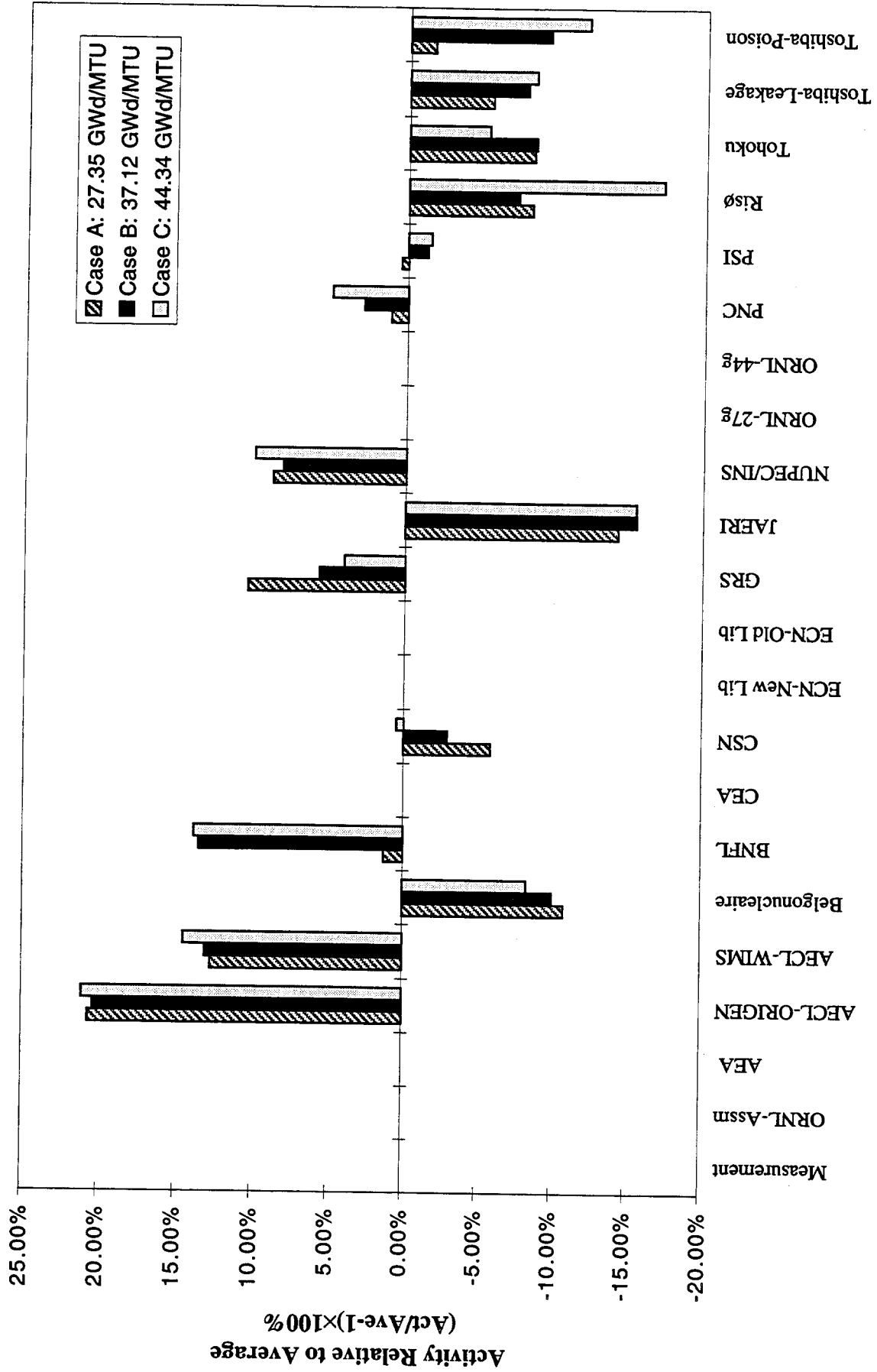


Fig. 31. Relative Am-243 activities.

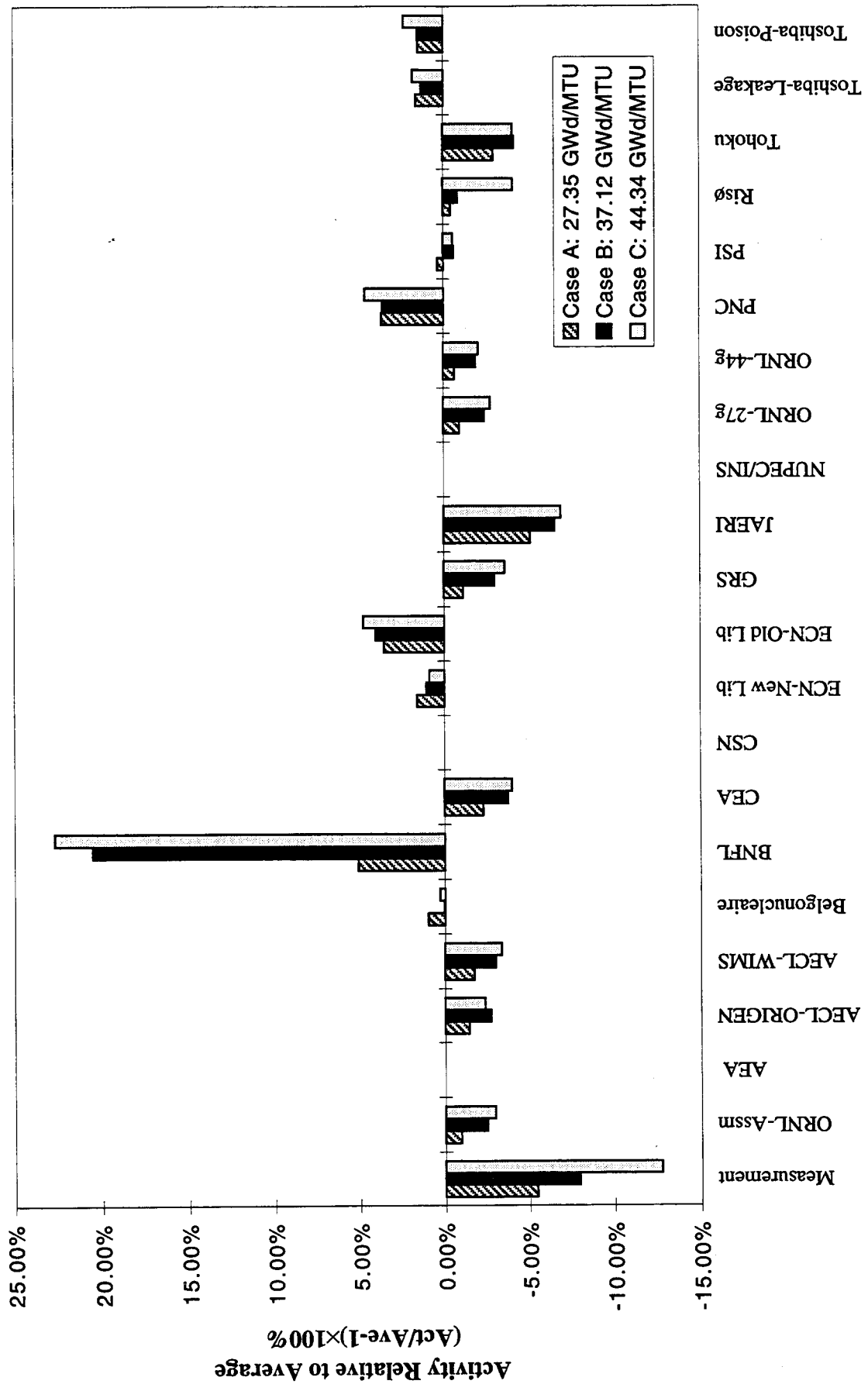


Fig. 32. Relative Tc-99 activities.

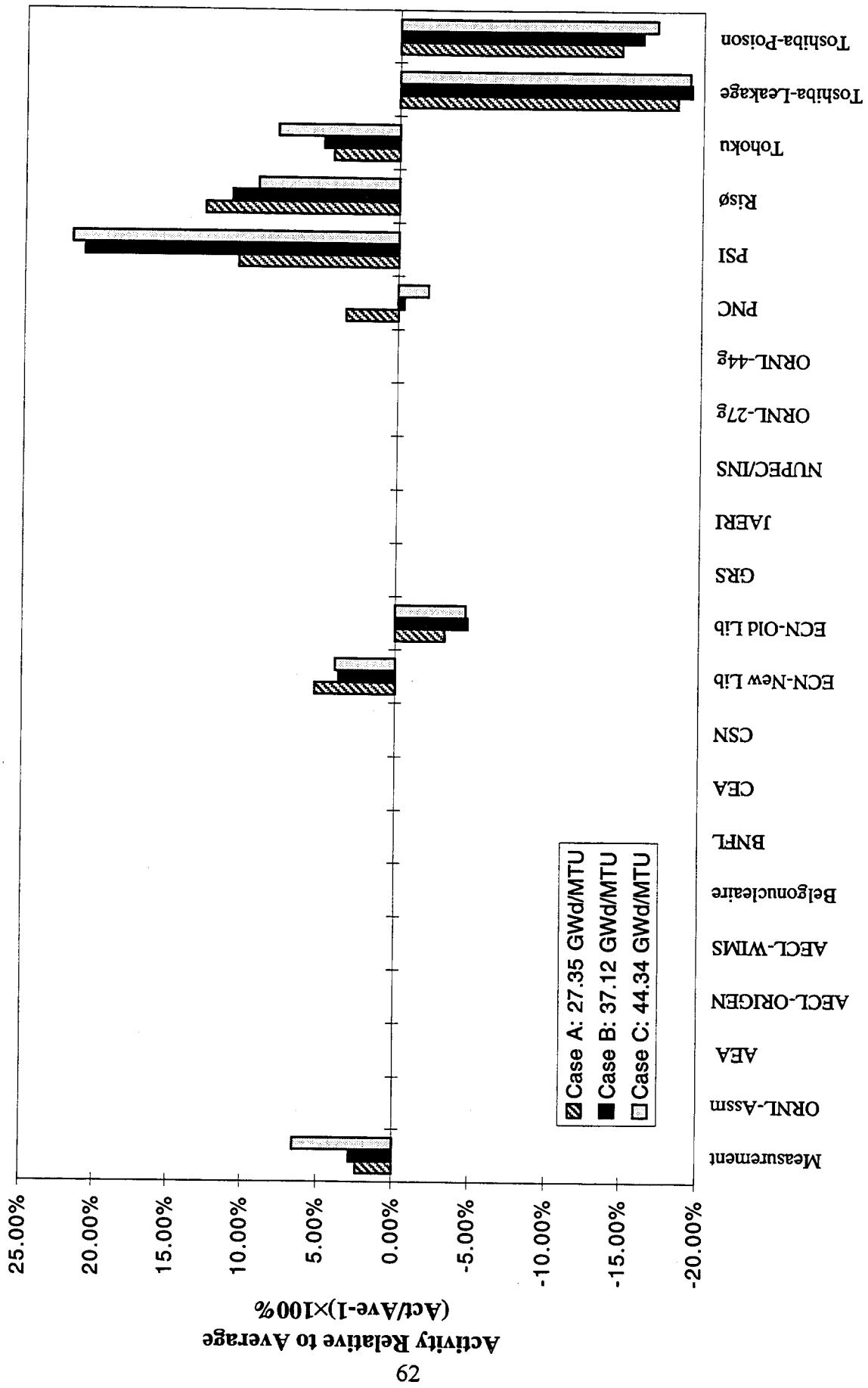


Fig. 33. Relative Cs-135 activities.

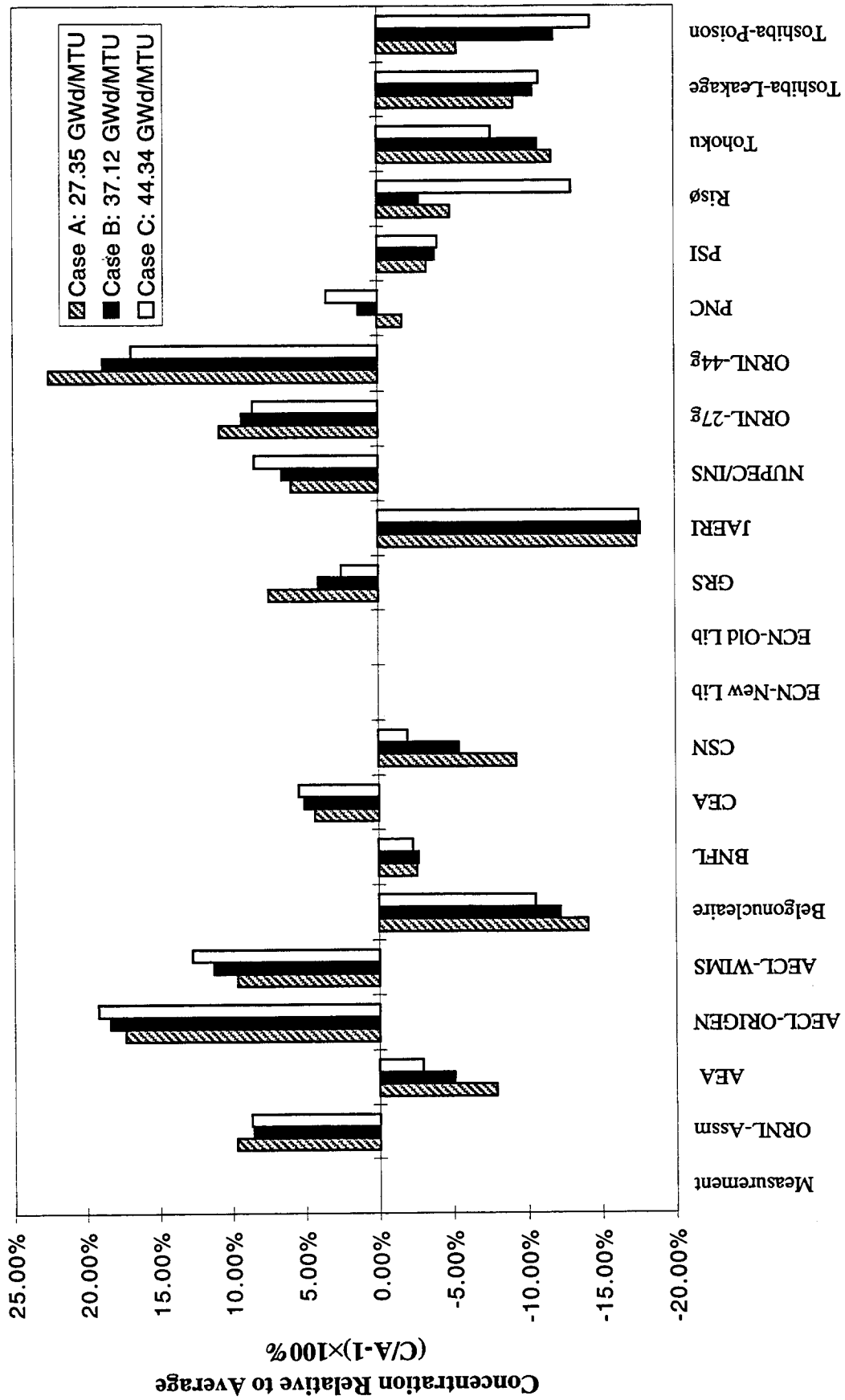


Fig. 34. Relative Am-243 concentrations with converted activities.

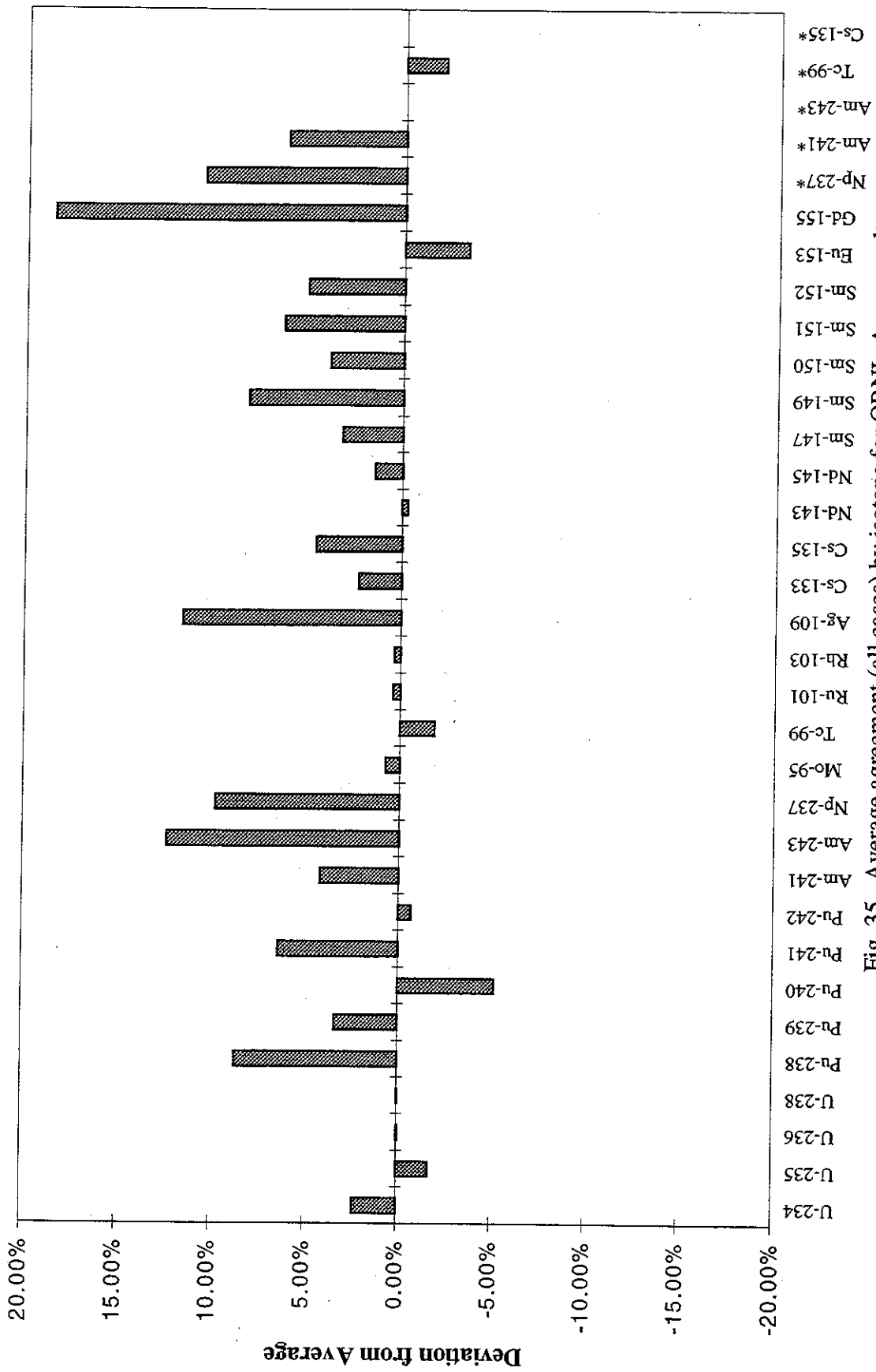


Fig. 35. Average agreement (all cases) by isotope for ORNL-Assm results.
 (*Isotopic abundance measured in terms of activity.)

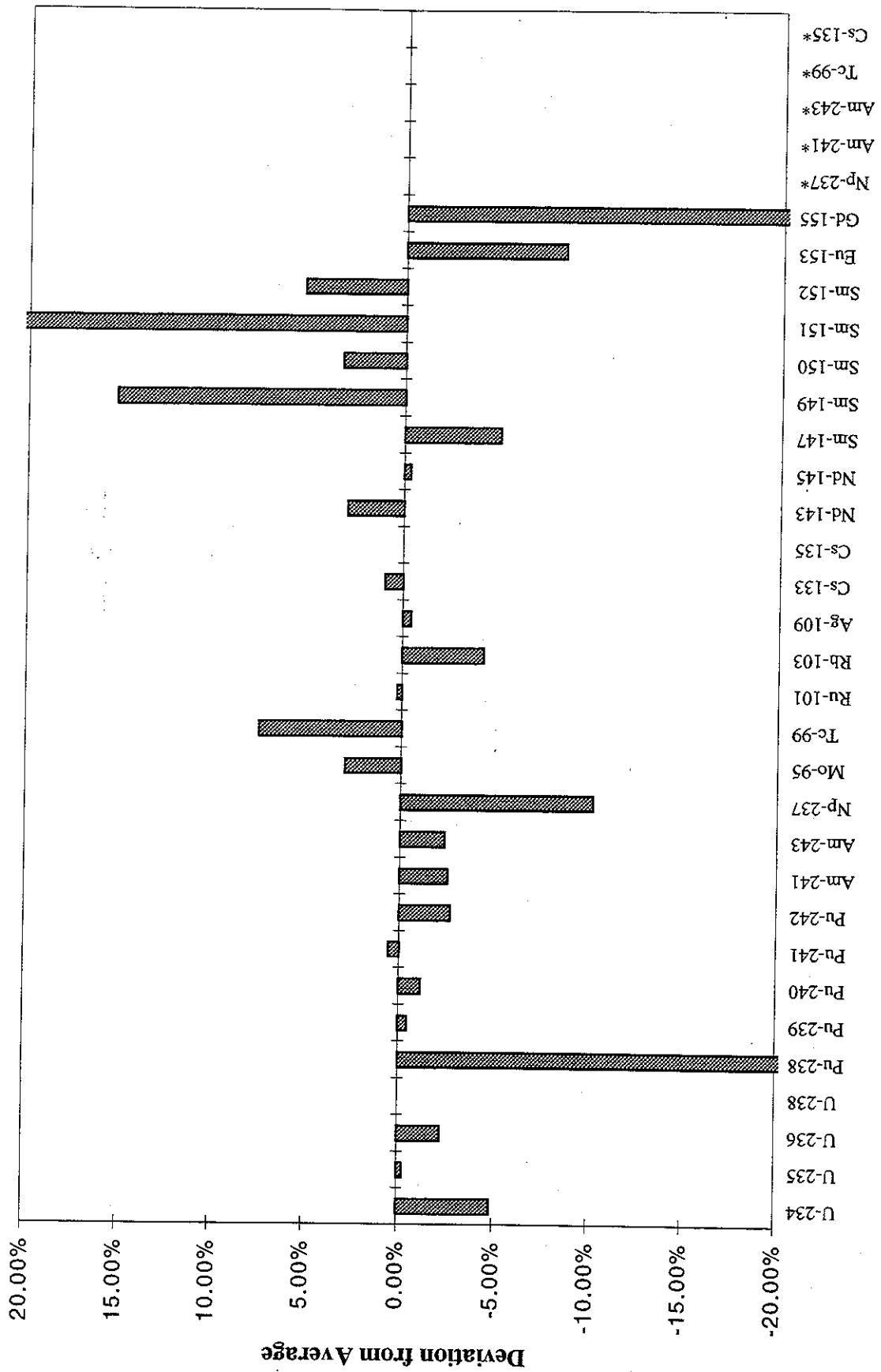


Fig. 36. Average agreement (all cases) by isotope for AEA results.
 (*Isotopic abundance measured in terms of activity.)

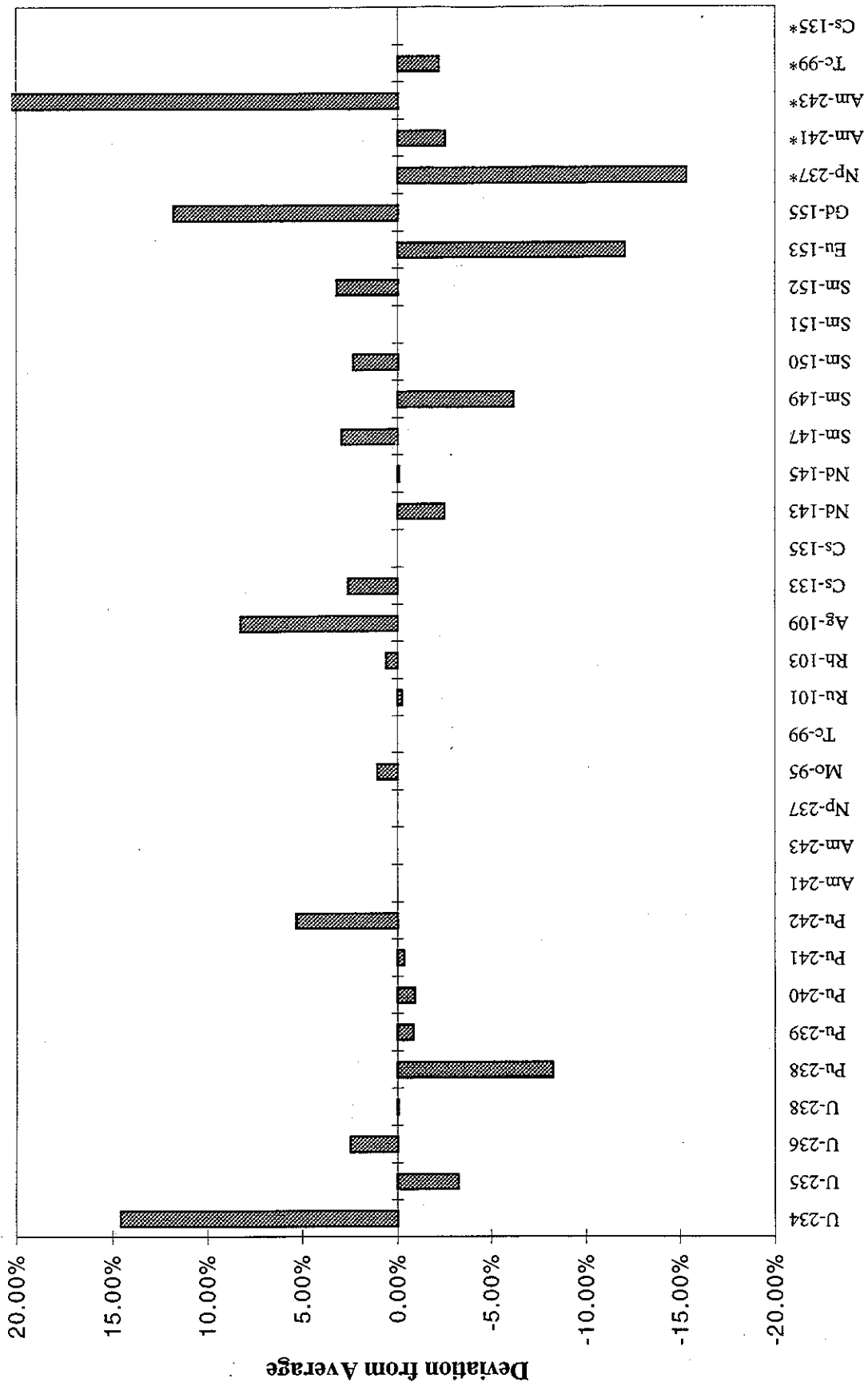


Fig. 37. Average agreement (all cases) by isotope for AECL-ORIGEN results.
 (* Isotopic abundance measured in terms of activity.)

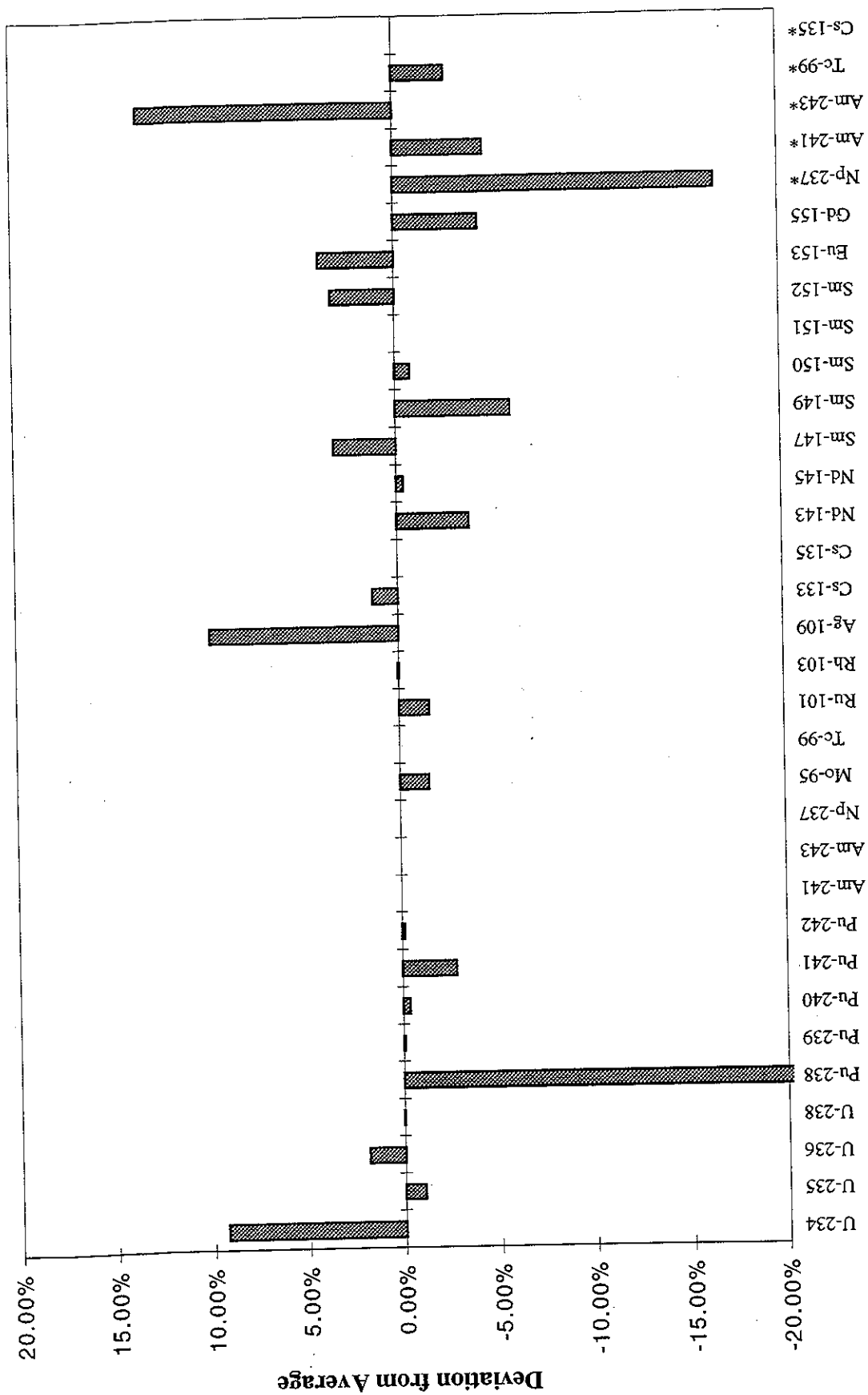


Fig. 38. Average agreement (all cases) by isotope for AECL-WIMS results.
 (*Isotopic abundance measured in terms of activity.)

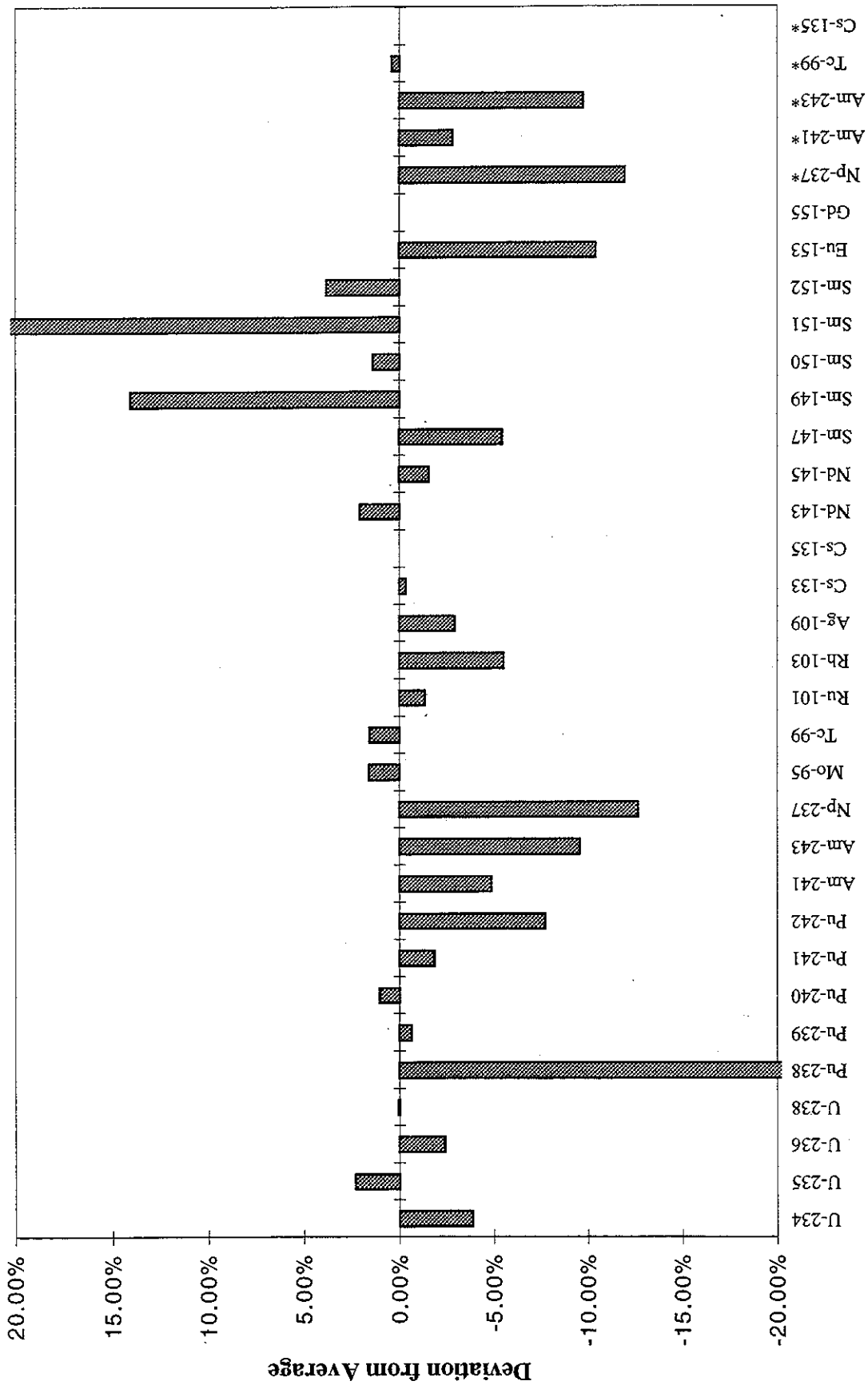


Fig. 39. Average agreement (all cases) by isotope for Belgonuclaire results.
 (*Isotopic abundance measured in terms of activity.)

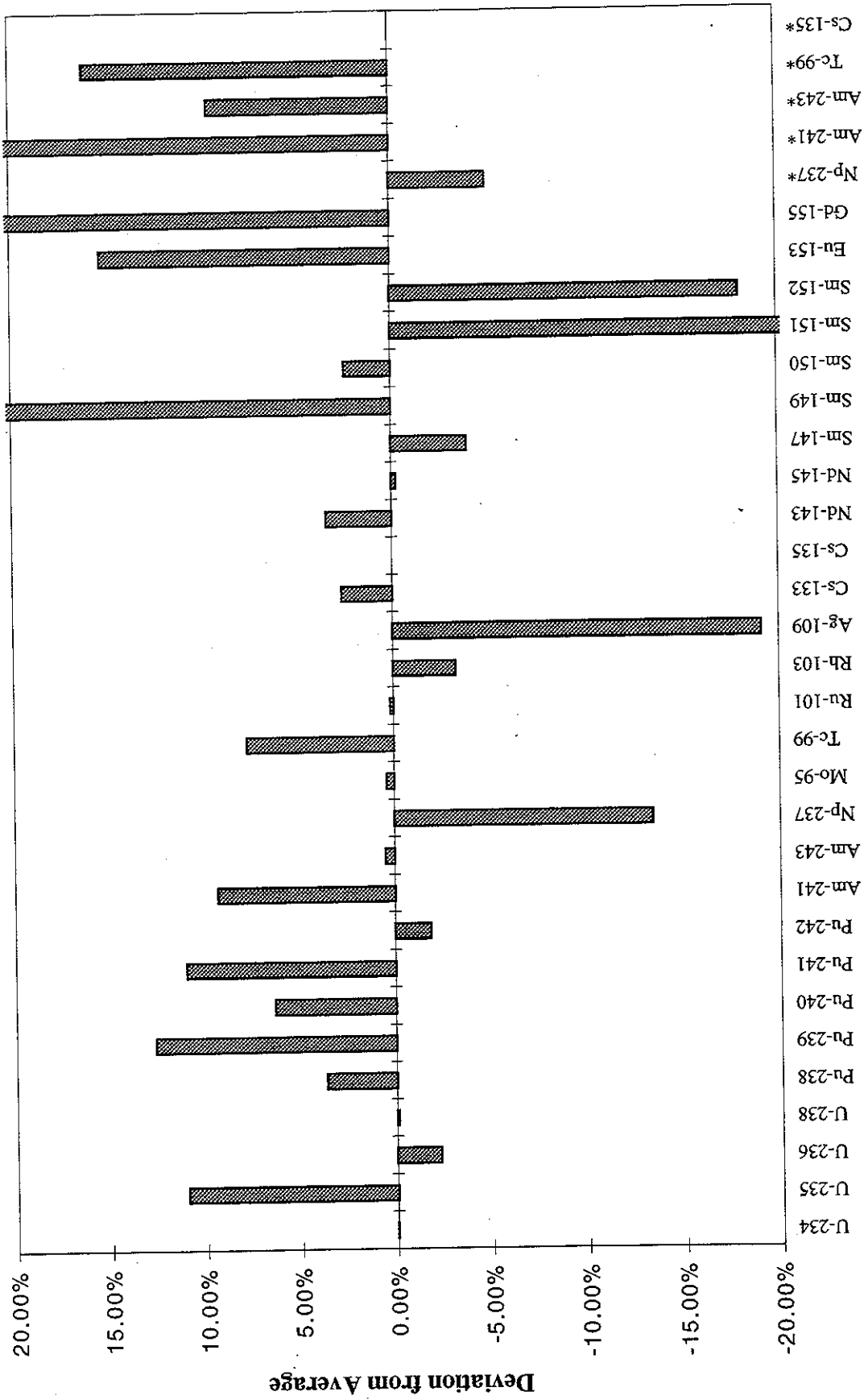


Fig. 40. Average agreement (all cases) by isotope for BNFL results.
 (*Isotopic abundance measured in terms of activity.)

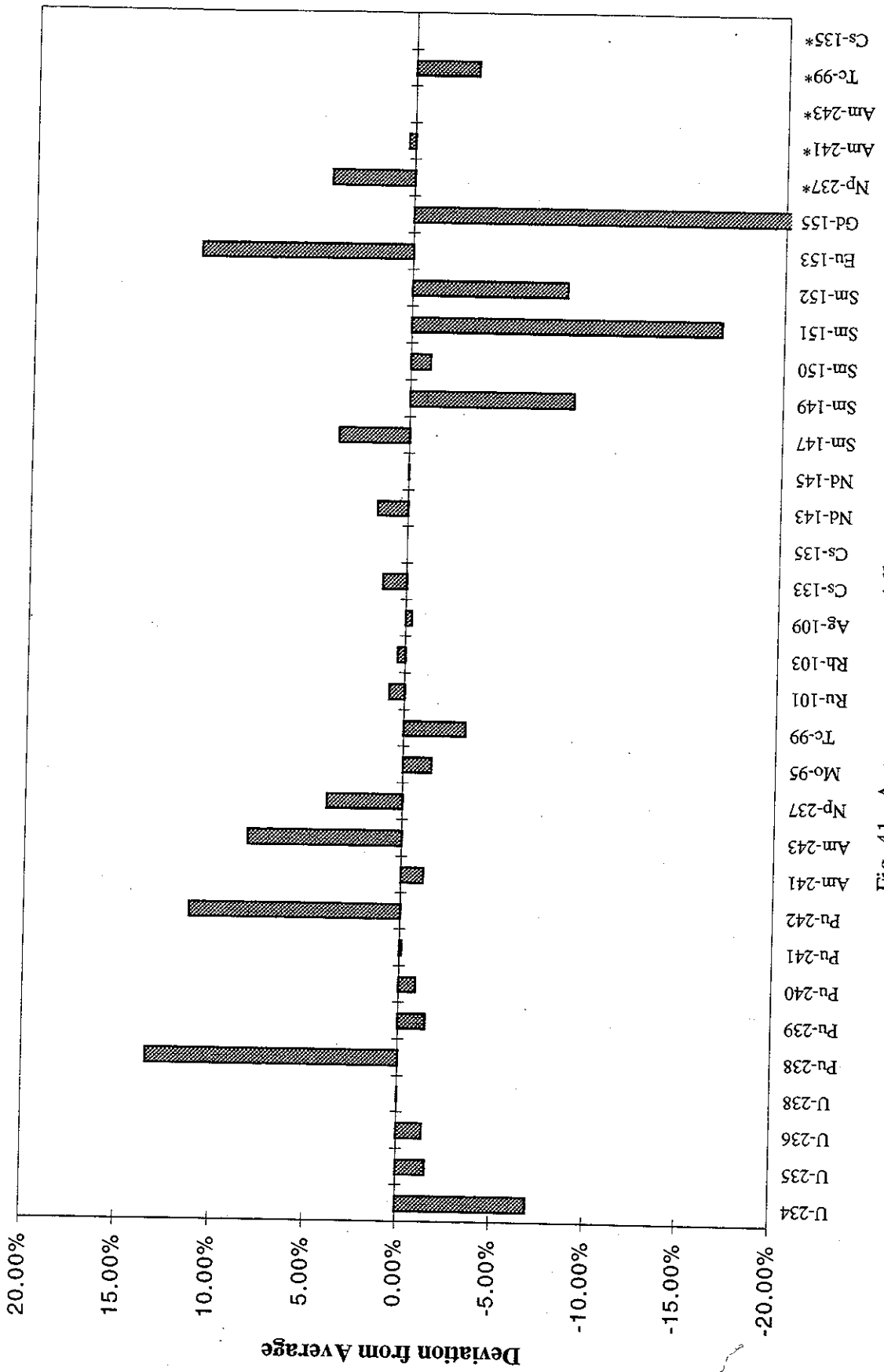


Fig. 41. Average agreement (all cases) by isotope for CEA results.
 (*Isotopic abundance measured in terms of activity.)

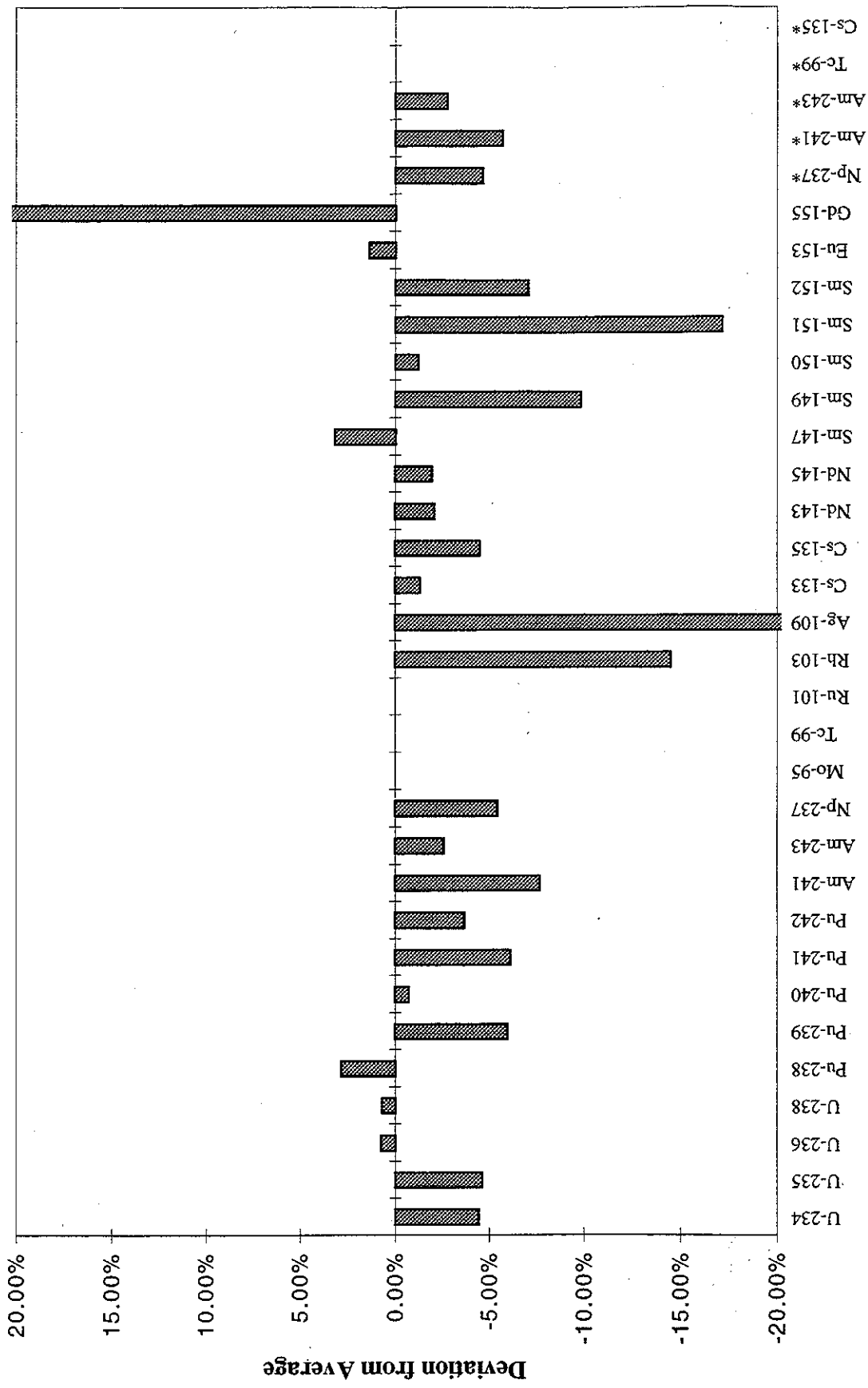


Fig. 42. Average agreement (all cases) by isotope for CSN results.
 (*Isotopic abundance measured in terms of activity.)

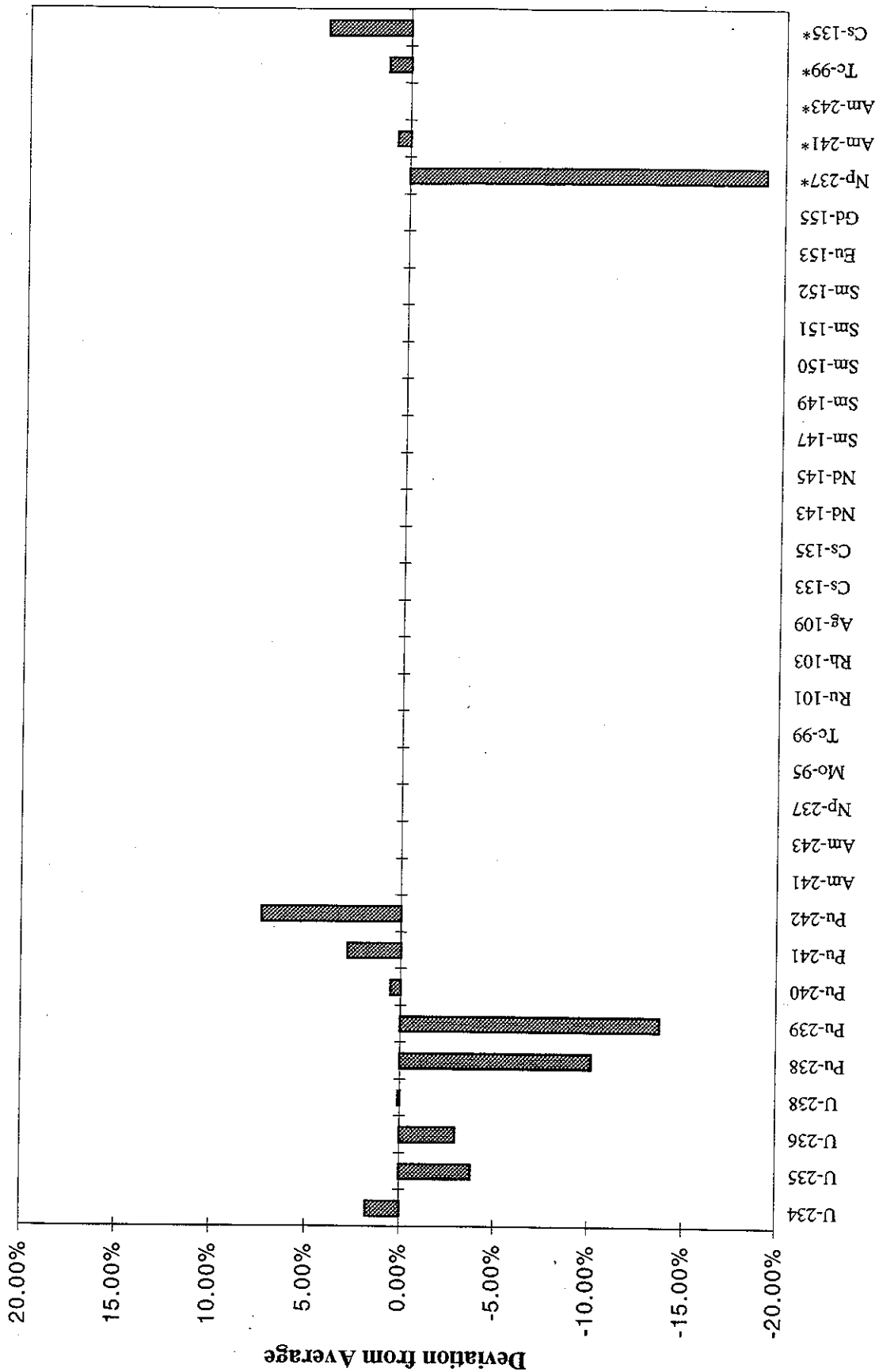


Fig. 43. Average agreement (all cases) by isotope for ECN-New Lib results.
 (* Isotopic abundance measured in terms of activity.)

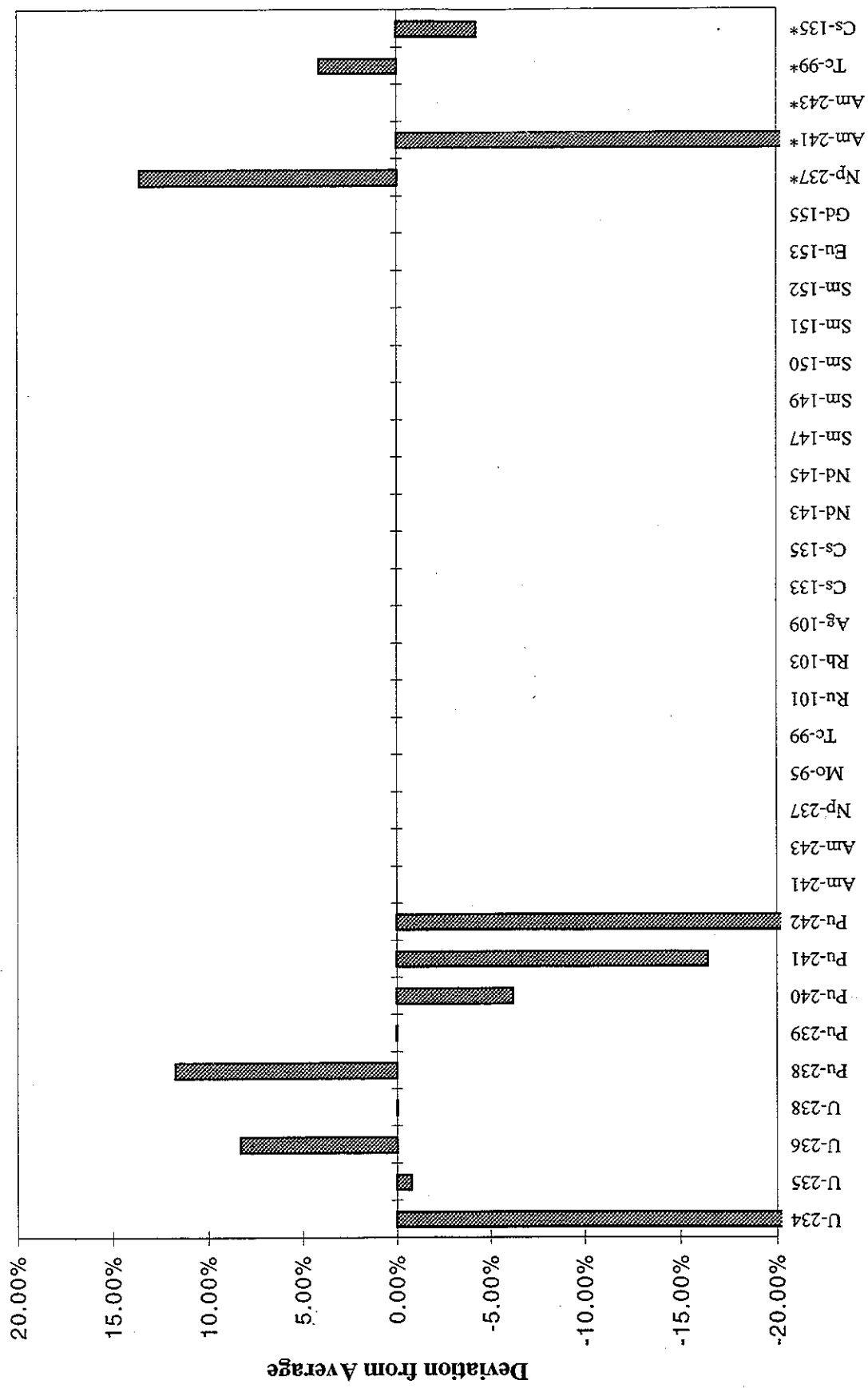


Fig. 44. Average agreement (all cases) by isotope for ECN-Old Lib results.
 (*Isotopic abundance measured in terms of activity.)

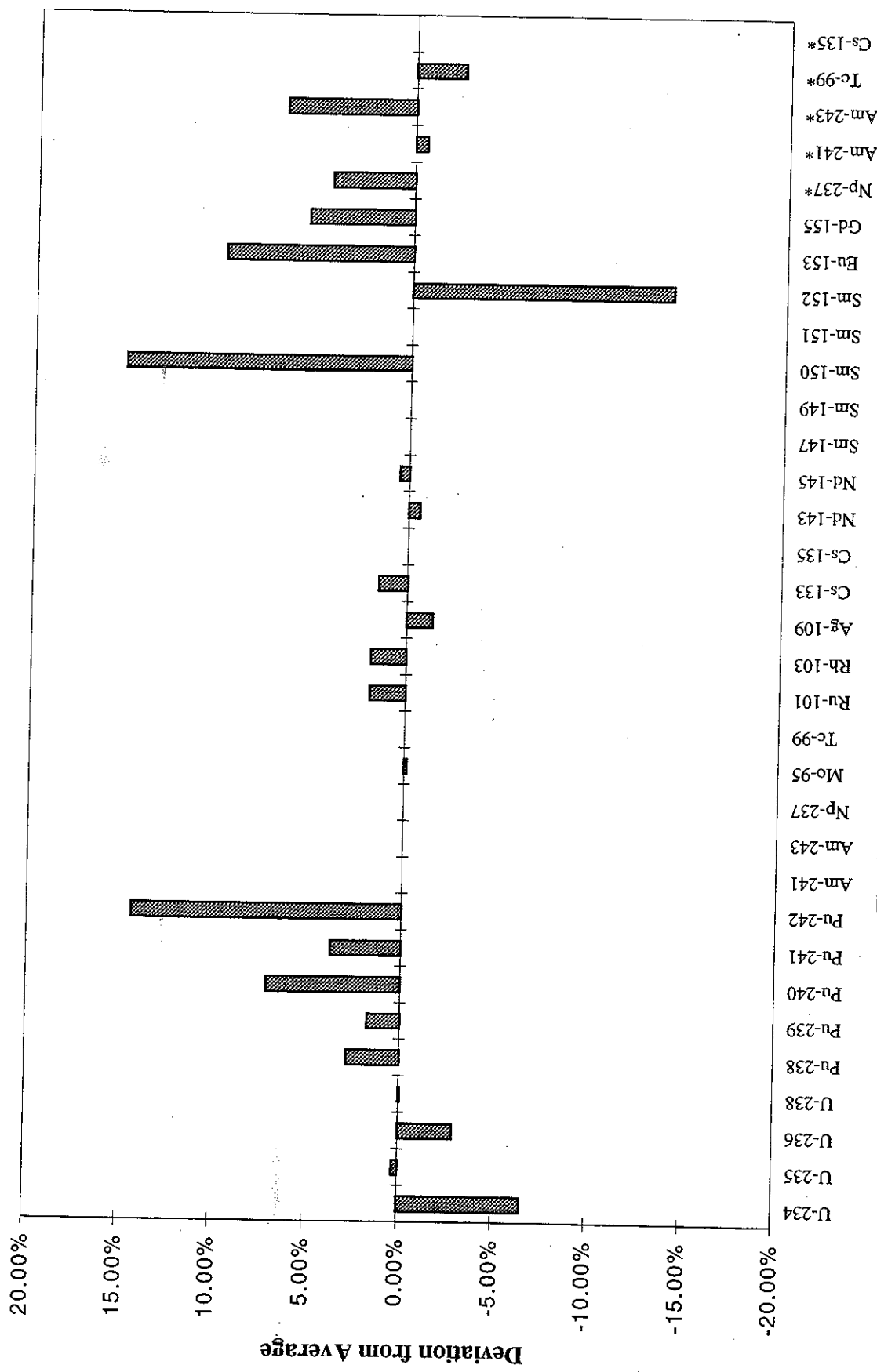


Fig. 45. Average agreement (all cases) by isotope for GRS results.
 (*Isotopic abundance measured in terms of activity.)

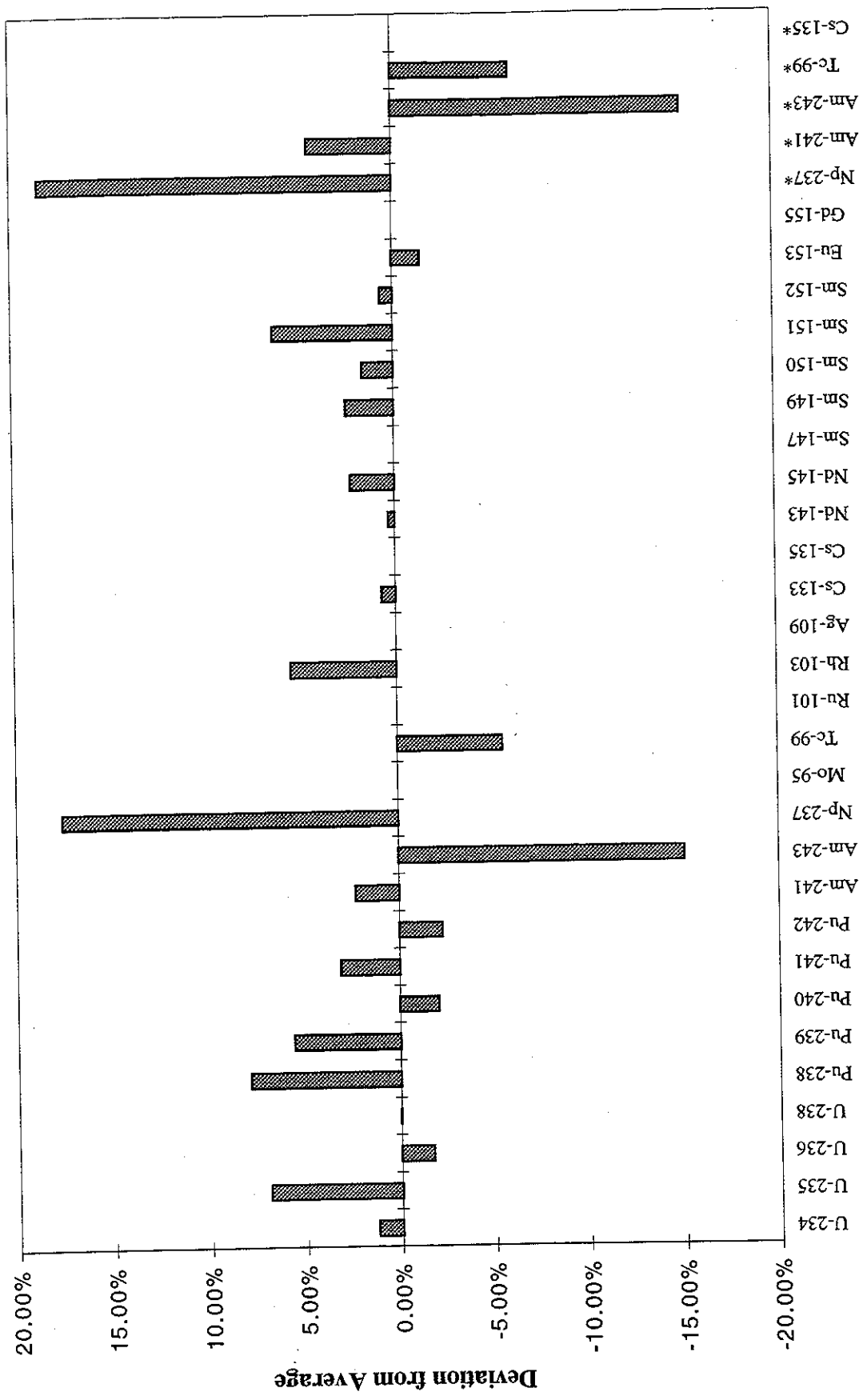


Fig. 46. Average agreement (all cases) by isotope for JAERI results. (* Isotopic abundance measured in terms of activity.)

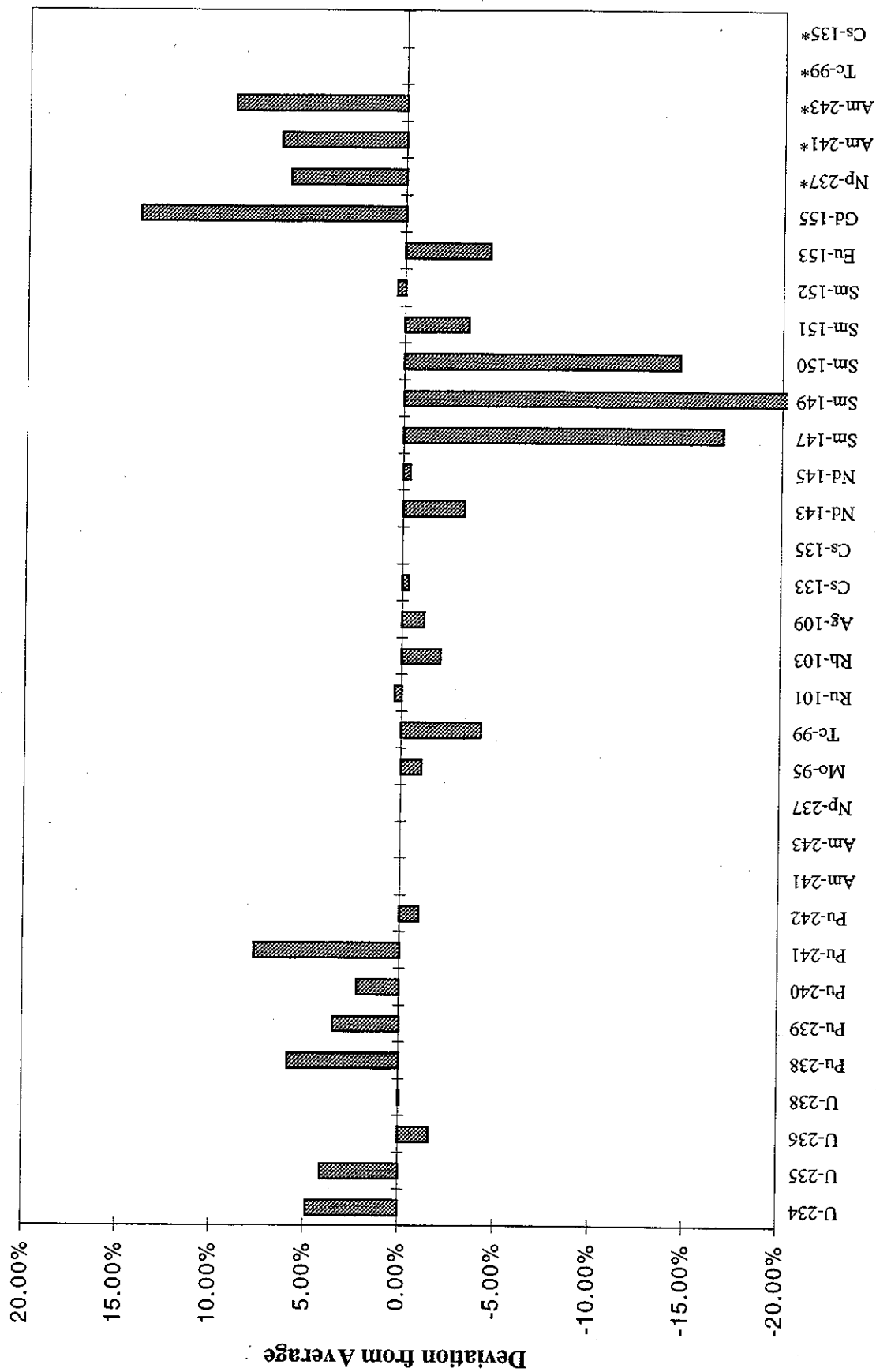


Fig. 47. Average agreement (all cases) by isotope for NUPEC/INS results.
 (* Isotopic abundance measured in terms of activity.)

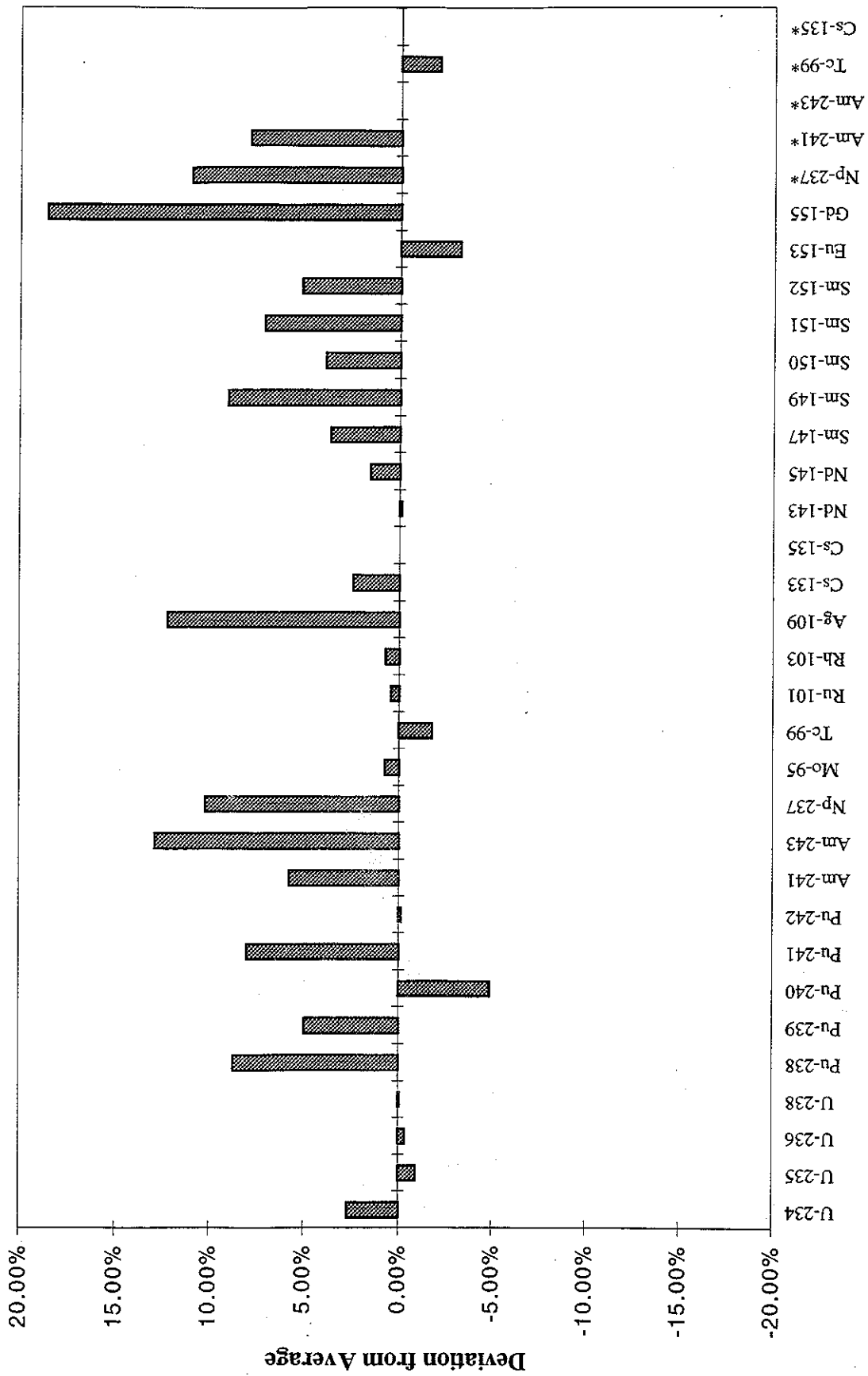


Fig. 48. Average agreement (all cases) by isotope for ORNL-27g results.
 (*Isotopic abundance measured in terms of activity.)

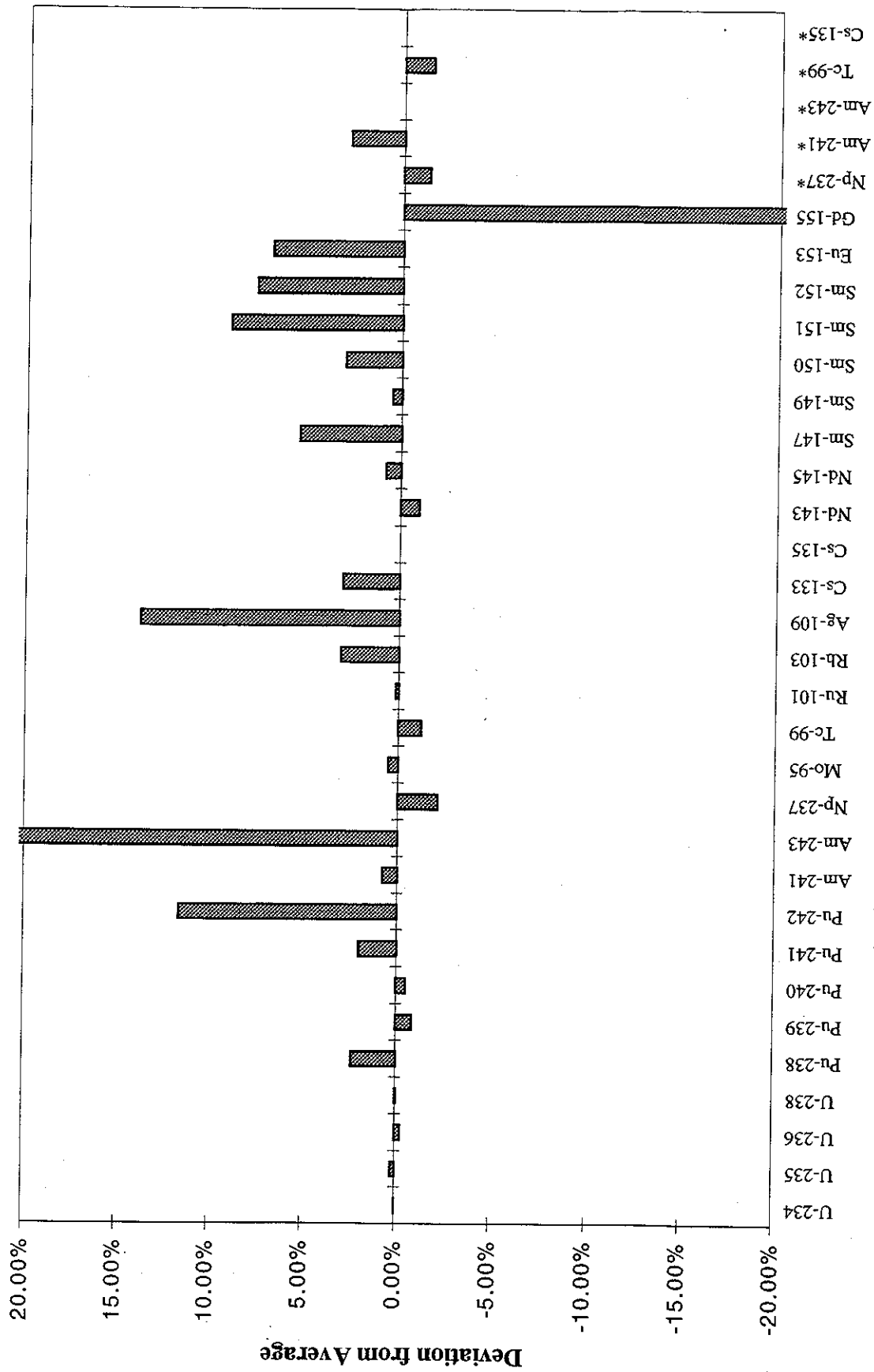


Fig. 49. Average agreement (all cases) by isotope for ORNL-44g results.
 (*Isotopic abundance measured in terms of activity.)

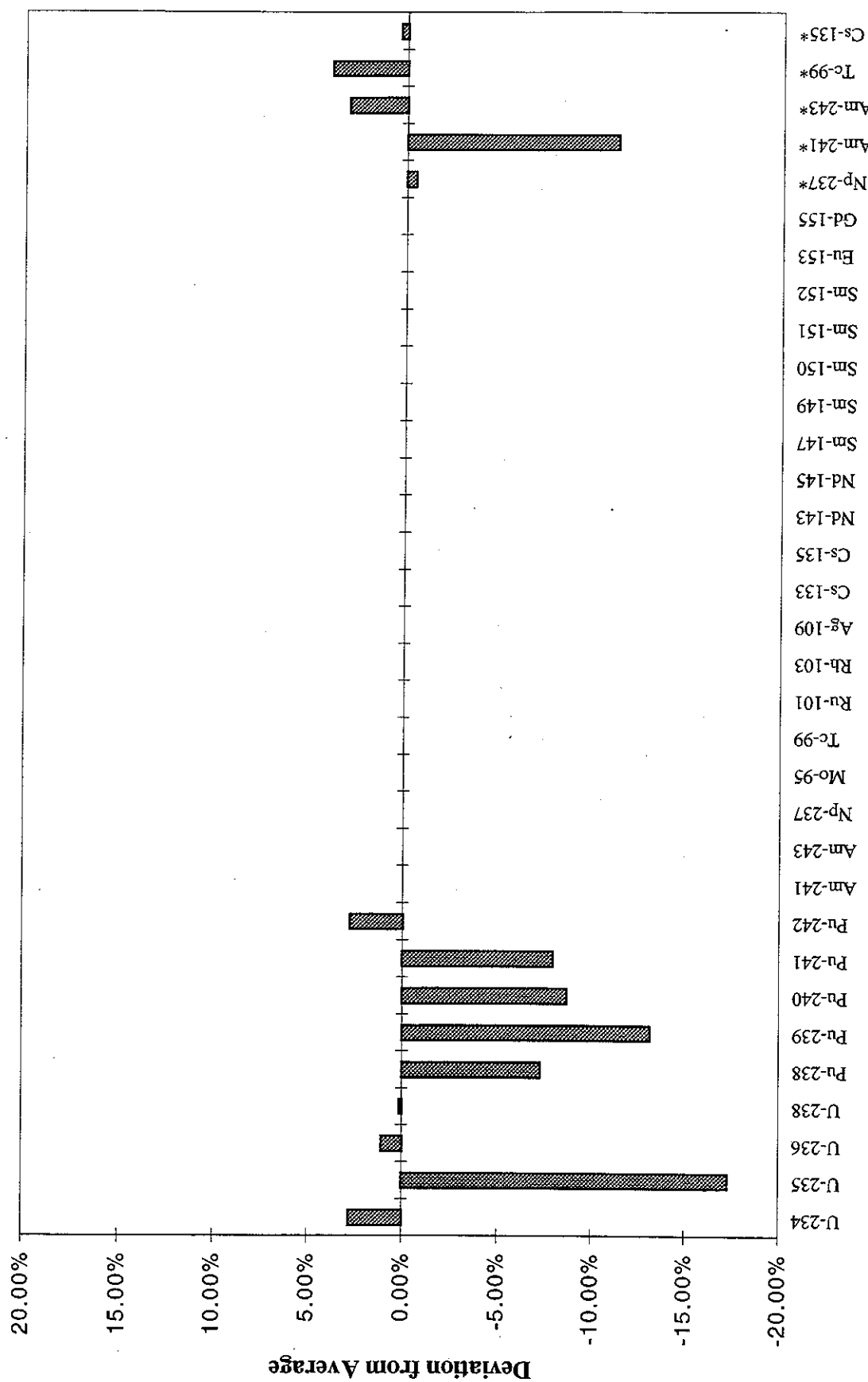


Fig. 50. Average agreement (all cases) by isotope for PNC results.
 (*Isotopic abundance measured in terms of activity.)

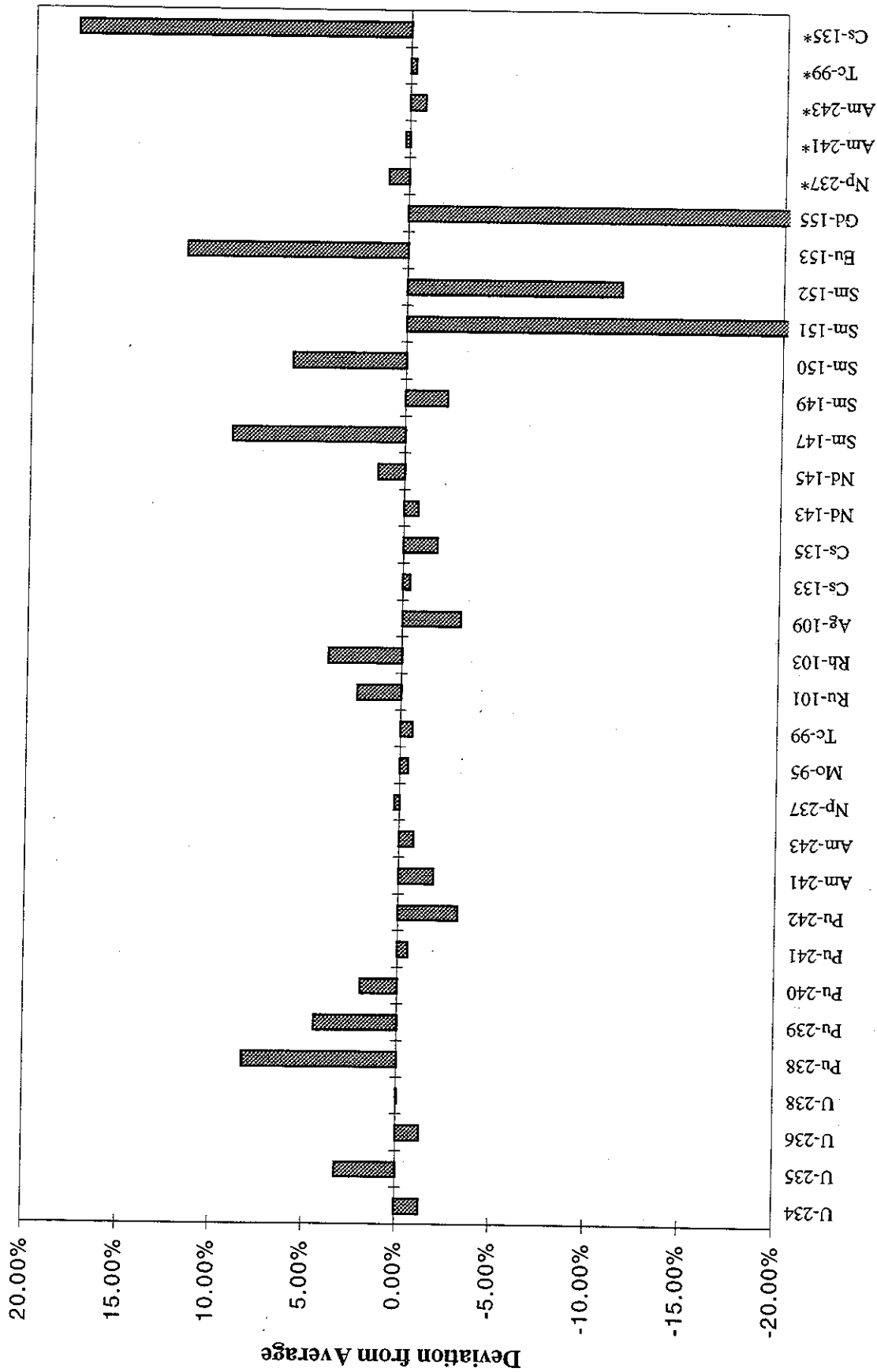


Fig. 51. Average agreement (all cases) by isotope for PSI results.
 (* Isotopic abundance measured in terms of activity.)

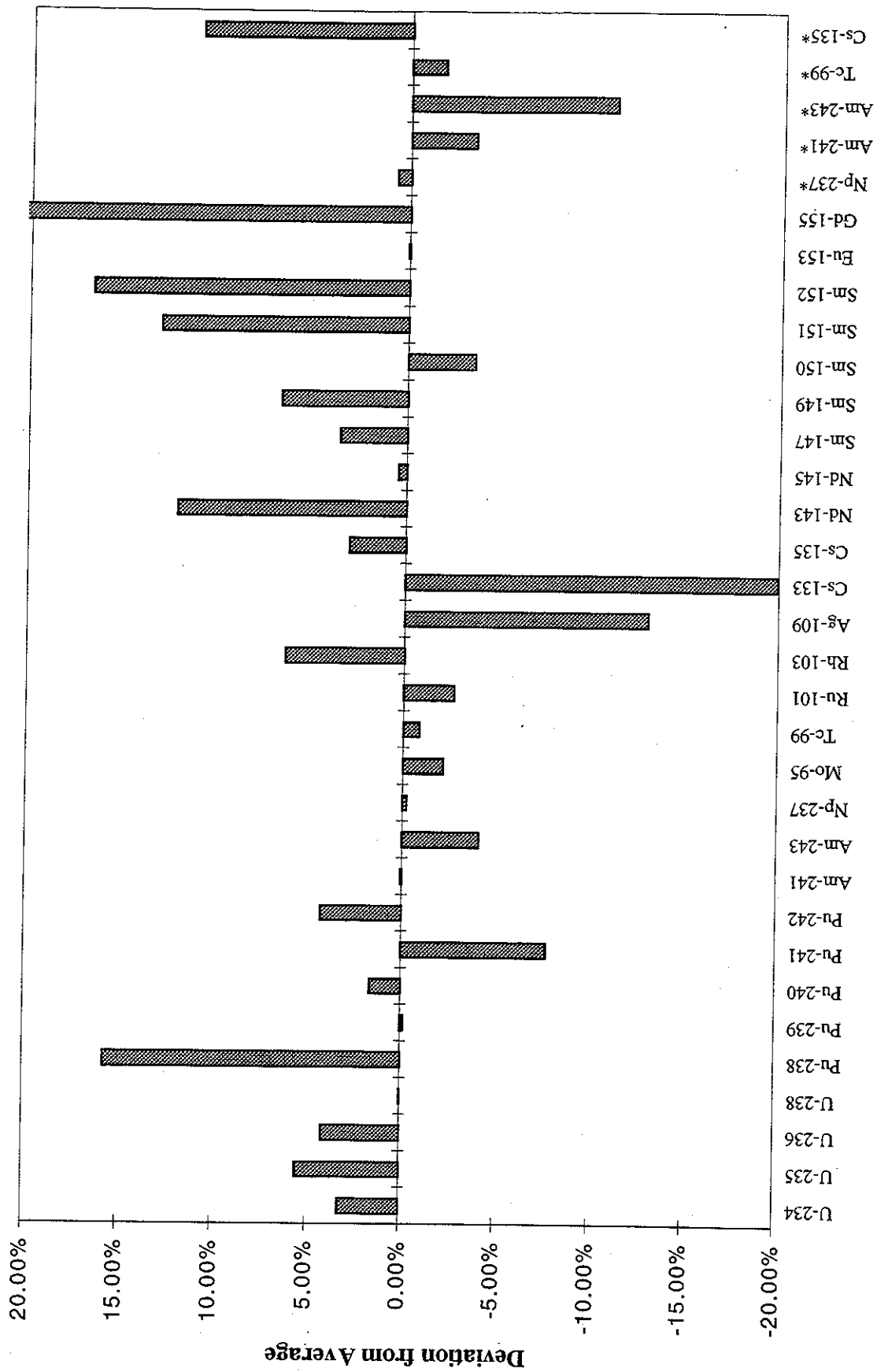


Fig. 52. Average agreement (all cases) by isotope for Risø results.
 (*Isotopic abundance measured in terms of activity.)

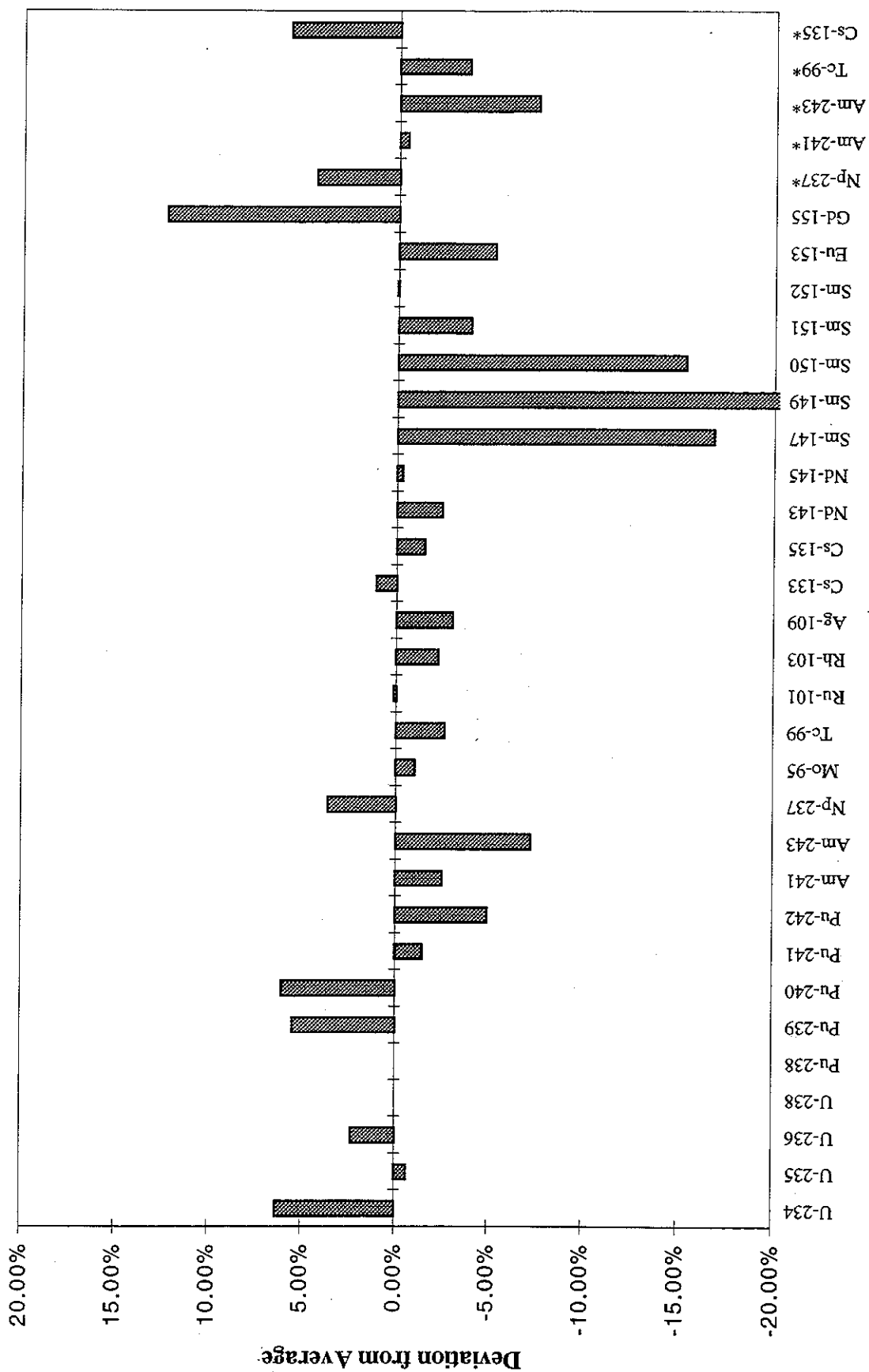


Fig. 53. Average agreement (all cases) by isotope for Tohoku results.
 (*Isotopic abundance measured in terms of activity.)

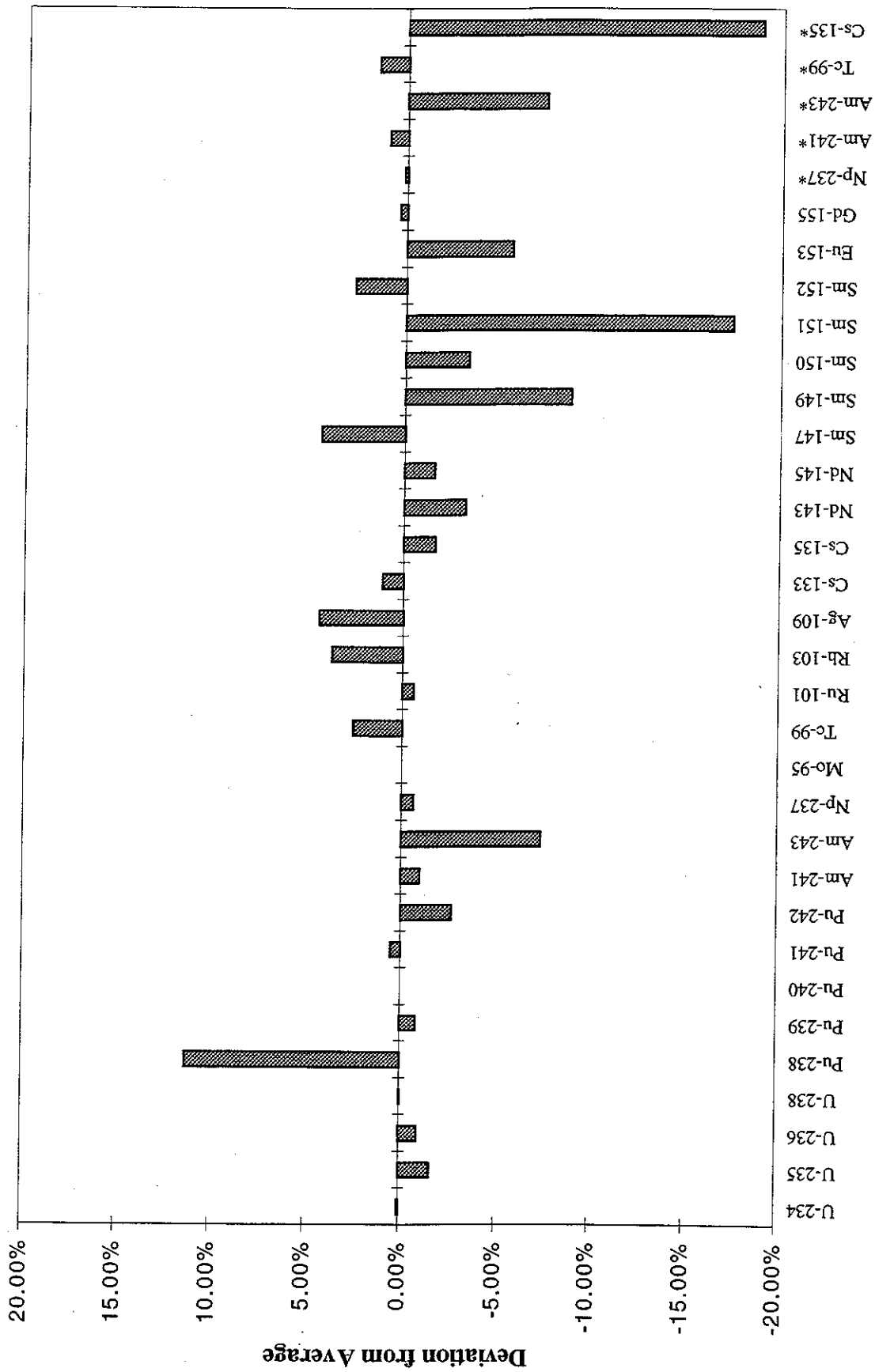


Fig. 54. Average agreement (all cases) by isotope for Toshiba-Leakage results.
 (*Isotopic abundance measured in terms of activity.)

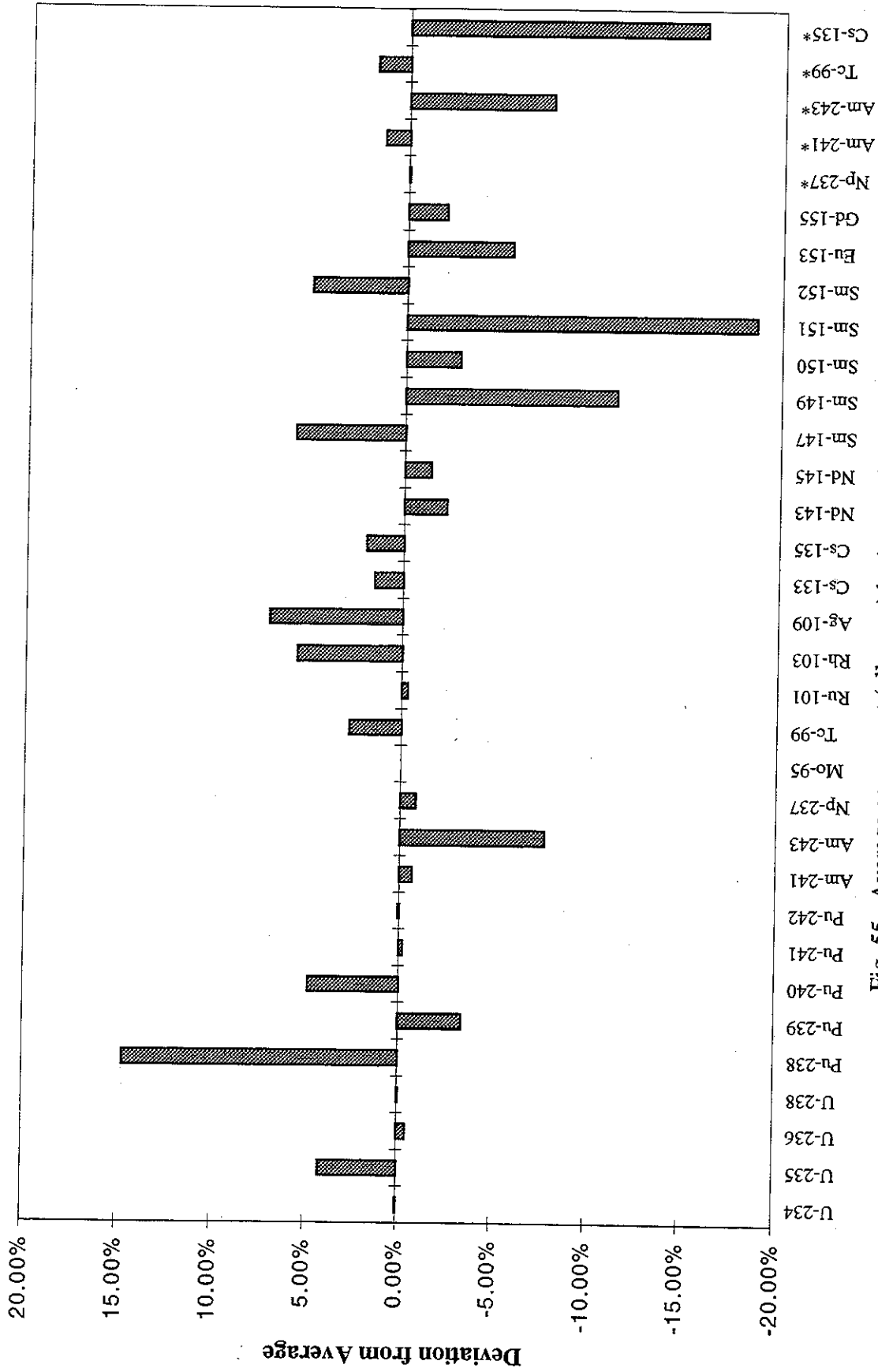


Fig. 55. Average agreement (all cases) by isotope for Toshiba-Poison results.
 (*Isotopic abundance measured in terms of activity.)

5. CONCLUDING REMARKS

Based on the standard deviation of the compiled results for each isotope, as given in Table 15, one can conclude that most methods are within 10% agreement in their estimate of isotopic concentrations for actinides. The two exceptions are ^{238}Pu and ^{243}Am . The deviation in ^{238}Pu was determined to be the result of incomplete/inadequate data used by certain participants; by excluding these results, a deviation of less than 10% is also noted. The deviation in ^{243}Am results, on the order of 11%, appears to be the result of poor data as well; however, the nature and source of the deficiency are not clear and will require further study.

It is also observed that with only three significant exceptions, all methods are within 11% agreement about the average for all fission products studied. Furthermore, most deviations are less than 10% and many less than 5%. The exceptions are ^{149}Sm , ^{151}Sm , and ^{155}Gd . For each of these nuclides, variation in the ability to predict nuclide concentrations is believed to result from inconsistencies in cross-section and fission yield data. In addition, there are a significant number of production paths for most of these isotopes, and all are sensitive to the fraction of ^{239}Pu fission. The most significant cause for the extremely large differences in ^{155}Gd concentrations is felt to be the result of inadequate cross-section data for ^{155}Eu in many cross-section libraries. Once this deficiency is corrected, results are likely to be in significantly better agreement; however, it is unclear if this is the only source of deficient data in the production of ^{155}Gd .

The ultimate goal of depletion methods is to provide an acceptable estimate of spent fuel isotopic contents in order to obtain a reasonable prediction of neutron multiplication in a spent fuel configuration for criticality safety analysis. Thus the reactivity associated with uncertainties in isotopic predictions can be used to assess the uncertainty in the calculation of neutron multiplication. A study of the reactivity associated with variations in isotopic compositions was undertaken by CSN and is summarized in Appendix A. This work presents the change in reactivity associated with changes in the concentration of individual isotopes, as calculated with the lattice code CASMO-3. Combined nuclide worths reported in Appendix A are consistent with results computed at ORNL.

6. REFERENCES

1. R. J. Guenther et al., *Characterization of Spent Fuel Approved Testing Material ATM-104*, PNL-5109-104, Pacific Northwest Laboratories, Richland, Washington, December 1991.
2. S. R. Bierman, "Spent Reactor Fuel Benchmark Composition Data for Code Validation," *Proceedings of the International Conference on Nuclear Criticality Safety - ICNC '91*, September 9-13, 1991, Oxford, United Kingdom, p. II-113.
3. O. W. Hermann et al., *Validation of the SCALE System for PWR Spent Fuel Isotopic Composition Analyses*, ORNL/TM-12667, Martin Marietta Energy Systems, Inc., Oak Ridge Natl. Lab., 1995.

APPENDIX A

**THE EFFECT ON REACTIVITY OF THE DIFFERENCES IN THE
COMPUTED ISOTOPIC COMPOSITION OF SPENT FUEL**

José M. Conde, M. Recio, A. I. Alvarez
Nuclear Engineering Division, Core Analysis Branch
Consejo de Seguridad Nuclear
Madrid, Spain

A.1 INTRODUCTION

The NEA of the OECD proposed a suite of benchmarks designed to study different aspects inherent to the use of burnup credit for the criticality safety analysis of the storage and transport of spent fuel. This benchmark is conceived as a code intercomparison and has been divided in several parts.

Part I of the benchmark focused on basic effects and was divided in two phases:

- Phase A¹ compared the multiplication factor calculated by different codes using the same PWR fuel isotopic composition. The comparison included both fresh and spent fuel at several burnup values.
- Phase B compared the isotopic composition calculated by different methods for a predefined PWR fuel burnup history. Comparison has been performed at three different burnup levels.

During the last meeting of the Criticality Calculations Group (Albuquerque, N.M., September 1995), the question was raised as to whether the Group should evaluate the impact on reactivity of the isotopic composition differences obtained in Phase I-B. It was considered that the assessment performed by a few participants could be enough to address this subject.

This work presents the change in reactivity associated with changes in the concentration of individual isotopes, as calculated with the lattice code CASMO-3 [ref. A.2].

A.2 METHOD

The results of Phase I-B were reported in the body of this report. For the purpose of this work, three sets of isotopic composition results have been used (cf. Tables 8 through 14):

1. CSN results calculated with CASMO-3;
2. concentration measurements;^{A.3} and
3. average of the results submitted by the participants.

The calculation procedure for each of the three burnup values included in the benchmark has been the following:

1. determination of the multiplication factor using the CASMO-calculated concentrations.

2. determination of the multiplication factor using both the experimental measurements and the average concentration values. For each case, the nuclides not included in the benchmark (or not measured) have been kept as the original CASMO-calculated value;
3. calculation of a new reactivity value by individually changing each isotope concentration, using both the measured and the average values.

Although not of definite importance for the purpose of this work, the conditions assumed for the reactivity calculation are coherent with the benchmark specification. The fuel rod data and pitch have been maintained, but an infinite array of infinite-length fuel rods has been considered. The temperature corresponds to storage conditions (300 K).

A.3 RESULTS

The reactivity obtained using the CASMO concentrations, the measured values, and the average of the participants' results are shown in Table A.1.

Table A.1. Reactivity values obtained with different concentration sets

Burnup (GWd/MTU)	CASMO concentrations	Measured values	Average values
27.35	1.00934	1.01842	1.01721
37.12	0.89869	0.92193	0.91776
44.34	0.82784	0.85320	0.85474

The differences found range from below 1% (lower-burnup case) up to 3% in the higher burnup case. To put these results in proper perspective, it has to be taken into account that neither the experimental uncertainty of the measured values nor the standard deviation of the average values has been taken into account. However, it is felt that these values give a fair idea of the maximum differences that can be obtained in a wide burnup range.

The origin of this reactivity difference can be tracked back to the individual isotopes by means of calculations where only a specific isotope is modified at a time. The reactivity values obtained for each burnup statepoint are shown in Tables A.2 through A.4. For each burnup point, the difference in the concentration of every individual isotope relative to the CASMO-calculated value is given, followed by the reactivity difference obtained by replacing the CASMO concentration value with the experimental (or average) value. Finally, the ratio of the reactivity

Table A.2. Effect of individual isotopes for Case A (27.35 GWd/MTU)

Nuclide	Experimental values			Average values		
	Concentration relative to CASMO (E/C-1*100)	$\Delta\rho$ (pcm)	Reactivity change rate (pcm/%)	Concentration relative to CASMO (A/C-1*100)	$\Delta\rho$ (pcm)	Reactivity change rate (pcm/%)
U-234	2.041	3	1.5	1.403	2	1.4
U-235	4.529	665	146.8	1.074	159	148.0
U-236	-2.907	17	-5.9	-0.309	2	-6.5
U-238	0.119	-20	-168.1	-0.475	82	-172.6
Pu-238	7.820	-17	-2.2	-3.825	8	-2.1
Pu-239	5.362	734	136.9	4.522	621	137.3
Pu-240	1.957	-101	-51.6	1.424	-74	-52.0
Pu-241	6.738	232	34.4	4.936	170	34.4
Pu-242	9.859	-29	-2.9	5.101	-15	-2.9
Am-241				6.919	-77	-11.1
Am-243				7.160	-5	-0.7
Np-237	-1.903	8	-4.2	6.589	-28	-4.3
Rh-103				15.248	-156	-10.2
Ag-109				29.680	-39	-1.3
Cs-133	2.262	-13	-5.7	1.239	-7	-5.7
Cs-135	-4.560	3	-0.7	1.299	-1	-0.8
Nd-143	-0.519	8	-15.4	1.136	-17	-15.0
Nd-145	2.286	-7	-3.1	1.605	-5	-3.1
Sm-147				-2.220	5	-2.3
Sm-149	55.496	-539	-9.7	10.134	-99	-9.8
Sm-150	7.254	-14	-1.9	1.192	-2	-1.7
Sm-151				17.842	-120	-6.7
Sm-152	-1.483	7	-4.7	6.375	-29	-4.6
Eu-153	0.752	-3	-4.0	-2.372	9	-3.8
Gd-155				-28.524	446	-15.7

Table A.3. Effect of individual isotopes for Case B (37.12 GWd/MTU)

Nuclide	Experimental values			Average values		
	Concentration relative to CASMO (E/C-1*100)	$\Delta\rho$ (pcm)	Reactivity change rate (pcm/%)	Concentration relative to CASMO (A/C-1*100)	$\Delta\rho$ (pcm)	Reactivity change rate (pcm/%)
U-234	7.362	-8	-1.1	4.525	-5	-1.1
U-235	10.944	1167	106.6	4.700	507	107.9
U-236	-3.605	21	-5.8	-0.792	4	-5.1
U-238	-0.395	58	-146.8	-0.670	98	-146.3
Pu-238	5.518	-21	-3.8	-2.676	10	-3.8
Pu-239	7.554	1324	175.3	6.492	1133	174.5
Pu-240	2.848	-157	-55.1	0.551	-31	-56.3
Pu-241	8.614	467	54.2	6.581	358	54.4
Pu-242	6.962	-36	-5.2	3.843	-20	-5.2
Am-241				8.299	-106	-12.8
Am-243				2.617	-5	-1.9
Np-237	-10.078	56	-5.6	5.658	-32	-5.7
Rh-103				17.200	-194	-11.3
Ag-109				28.683	-52	-1.8
Cs-133	1.774	-13	-7.3	1.307	-10	-7.7
Cs-135	0.832	-1	-1.2	4.563	-3	-0.7
Nd-143	0.196	-4	-20.4	2.043	-33	-16.2
Nd-145	3.225	-12	-3.7	2.023	-8	-4.0
Sm-147				-3.226	7	-2.2
Sm-149	50.830	-492	-9.7	11.011	-108	-9.8
Sm-150	0.148	-1	-6.8	1.183	-3	-2.5
Sm-151				21.374	-142	-6.6
Sm-152	-6.052	30	-5.0	7.949	-41	-5.2
Eu-153	-5.382	28	-5.2	-1.129	6	-5.3
Gd-155				-25.324	619	-24.4

Table A.4. Effect of individual isotopes for Case C (44.34 GWd/MTU)

Nuclide	Experimental values			Average values		
	Concentration relative to CASMO (E/C-1*100)	$\Delta\rho$ (pcm)	Reactivity change rate (pcm/%)	Concentration relative to CASMO (A/C-1*100)	$\Delta\rho$ (pcm)	Reactivity change rate (pcm/%)
U-234	6.952	-5	-0.7	8.289	-7	-0.8
U-235	20.654	1575	76.3	9.100	704	77.4
U-236	-3.073	17	-5.5	-0.998	5	-5.0
U-238	-0.806	105	-130.3	-0.830	108	-130.1
Pu-238	7.822	-38	-4.9	-1.645	8	-4.9
Pu-239	9.363	1827	195.1	8.007	1570	196.1
Pu-240	4.607	-251	-54.5	0.247	-13	-52.6
Pu-241	11.390	759	66.6	8.027	536	66.8
Pu-242	7.913	-52	-6.6	2.569	-17	-6.6
Am-241				9.703	-124	-12.8
Am-243				-1.389	4	-2.9
Np-237	-1.866	12	-6.4	4.949	-31	-6.3
Rh-103				18.560	-211	-11.4
Ag-109				29.435	-60	-2.1
Cs-133	1.142	-8	-7.0	1.468	-11	-7.5
Cs-135	8.122	-5	-0.6	8.574	-5	-0.6
Nd-143	1.666	-26	-15.6	3.238	-51	-15.8
Nd-145	3.766	-14	-3.7	2.357	-9	-3.8
Sm-147				-3.721	8	-2.2
Sm-149	124.451	-1172	-9.4	11.557	-111	-9.6
Sm-150	10.499	-30	-2.9	1.347	-4	-3.0
Sm-151				23.004	-158	-6.9
Sm-152	-3.123	16	-5.1	8.487	-44	-5.2
Eu-153	5.488	-32	-5.8	-0.428	2	-4.7
Gd-155				-23.052	685	-29.7

difference per percent unit change in concentration is noted to give an idea of the nuclide's importance with respect to reactivity. A negative result for this "reactivity change rate" means that the nuclide has an overall absorption effect.

The tables include all nuclides considered in the benchmark but ⁹⁵Mo, ⁹⁹Tc, and ¹⁰¹Ru, which are not included in the CASMO nuclear data library. Also, experimental measurements for some nuclides have not been performed.

To decide which of the isotopes are more relevant for the reactivity calculation, a numeric limit has to be defined. If we arbitrarily decide that the isotopes having an impact on reactivity smaller than 10 pcm/% can be neglected, then the list of the most relevant isotopes becomes the following: ²³⁵U, ²³⁸U, ²³⁹Pu, ²⁴⁰Pu, ²⁴¹Pu, ²⁴¹Am, ¹⁰³Rh, ¹⁴³Nd, ¹⁴⁹Sm, and ¹⁵⁵Gd. However, some isotopes not meeting the criteria may also be important because of the high calculation uncertainty they have. The best example of this group is ¹⁵¹Sm.

In order to assess the impact on reactivity of the isotopic compositions calculated by the Benchmark participants, the average standard deviations of the participants' results reported for each case in Table 15 of this report have been used, together with the sensitivities calculated taking the average concentration values as a base (Tables A.2 through A.4). The final results are included in Table A.5, while Table A.6 shows the individual results by isotope and burnup case.

Table A.5. Total impact on reactivity of the standard deviation of the isotope concentrations

Case	Reference reactivity	$\Delta\rho$ (pcm)	$\Delta\rho$ (%)
A	1.01721	2809	2.76
B	0.91776	3961	4.32
C	0.85474	4711	5.51

Table A.6. Impact on reactivity of the standard deviation of each isotope concentration

Nuclide	Case A		Case B		Case C	
	Standard deviation (%)	$\Delta\rho$ (pcm)	Standard deviation (%)	$\Delta\rho$ (pcm)	Standard deviation (%)	$\Delta\rho$ (pcm)
U-234	5.19	7.3	7.08	7.8	8.99	7.2
U-235	2.98	441.0	6.01	648.5	8.12	628.5
U-236	2.91	18.9	2.72	13.9	2.60	13.0
U-238	0.12	20.7	0.17	24.9	0.21	27.3
Pu-238	15.68	32.9	14.80	56.2	13.86	67.9
Pu-239	5.16	708.5	6.08	1061.1	7.12	1396.2
Pu-240	3.95	205.4	4.27	240.4	5.27	277.2
Pu-241	6.45	221.9	5.97	324.8	6.86	458.3
Pu-242	8.69	25.2	8.28	43.1	8.39	55.4
Am-241	4.22	46.8	4.35	55.7	5.29	67.7
Am-243	11.31	7.9	10.41	19.8	10.40	30.2
Np-237	8.61	37.0	8.86	50.5	9.42	59.4
Rh-103	4.57	46.6	5.15	58.2	5.40	61.6
Ag-109	11.03	14.3	10.61	19.1	10.21	21.4
Cs-133	4.87	27.8	4.90	37.8	5.60	42.0
Cs-135	2.49	2.0	2.98	2.1	3.63	2.2
Nd-143	2.76	41.4	3.93	63.7	4.51	71.3
Nd-145	1.02	3.2	1.25	5.0	1.46	5.6
Sm-147	6.03	13.9	7.95	17.5	9.12	20.1
Sm-149	14.14	138.6	15.01	147.1	15.61	149.9
Sm-150	5.30	9.0	7.07	17.7	8.50	25.5
Sm-151	22.41	150.2	21.72	143.4	22.31	153.9
Sm-152	7.20	33.1	9.01	46.9	9.68	50.3
Eu-153	7.90	30.0	8.19	43.4	8.52	40.1
Gd-155	33.45	525.2	33.28	812.0	32.97	979.2

A.4 REFERENCES

- A.1. M. Takano, *OECD/NEA Burnup Credit Criticality Benchmark. Result of Phase-1A* NEA/NSC/DOC(93)22; also JAERI-M 94-003, January 1994.
- A.2. M. Edenius et al., *CASMO-3 A Fuel Assembly Burnup Program*, STUDSVIK/NFA-89/2, November 1989.
- A.3. S. R. Bierman, *Spent Reactor Fuel Benchmark Composition Data for Code Validation*, Proceedings of the International Conference on Nuclear Criticality Safety ICNC-91, September 9-13, 1991, Oxford, United Kingdom, p. II-113.

APPENDIX B

**REVISED PSI RESULTS FOR THE BURNUP CREDIT CRITICALITY BENCHMARK,
PART I-B**

Peter Grimm and Jean-Marie Paratte

Paul Scherrer Institute
CH-5232 Villigen PSI
Switzerland

November 15, 1995

Recently, PSI has improved its depletion calculation method, more specifically the analytical formula used for nuclides with high destruction rates (i.e., short-lived or strongly absorbing nuclides). Relatively substantial changes have occurred in the densities of the following nuclides: ^{149}Sm , ^{151}Sm , ^{153}Eu (up to 5%), ^{155}Gd (up to 7%), ^{238}Pu (approximately 7%), and ^{243}Am (approximately 10%). The previous method overpredicted the densities of these nuclides which have short-lived precursors treated by the mentioned analytical method. The nuclide inventories for the three cases, given as mass fractions in the fuel and as specific activities (for Np and Am as well as for the radioactive fission products ^{99}Tc , ^{135}Cs , and ^{151}Sm), are listed in Table B-1.

Table B.1. Revised (11/15/95) results for PSI Phase I-B benchmark

Nuclide	Case A		Case B		Case C	
	Mass fract. (mg/g)	Activity (mCi/g)	Mass fract. (mg/g)	Activity (mCi/g)	Mass fract. (mg/g)	Activity (mCi/g)
U-234	1.5632E-1		1.3416E-1		1.2002E-1	
U-235	8.4014E+0		5.0361E+0		3.3162E+0	
U-236	3.1722E+0		3.5878E+0		3.7349E+0	
U-238	8.3737E+2		8.3013E+2		8.2438E+2	
Pu-238	9.0634E-2		1.7515E-1		2.4646E-1	
Pu-239	4.3591E+0		4.4464E+0		4.4228E+0	
Pu-240	1.6866E+0		2.1952E+0		2.4720E+0	
Pu-241	6.5963E-1		8.7337E-1		9.7663E-1	
Pu-242	2.6492E-1		5.4157E-1		7.8502E-1	
Am-241	2.3465E-1	8.0609E-1	3.0370E-1	1.0433E+0	3.3283E-1	1.1433E+0
Am-243	3.6427E-2	7.2744E-3	1.0113E-1	2.0195E-2	1.7231E-1	3.4411E-2
Np-237	2.8637E-1	2.0195E-4	4.1286E-1	2.9115E-4	4.9598E-1	3.4976E-4
Mo-95	5.6267E-1		7.2696E-1		8.3719E-1	
Tc-99	5.8920E-1	1.0148E-2	7.6829E-1	1.3233E-2	8.8950E-1	1.5320E-2
Ru-101	5.7299E-1		7.7494E-1		9.2141E-1	
Rh-103	3.5446E-1		4.5294E-1		5.1228E-1	
Ag-109	5.1069E-2		7.9584E-2		1.0121E-1	
Cs-133	8.3309E-1		1.0755E+0		1.2347E+0	
Cs-135	3.7170E-1	4.9281E-4	4.0527E-1	5.3732E-4	4.2340E-1	5.6136E-4
Sm-147	1.9293E-1		2.1980E-1		2.2996E-1	
Sm-149	1.9280E-3		2.0882E-3		2.2217E-3	
Sm-150	1.9945E-1		2.8482E-1		3.4882E-1	
Sm-151	7.5510E-3	1.9246E-1	8.2499E-3	2.1028E-1	8.8636E-3	2.2592E-1
Sm-152	8.3968E-2		1.0383E-1		1.1698E-1	
Nd-143	6.1582E-1		7.1915E-1		7.6282E-1	
Nd-145	5.0995E-1		6.5196E-1		7.4444E-1	
Eu-153	8.1460E-2		1.2064E-1		1.4842E-1	
Gd-155	2.3370E-3		3.8197E-3		5.2089E-3	

INTERNAL DISTRIBUTION

- | | | | |
|--------|-----------------|--------|-------------------------------|
| 1. | S. M. Bowman | 20. | R. W. Roussin |
| 2. | B. L. Broadhead | 21. | C. H. Shappert |
| 3-7. | M. D. DeHart | 22. | R. M. Westfall |
| 8. | O. W. Hermann | 23. | G. E. Whitesides |
| 9. | C. M. Hopper | 24. | Central Research Library |
| 10. | W. C. Jordan | 25-26. | ORNL Y-12 Research Library |
| 11. | M. A. Kuliasha | | Document Reference Section |
| 12. | B. D. Murphy | 27. | Laboratory Records Department |
| 13. | L. F. Norris | 28. | Laboratory Records, ORNL (RC) |
| 14-18. | C. V. Parks | 29. | ORNL Patent Office |
| 19. | L. M. Petrie | | |

EXTERNAL DISTRIBUTION

30. M. Akimoto, General Manager, Computing & Information Systems Center, JAERI, Tokai-Mura, Naka-gun, Ibaraki-ken 319-11 Japan
31. P. Albarede, C.E.N. - Cadarache, Bat. 230, CEA/DEDR/DRP/SPRC, F-13108 St. Paul Lez Durance, Cedex, France
32. A. I. Alvarez, CSN, Justo Dorado, 11, 28003 Madrid, Spain
33. R. E. Anderson, Los Alamos National Laboratory, NIS-6, MS J562, Los Alamos, NM 87545
34. Y. Ando, Nuclear Engineering Lab., Toshiba Corporation, 4-1 Ukishima-cho, Kawasaki-ku, Kawasaki 210 Japan
35. P. Angelo, 3080 Fennec Lane, Idaho Falls, Idaho 83401
36. M. Anttila, Technical Research Centre of Finland, VTT Energy, Nuclear Energy, P.O. Box 1604, SF-02044 VTT Tekniikantie 4C, Finland
37. C. E. Apperson, Westinghouse Savannah River Company, Savannah River Site, Bldg. 773-11A, Aiken, SC 29808-0001
38. M. G. Bailey, Office of Nuclear Material Safety & Safeguards, U.S. Nuclear Regulatory Commission, MS TWFN-8F5, Washington, DC 20555
39. F. Barbry, C.E.A., Centre d'Etudes de Valduc, Chef de Service, IPSN/DRS/SRSC, 21120 IS-SUR-TILLE, France
40. J. M. Aragonés Beltrán, Escuela Técnica Superior de Ingenieros Industriales, Prof. Cat. Física Nuclear, Jose Gutierrez Abascal 2, E-28006 Madrid 6, Spain
41. K. Bendiksen, Director, Institute for Energy, Technology, P.O. Box 40, N-2007 Kjeller, The Netherlands

42. H. Bernard, DRN/DEC/DIR, Bat. 220, CEN Cadarache, F-13108 St. Paul-Lez-Durance, Cedex, France
43. W. Bernnat, Universitaet Stuttgart, Institut fuer Kernenergetik, und Energiesysteme, Postfach 801140, D-70550 Stuttgart 80 Germany
44. P. G. Boczar, Lead Manager, Advanced Fuel & Fuel Cycle Tech. Program, AECL Chalk River Laboratories, Chalk River, Ontario KOJ 1J0 Canada
45. R. Bowden, Nuclear Technology Section, British Nuclear Fuels plc, BNFL Engineering Group, Risley, Warrington, Cheshire WA3 6AS United Kingdom
46. M. C. Brady, Sandia National Laboratories, 101 Convention Center Drive, Suite 880, M/S 465, Las Vegas, NV 89109
47. R. W. Brewer, Los Alamos National Laboratory, SM30 Warehouse Bikini Road, MS F691, Los Alamos, NM 87545
48. J. B. Briggs, Idaho National Engineering Laboratory, P.O. Box 1625, MS-3890, Idaho Falls, ID 83415-3890
49. C. H. M. Broeders, Institut fuer Neutronenphysik, und Reaktortechnik, Kernforschungsanz. Karlsruhe, Postfach 3640, D-76021 Karlsruhe, Germany
50. D. E. Cabrilla, U.S. Department of Energy, EM-431, 1000 Independence Avenue, Washington, DC 20585
51. C. R. Carlos, Instituto Tecnologico e Nucl., Dpto. de Energia e Engenharia, Nucleares, Estrada Nacional N. 10, 2685 - Sacavem, Portugal
52. R. Carlson, Lawrence Livermore National Laboratory, P.O. Box 808, Livermore, CA 94550
53. A. Charlier, Belgonucleaire, Avenue Ariane 2-4, B-1200 Brussels, Belgium
54. J.-S. Choi, Lawrence Livermore National Laboratory, P.O. Box 808, 7000 East Avenue, L-390, Livermore, CA 94551
55. D. Y. Chung, Leader, Risk & Safety Support, U.S. Department of Energy, Office of Defense Programs, 19901 Germantown Road, Germantown, MD 20874
56. J. M. Conde Lopez, Head, Nuclear Engineering D., CSN, Justo Dorado, 11, 28003 Madrid, Spain
57. A. J. Cooper, British Nuclear Fuels, Technical Department, R116, Rutherford House, Risley Warrington WA3 6AS United Kingdom
58. P. Cousinou, Chef de Service IPSN/DRS/SEC, Centre d'Etudes Nucleaires, B.P. 6, F-92265 Fontenay Aux Roses, Cedex, France
59. A. De La Paz, Defense Nuclear Facility Safety Board, 625 Indiana Avenue, Suite 700, Washington, DC 20004
60. P. F. A. De Leege, Delft University of Techn., Interfaculty Reactor Inst., Reactor Physics Dept., Mekelweg 15, 2629 JB Delft, The Netherlands
61. A. J. Deruytter, Division Head, Nuclear Physics and Measurements, Institute for Reference Materials, and Measurements, JRC GEEL, Belgium
62. P. D'Hondt, Centre d'Etude de l'Energie Nucleaire, 200 Boeretang, B-2400 Mol, Belgium
63. C. Diop, CE Saclay, DRN/DMT/SERMA/LEPP, Bat. 470, F-91191 Gif-Sur-Yvette Cedex, France
64. T. W. Doering, TESS, B&W Fuel Co., MS 423, Suite 527, P.O. Box 98608, 101 Convention Center Drive, Las Vegas, NV 89109
65. M. J. S. Dyke, Pantex, P.O.Box 30020, Bldg 12-127, Amarillo, TX 79177
66. K. Ekberg, Studsvik AB, Fack, S-611 82 Nykoeping, Sweden
67. L. M. Farrington, British Nuclear Fuels plc, Technical Services, R101, Rutherford House, Risley, Warrington WA3 6AS United Kingdom
68. I. E. Fergus, U.S. Department of Energy, EH-22/GTN, Washington, DC 20585

69. P. J. Finck, CEA, Centre d'Etudes de Cadarache, DER/SPRC/Bat 230, 13108 St Paul Lez Durance, Cedex, France
70. H. Finnemann, Siemens AG/KWU, BT2, Postfach 3220, Hammerbacher Str. 12+14, D-91050 Erlangen, Germany
71. E. K. Fujita, Engineering Physics Division, Argonne National Laboratory, 9700 South Cass Avenue, Argonne, IL 60439-4801
72. A. Y. Gagarinski, NSR Vice-President, RRC Kurchatov Institute, Kurchatov Square, 123182 Moscow, Russia
73. D. Galvin, U.S. Department of Energy, Systems Engineering, Division DP-31, 19901 Germantown Road, Germantown, MD 20874
74. L. Garcia de Viedma, Deputy Director, Computing, Consejo de Seguridad Nuclear, C/Justo Dorado, 11, 28040 Madrid, Spain
75. B. Gillet, COGEMA, 2 rue Paul Dautier, 78141 Velizy Villacoublay, Cedex, France
76. E. S. Gluchkov, RRC Kurchatov Institute, Kurchatov Square 1, 123182 Moscow, Russia
77. I. C. Gauld, Whiteshell Laboratories, AECL Research, Pinawa, Manitoba ROE 1LD Canada
78. B. Gmal, Gesellschaft fuer Anlagen-und Reaktorsicherheit, Postfach 1328, D-85739 Garching, Germany
79. C. Gragg, Studsvik Core Analysis AB, Fack, S-611 82 Nykoeping, Sweden
80. P. Grimm, Paul Scherrer Institute, CH-5232 Villigen PSI, Switzerland
81. H. Gruppelaar, Head, Nuclear Analysis Group, REACP NL, Foundation ECN, Postbus 1, NL-1755 ZG Petten, The Netherlands
82. N. T. Gulliford, Reactor Physics, Criticality, and Shielding Laboratory, AEA Technology, Winfrith Technology Centre, Dorchester, Dorset DT2 8DH United Kingdom
83. N. Haberman, U.S. Dept. of Energy, Washington DC, 20585
84. W. Heinicke, Gesellschaft fuer Anlagen-und Reaktorsicherheit, Forschungsgelaende, D-8046 Garching, Germany
85. S. Helmersson, ABB-ATOM AB, Reactor Core Engineering, S-72163 Vasteras, Sweden
86. K. Hesketh, British Nuclear Fuels plc, Springfields, Preston, Lancashire PR4 0XJ United Kingdom
87. N. Hirakawa, Reactor Physics Laboratory, Dept. of Nuclear Engineering, University of Tohoku, Aoba, Aramaki-ku, SENDAI-SHI 980 Japan
88. C. F. Hoejerup, Head, Reactor Physics Section, Risoe National Laboratory, P.O. Box 49, DK-4000 Roskilde, Denmark
89. M. Houts, Los Alamos National Laboratory, SM30 Warehouse Bikini Road, MS-K551, Los Alamos, NM 87545
90. R. Hueggenberg, Gesellschaft fuer, Nukleare Behaelter (GNB), Hollestr. 7A, D-45127 Essen, Germany
91. Y. H. Huh, Principal Researcher, KAERI, P.O. Box 7, Daeduk-danji, Taejon 305-606 Korea
92. M. Itagaki, JAERI, Criticality Safety Laboratory, Dept. of Fuel Cycle Research, 2-4 Shirakata-Shirane, Tokai-mura Ibaraki 31911 Japan
93. T. Iwasaki, Reactor Physics Laboratory, Dept. of Nuclear Engineering, University of Tohoku, Aoba, Aramaki-ku, SENDAI-SHI 980 Japan
94. R. Jeffree, Counsellor, Australian High Commission, Australia House, Strand, London, WC2B 4LA Australia
95. S. C. Keeton, Lawrence Livermore National Laboratory, P.O. Box 808, 7000 East Ave., Building 451, L-561, Livermore, CA 94550
96. J. S. Kim, Vice President, Nuclear Power Engineering, KAERI, P.O. Box 7, Daeduk-Danji, Daejon, 305-606 Korea

97. J. L. Kloosterman, Foundation (ECN), B.U. Nuclear Energy, P.O. Box 1, NL-1755 ZG Petten, The Netherlands
98. A. D. Knipe, General Manager, Plant Support Services Group, A32/317, Winfrith Technology Center, Dorchester, Dorset DT2 8DH United Kingdom
99. Y. Komuro, JAERI, Department of Fuel Cycle Research, 2-4 Shirakata Shirane, Tokai-mura, Ibaraki-ken, 319-11 Japan
100. T. Koyama, Power Reactor & Nuclear Fuel Development Corporation, 9-13, 1-chome, Akasaka, Minato-ku, Tokyo, Japan
101. M. Kuvshinov, All Russian Research Institute of Experimental Physics, Nizhni Novgorod Region, ARZAMAS-16 607200 Russia
102. R. LaBauve, Los Alamos National Laboratory, SM30 Warehouse Bikini Road, MS K551, Los Alamos, NM 87545
103. W. H. Lake, Office of Civilian Radioactive Waste Management, U.S. Department of Energy, RW-33, Washington, DC 20585
104. D. B. Lancaster, TRW Environmental Safety Systems Inc., 2650 Park Tower Drive, Suite 800, Vienna, VA 22180
105. P. Landeyro, ENEA-DRI/COMB, CRE Casaccia, S.P. Anguillarese, 301, 00100 Rome, Italy
106. J. D. Lee, Lawrence Livermore National Laboratory, P.O. Box 808, 7000 East Ave., Building 451, L-561, Livermore, CA 94550
107. J. I. Lee, Project Manager, Safety Rev. & Assessmt, KINS, P O Box 114, Yusong, Taejon 305-600 Korea
108. Y-K. Lee, CEN Saclay, DMT/SERMA/LEPP, F-91191 Gif-Sur-Yvette Cedex, France
109. T. Lefvert, Vattenfall AB, Electricity Generation, S-162 87 Vallingby, Sweden
110. W. Lipiec, BRM, ABB Atom AB, S-721 63 Vasteras, Sweden
111. D. Lutz, Universitaet Stuttgart, Institut fuer Kernenergetik und Energiesysteme, Postfach 801140, D-70550 Stuttgart 80 Germany
112. J. C. Luxat, Reactor Safety and Operations Analysis, Ontario Hydro, 700 University Ave, H11-F1, Toronto, Ontario M5G 1X6 Canada
113. C. Madic, DRDD/SEMP, CEA/VALRHU/MARCOULE, B.P. 171, 30207 Bagnols Sur Ceze Cedex, France
114. T. Maldague, Belgonucleaire S.A., Avenue Ariane 4, B-1200 Brussels, Belgium
115. L. Markova, Ustav jaderneho vyzkumu Rez, Theoretical Reactor Physics, Nuclear Research Institute, 25068 RE Czech Republic
116. S. Matsuura, Vice-President, Japan Atomic Energy Institute, Fukoku Seimei Bldg., 2-2-2, Uchisaiwai-cho, Chiyoda-ku, Tokyo, 100 Japan
117. H. F. McFarlane, Argonne National Laboratory, P.O. Box 2528, Idaho Falls, ID 83403-2528
118. R. McKnight, Argonne National Laboratory, RA-208, 9700 South Cass Avenue, Argonne, IL 60439
119. D. E. Mennerdahl, Mennerdahl Systems, Starvögen 12, S-183 51 TjBY Sweden
120. S. Mitake, Japan Institute of Nuclear Safety, Fujita Kankou Toranomom B.7F, 3-17-1 Toranomom, Minato-ku, Tokyo 105 Japan
121. I. Mitsuhashi, Toshiba Corporation, Nuclear Engineering Lab., 4-1 Ukishima-cho, Kawasaki-ku, Kawasaki 210 Japan
122. Y. Miyoshi, JAERI, Criticality Safety Laboratory, Department of Fuel Cycle Safty. Res., 2-4 Shirakata-Shirane, Tokai-mura Ibaraki 31911 Japan
123. E. Moser, Gesellschaft fuer Anlagen-und Reaktorsicherheit, Postfach 1328, D-85739 Garching, Germany

124. R. Mosteller, Los Alamos National Laboratory, SM30 Warehouse Bikini Road, TSA-12, MS K551, Los Alamos, NM 87545
125. H. Nagano, Director, Research and International Affairs Division, Atomic Energy Bureau, STA, 2-2-1 Kasumgaseki, Chiyoda-ku, Tokyo, Japan
126. Y. Naito, Director, Department of Fuel Cycle Safety Research, JAERI, 319-11 Tokai-mura, Naka-gun, Ibaraki-ken, Japan
127. M. Narita, Faculty of Engineering, Hokkaido University, Kita-13 Nishi 8, SAPPORO, Hokkaido 060 Japan
128. J-C. Nimal, CEN Saclay, IRDI/DEDR/DEMT/SERMA/LEPP, Bat. 470, F-91191 Gif/Yvette Cedex, France
129. C. Noble, U.S. Department of Energy, 785 DOE Place, MS 1220, Idaho Falls, ID 83415-3890
130. I. Nojiri, PNC, Tokai Works, Muramatsu Tokai-mura, Naka-gun Ibaraki-Ken 319-11 Japan
131. C. Nordborg, OECD/NEA Data Bank, Le Seine Saint-Germain, 12 boulevard des Iles, F-92130 Issy-les-Moulineaux, France
132. A. Nouri, C.E.A., IPSN/DRS/SEC, B.P. No 6, 92265 Fontenay Aux Roses, Cedex, France
- 133-134. Office of Scientific and Technical Information, U.S. Department of Energy, P.O. Box 62, Oak Ridge, TN 37831
135. Office of the ORNL Site Manager, U.S. Department of Energy, Oak Ridge National Laboratory, P.O. Box 2008, Oak Ridge, TN 37831
136. H. Okuno, Department of Fuel Cycle Safety Research, JAERI, 319-11 Tokai-mura, Naka-gun, Ibaraki-ken, Japan
137. N. Otani, Criticality Engineering Lab., PNC, 4002 Naritacho, Oarai-machi, Higashi-ibaraki, Ibaraki 311-13 Japan
138. O. Ozer, Electric Power Research Institute, 3412 Hillview Ave., Palo Alto, CA 94304
139. J.-M. Paratte, Paul Scherrer Institute, CH-5232 VILLIGEN PSI, Switzerland
140. S. Pearlstein, Brookhaven National Laboratory, 53 Bell Avenue, Bldg. 475C, Upton, NY 11973
141. R. T. Perry, Los Alamos National Laboratory, TSA-10, MS K551, Los Alamos, NM 87545
142. J. S. Philbin, Sandia National Laboratories, P.O.Box 5800, MS 1146, Albuquerque, NM 87185-5800
143. B. Pohl, Lawrence Livermore National Laboratory, 7000 East Avenue, Building 311, L-298, Livermore, CA 94550
144. G. Poullot, CEA/IPSN/DRS/SEc, CEN Fontenay-Aux-Roses, B.P. No. 6, F-92265 Fontenay-Aux-Roses, France
145. S. M. Qaim, Division Head, Institut fuer Nuclearchemie, Forschungszentrum Juelich, Postfach 1913, D-52425 Juelich 1 Germany
146. M. Rahimi, 2650 Park Tower Drive, Suite 800, Vienna, VA 22180
147. G. Reffo, E.N.E.A. - Centro Ricerche, Energia Centro Dati Nucleari, V. Martiri di Monte Sole 4, I-40129 Bologna, Italy
148. B. Riazanov, Head of Nuclear Safety Division, SATE Scientific Center of Russian Federation, IPPE, Bondarenko Square 1, 249020 Obninsk, Russia
149. S-G. Ro, Storage & Transportation, Research Division, NEMAC, KAERI, P.O. Box 7, Daeduk-Danji, Daejeon, 305-606 Korea
150. B. Roque, C.E. - Cadarache, Bat. 230, CEA/DRN/DER, F-13108 St. Paul Lez Durance, Cedex, France
151. B. Rothleder, U.S. Department of Energy, EH-64, 19901 Germantown Road, Germantown, MD 20874

152. J. Roussignol, CEA/IPSN/DRS/SEc, CEN Fontenay-aux-Roses, B.P. No. 6, F-92265 Fontenay-Aux-Roses, France
153. A. Rudge, AEA Technology, Safety & Reliability Direct., Wigshaw Lane, Culcheth, Warrington WA3 4NE United Kingdom
154. Dr. Rypar, Nuclear Research Institute, 25068 Rez, Prague, Czech Republic
155. M. Salvatores, Directeur de Recherche, Dir. des Reacteurs Nucleaires, Bat. 707 - CE/Cadarache, F-13108 St. Paul-Lez-Durance, Cedex, France
156. A. Santamarina, C.E. - Cadarache, Bat. 230, CEA/DRN/DER, F-13108 St. Paul Les Durance, Cedex, France
157. M. Recio Santamarina, Consejo de Seguridad Nuclear, Justo Dorado, 11, 28040 Madrid, Spain
- 158-187. E. Sartori, OECD/NEA Data Bank, Le Seine-Saint Germain, 12 boulevard des Iles, F-92130 Issy-Les-Moulineaux, France
188. O. Sato, Mitsubishi Research Institute, Inc., Time & Life Bldg., 2-3-6 Otemachi, Chiyoda-ku, Tokyo 100 Japan
189. H. H. Schweer, Bundesamt fuer Strahlenschutz, Albert Schweitzerst. 18, D-38226 Salzgitter, Germany
190. P. Sentieri, Lockheed Idaho Technologies Company, MS-3428, Idaho Falls, ID 83403-2528
191. J-i. Shin, President, KAERI, P.O. Box 105, Yuseong, Taejon 305-600 Korea
192. F. Siciliano, ENEA - Centro Comb Trisaia, S.S. 106 Jonica, Km 419+500, I-75025 Policoro (Matera) Italy
193. S. E. Simopoulos, Nuclear Engineering Section, National Technical University of Athens, 15780 Athens, Greece
194. N. R. Smith, AEA Technology, Winfrith Technology Centre, Dorchester, Dorset DT2 8DH United Kingdom
195. J. T. Stewart, Department of Transport Radioactive Materials, Transport Division, P2/23C, 2 Marsham Street, London SW1P 3EB United Kingdom
196. T. Suto, 2nd Chemical Processing Section, Tokai Reprocessing Plant, PNC Tokai Works, Tokai-Mura, Naka-gun, Ibaraki-ken 319-11 Japan
197. K. Suyama, Fuel Cycle Safety Eval. Lab., Department of Fuel Cycle & Safety, Japan Atomic Energy Institute, Tokai-mura, Naka-gun, Ibaraki-ken 319-11 Japan
198. Z. Szatmary, Institute of Nuclear Techniques, Technical University of Budapest, H-1521 Budapest, Hungary
199. M. Takano, JAERI, Fuel Cycle Safety Eval. Lab., Tokai Research Establishment, Tokai-Mura, Naka-gun, Ibaraki-ken 319-11 Japan
200. E. Tanker, Terkiye Atom Enerjisi Kurumu, Baskanligi, Alacam Sokak No. 9 Cankaya, 06530 Ankara, Turkey
201. J. T. Taylor, Lockheed Idaho Technologies Company, MS-3428, Idaho Falls, ID 83403
202. Jean-Pol Tesch, AVN, Avenue du Roi 157, 1060 Brussels, Belgium
203. P. R. Thorne, British Nuclear Fuels plc, Safety & Nuclear Technology, R101, Rutherford House, Risley Warrington WA3 6AS United Kingdom
204. J. R. Thornton, Duke Engineering & Services, Inc., 2300 S. Tryon St., P.O. Box 1004, Charlotte, NC 28201-1004
205. A. Tsiboulia, Institute of Physics and Power Engineering (IPPE), Fiziko-Energiticheskij Institute, 1, Bondarenko Square, 249020 Obninsk, Russia
206. F. J. Turvey, Assistant Chief Executive, Radiological Protection Inst., 3 Clonskeagh Square, Clonskeagh Road, Dublin 14 Eire

207. M. Medina Vaillard, Director General, Comision Nacional Seguridad, Nuclear y Salvaguardias, Dr.Barragan 779, Col.Narvarte, 03020 Mexico, D.F.
208. Y. Vanderborck, Belgonucleaire, Avenue Ariane 4,, 1200 Brussels, Belgium
209. I. van Gerwen, CEC, DG XVII C-3, 200, rue de la Loi, B-1000 Brussels, Belgium
210. A. P. Vasilyev, Russian Federal Nuclear Center, Institute of Technical Physics, Theoretical Division, P.O. Box 245, 456770 Snezhinsk, Chelyabinsk Region, Russia
211. I. Vidovszky, Hungarian Academy of Sciences, Institute of Atomic Energy, P.O. Box 49, H-1525 Budapest 114 Hungary
212. N. P. Voloshin, Institute of Technical Physics, P.O.Box 245, Snezhinsk (Chelyabinsk-70), Chelyabinsk oblast 456770 Russia
213. H. Vonach, Inst. f. Radiumforschung und Kernphysik der Univ. Wien, Boltzmanngasse 3, A-1090 Wien, Austria
214. S. J. Walls, British Nuclear Fuels Plc, B113, Sellafield, Seascale, Cumbria CA20 1PG United Kingdom
215. M. E. Wangler, Office of Facility Safety Analysis, Mail Stop EH-32, U.S. Department of Energy, Washington, DC 20485
216. P. S. Webb, M. . Chew & Assoc., Inc., 1424 Concannon Blvd., Livermore, CA 94550
217. W-J. Weber, Gesellschaft fuer Anlagen-und Reaktorsicherheit, Forschungsgelaende, Postfach 1328, D-85739 Garching, Germany
218. A. Wells, 2846 Peachtree Walk, Duluth, GA 30136
219. C. J. Withee, Nuclear Material Safety & Safeguards, U.S. Nuclear Regulatory Commission, MS TWFN 8F5, Washington, DC 20555
220. P. Wydler, Paul Scherrer Institute, CH-5232 Villigen PSI, Switzerland
221. M. Yamamoto, Nuclear Engineering Lab., Toshiba Corporation, 4-1 Ukishima-cho, Kawasaki-ku, Kawasaki 210 Japan
222. R. Yang, Electric Power Research Institute, 3412 Hillview Ave., Palo Alto, CA 94304
223. V. I. Yuferev, Russian Federal Research Institute of Experimental Physics, Nizhni Novgorod Region, Arzamas-16, 607190 Russia

